AD NUMBER: AD0912123

LIMITATION CHANGES

TO:

Approved for public release; distribution is unlimited.

FROM:

Distribution authorized to U.S. Gov't. agencies only; Test and Evaluation Use; OCT 1972 Other requests shall be referred to Air Force Rocket Propulsion Laboratory, Edwards, CA 93523.

AUTHORITY

AFRPL ltr dtd 11 DEC 1973

AFRPL-TR-72-107

SIMULATION TESTING OF A MODIFIED BOMB DUMMY UNIT (BDU) (U) (AFRPL PROJECT DAME) (U)

Prepared by

ROCKETDYNE
North American Rockwell
McGregor, TX, 76657

Technical Report AFRPL TR-72-107

December 1972

AIR FORCE ROCKET PROPULSION LABORATORY
DIRECTOR OF SCIENCE AND TECHNOLOGY
AIR FORCE SYSTEMS COMMAND
UNITED STATES AIR FORCE
EDWARDS, CALIFORNIA

AFRPL-TR-72-107

SIMULATION TESTING OF A MODIFIED BOMB DUMMY UNIT (BDU) [redacted] (AFRPL PROJECT DAME) [redacted]

Prepared by

ROCKETDYNE
North American Rockwell
McGregor, TX, 76657

Technical Report AFRPL TR-72-107

Dec[redacted]72

149p.

Final rept.

R-4739

F04611-69-C-0075

AF-3059

30-104

AIR FORCE ROCKET PROPULSION LABORATORY
DIRECTOR OF SCIENCE AND TECHNOLOGY
AIR FORCE SYSTEMS COMMAND
UNITED STATES AIR FORCE
EDWARDS, CALIFORNIA

FOREWORD

This final report fulfills requirements of Contract F04611-69-C-0075, P006, Subline Item 1AA, for the conduct of simulation test of a Modified Bomb Dummy Unit. The program was conducted in support of AFRPL's in-house project 305904AME, "Project DAME (Determination of Aircraft Missile Environment)." The specific objective of the program, to conduct a system checkout of the complete flight test vehicle while it was exposed in an environment test simulator to a predicted flight vibration and thermal environment, was successfully attained. This report carries the contractor's report number R-4739.

ACKNOWLEDGEMENT

The direction and assistance provided by the program technical monitor, Mr. Lee G. Meyer during the course of this key Air Force technology program is gratefully acknowledged. Coordinated professional efforts of Messrs. P. Mercado of Naval Weapons Center, China Lake, E. J. Zimmer of AF Rocket Propulsion Laboratory, Dr. H. Leeming, Consultant, and General Dynamics/Ft. Worth, Subcontractor, are also acknowledged. Their timely assistance and coordination support was generously offered and enabled the necessary program flexibility and direction to achieve the noted technological advancements commensurate with the program objectives.

CONTENTS

CONTENTS

(Continued)

FIGURES

FIGURES

(Continued)

FIGURES

(Continued)

FIGURES

(Continued)

TABLES

1. INTRODUCTION

Project DAME, initiated by AFRPL, is being conducted to assist in defining the dynamic flight environmental effects on a solid propellant grain in an air-launched tactical missiles application. An instrumented Bomb Dummy Unit (BDU) containing an instrumented inert solid propellant grain was fabricated and supplied to Rocketdyne, Solid Rocket Division (SRD), by AFRPL as an initial flight test vehicle. It was subjected to dynamic instrument checkout and preflight system evaluation at Rocketdyne. The preflight evaluation was conducted on a dynamic ground test station, with an MAU-12A/C launcher (soft-mount system) to simulate wing attachment dynamic mechanical flexibility and with a stiff hard mount system where the BDU was directly attached to the ground test station for better transmissibility and control of the BDU.

Impedance measurements were made at the interface between the ground test station vibration fixture and the MAU-12A/C launcher to provide load transfer, mode shape, and mechanical stiffness data for the BDU assembly. Since commercial impedance heads are not easily adapted to the flight configuration, the launcher was instrumented with strain gages to provide that data during flight. Data were measured from the instrumented launcher concurrent with the impedance head and BDU instrumentation during ground tests.

This program was a joint effort between AFRPL, NWC, and Rocketdyne. Rocketdyne subcontracted flight prediction environments of the BDU when attached to an F-111 to General Dynamics, Fort Worth. Data from General Dynamics were in turn translated into ground simulation test objectives by Rocketdyne. NWC, AFRPL, and Dr. H. Leeming and Associates assisted Rocketdyne in defining the final test plan. Dr. H. Leeming and Associates (HL&A) primarily provided propellant section instrumentation analysis and circuit design for the instrumented sway brace. NWC designed, fabricated, provided, and operated the on-board data acquisition system. AFRPL provided assistance in operation support of the on-board data acquisition during the preflight check-out effort at Rocketdyne.

The specific objective of this program was to conduct a system checkout of the completed flight test vehicle (BDU) for Project DAME while it was being exposed in the static environment test simulator to a predicted flight vibration and thermal environment. This checkout was accomplished by subjecting the BDU to numerous vibration and aero-heat test cycles using both soft- and hard-mounting systems. On each test cycle, both ground station and on-board data were acquired for comparison to expected values. By this comparative method, proper gain levels for each gage were established for the on-board data acquisition system, thus preparing the BDU for its ultimate Project DAME flight tests.

The environment predictions used in the checkout program were based on the flight test vehicle being attached to an F-111 aircraft conducting flight profiles defined in the flight environment prediction section.

The program was composed of three phases, as shown in Fig. 1-1. The organization of this report is similar.

Phase I, Environmental Prediction(s), was conducted by General Dynamics. They supplied Rocketdyne with expected flight environmental conditions when subjecting the BDU to various flight profiles. These flight environments were then used to define test environments for use in Phase II.

Phase II, Simulation Testing, was the main portion of the program and was composed of four subdivisions - Define Simulation Environment, Test Equipment Design and Fabrication, Testing, and Shipping the BDU.

Phase III, Analysis, involved data reduction and analysis of the data obtained under Phase II. Dr. Leeming and Associates were subcontracted to provide the major portion of the propellant section data

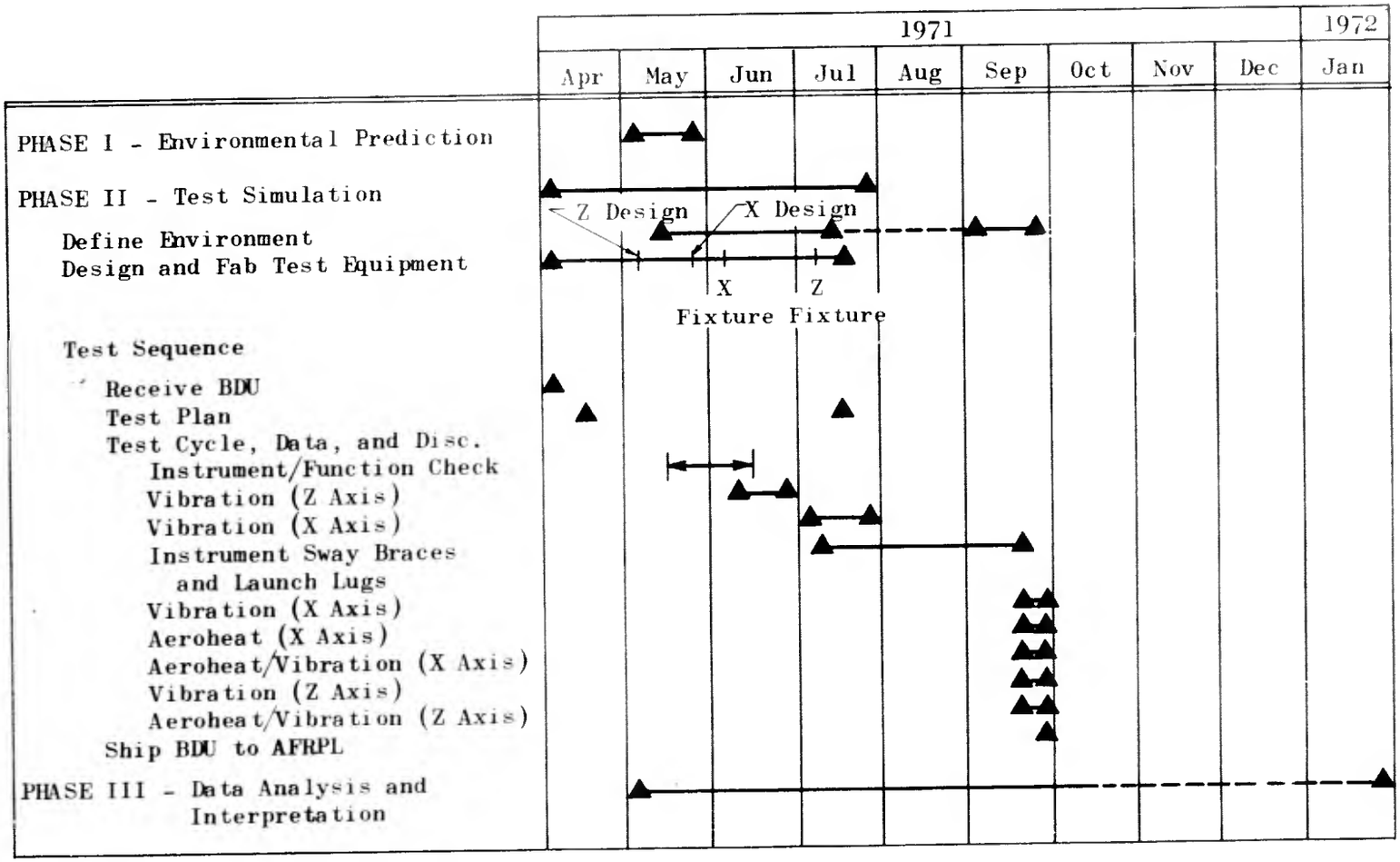

Figure 1-1. Bomb Dummy Unit Phasing Schedule

analysis while Rocketdyne provided ground-station data reduction of specified instruments and analysis of the instrumented sway braces and launch-lug data.

2. SUMMARY

The Bomb Dummy Unit (BDU) was subjected to testing preparatory to its captive flight on an F-111 aircraft. The objectives of the ground testing were to assess the safety aspects of flight, to (function) check the instrumentation and data acquisition system, and to calibrate the instruments in a simulated dynamic environment. The propellant grain was pressurized at several temperatures and instruments were read using precision equipment during both transient and equilibrium conditions. The BDU assembly was attached to an MAU-12A/C launcher (which was instrumented for force transfer measurements during the conduct of this program) to simulate in-flight attitude and configuration, and subjected to sine survey, random, aeroheat, and combined random and aeroheat testing. Simulated random and aeroheat testing environments were based on the data as determined by General Dynamics, Ft. Worth, to be expected during flight testing on an F-111 during certain specified mission profiles.

Redundant data were acquired from the BDU flight instrumentation using the on-board flight recorder and Rocketdyne's dynamic ground test station recorders. Data from the ground test station were reduced and are discussed in this report.

Acceleration and mechanical impedance data from instruments additional to those to be used on the flight configuration are also reported. The more salient items deduced from the mechanical dynamics are the BDU is a complex and nonlinear system that displays "bell-ringing" (X-axis), pitching (Z-axis) and bending modes (both axes). Fundamental resonance frequencies appear to be 11.5, 27, and 60 Hz respectively for these modes. These modes (notably the bell-ringing mode) can be excited by input forces in other axes at their fundamental and harmonic frequencies. From the apparent mass, instrumented launcher, and from what is known about the expected flight environment, it does not appear there will be

problems with large loadings induced to the BDU during flight although coupling between the 27 Hz pitching mode and the 25 Hz F-111 wing torsion mode should be closely examined.

During conduct of this program we were strongly reminded of the specialized requirements of a data acquisition system for solid rocket motor dynamic testing and that the value of data acquired during testing can be significantly enhanced through close coordination between the test engineer and the analyst. With over 70 channels of information being recorded most of it being high frequency data, there are a variety of internal comparisons (e.g., phase angles) that are very informative for data interpretation. In many tests, such comparisons cannot be made due to equipment limitations; consequently, the dynamic behavior of the system is not completely characterized.

In the BDU tests, data channels acquired by tape were rearranged for different axes and for successive tests in each axis. This facilitated a relatively complete dynamic characterization of the system. In circumstances in which repeated testing is not required, this technique would be costly and time consuming.

Dynamic preflight testing of the BDU has benefitted Project DAME. A defect was found, and repaired by the manufacturer, in the on-board flight recorder. The dynamic behavior of the BDU has been characterized in detail, and the instrumentation dynamic response has been measured through a ground-based analog system. These data can be used as a reference standard. Experimentation provided experience on this particular system to facilitate adjustment of the data acquisition electronics (e.g., VCO band width) that will subsequently minimize the risk of losing data during flight testing. Both system and propellant response data were measured and documented for reference. These data are available for comparison to responses measured during flight; and future additional in-depth analyses, thereby, are a significant contribution toward accomplishing the objectives of Project DAME.

3. PHASE I - ENVIRONMENTAL PREDICTION

General Dynamics (GD), Fort Worth, Texas, designer and builder of the F-111 aircraft, was subcontracted by Rocketdyne to predict the environmental (vibration, acoustic, and thermal) conditions for the bomb dummy unit. The F-111 aircraft will be used in the Project DAME flight tests. General Dynamics' final report is presented in Attachment 1 and only summarized in the text of this final report.

General Dynamics predicted vibration, acoustic, and thermal environments of a test store carried by an F-111 aircraft during specified flight profiles. Predictions have been made for external carriage on pylon stations 3, 4, 5, or 6 and for carriage in the weapons bay. Data are provided for the following specified flight profiles:

1. Taxi, take-off, and landing
2. Climb to 50,000 feet in 9 minutes, accelerate from M = 1.60 to M = 2.5 in 6 minutes, and maintain M = 2.5 at 50,000 feet for 4 minutes
3. Climb to 35,000 feet in 4 minutes, accelerate from M = 0.90 to M = 2.0 in 5 minutes, and maintain M = 2.0 for 8 minutes
4. Climb to 35,000 feet in 4 minutes and maintain M = 0.80 for 30 minutes at 35,000 feet
5. Fly terrain following radar mission at 500 feet (above ground level) and M = 0.9 for 30 minutes.

Profile No. 3 was specified by AFRPL for test simulation by Rocketdyne with the test store mounted on a wing pylon. Therefore the summary of the GD effort is concentrated on this one flight profile. The test store used in the prediction was a modified bomb dummy unit, (BDU) 12/B, Fig. 3-1, with the following characteristics:

length - 118.5 inches
diameter - 14.75 inches (maximum)
fin span - 25.395 inches
weight - 750 pounds

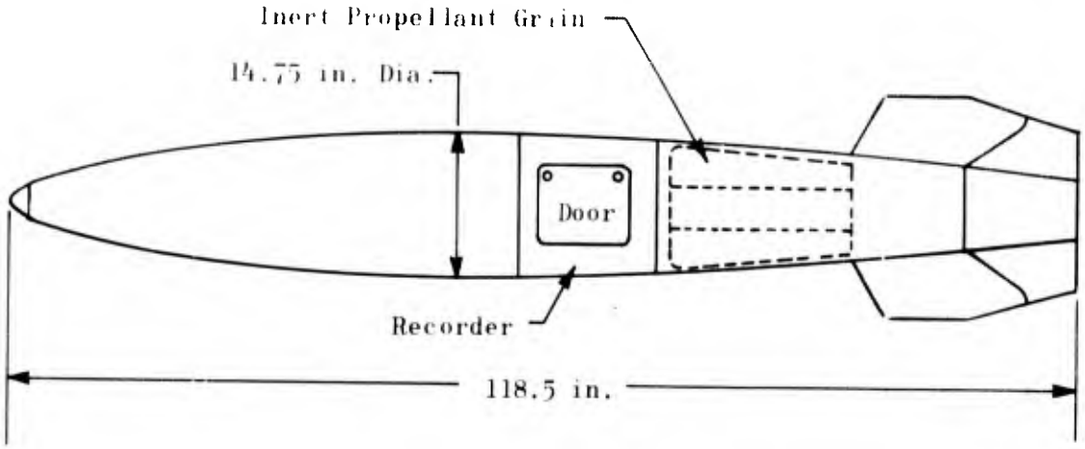

Figure 3-1. Bomb Dummy Unit, BDU-12/B

VIBRATION AND ACOUSTICS

Detailed vibration and acoustic data were derived for aircraft Taxi, Take-off, and Landing (Mission 1) and for the end point of each of the other four flight profiles. In addition, the variation of vibration and acoustic levels with flight dynamic pressure was defined. Proven deterministic techniques for predicting high frequency responses are generally not too reliable. In view of this limitation, extrapolation methods, wherein experimental data obtained on one vehicle are used to predict the response of another, are widely used. Such an approach was used to obtain the vibration and acoustic predictions. Data measured on stores during the F-111 flight test program are the principal bases for the vibration and acoustic predictions contained herein. Vibration data for flight profiles are shown in Fig. 3-2 through 3-5.

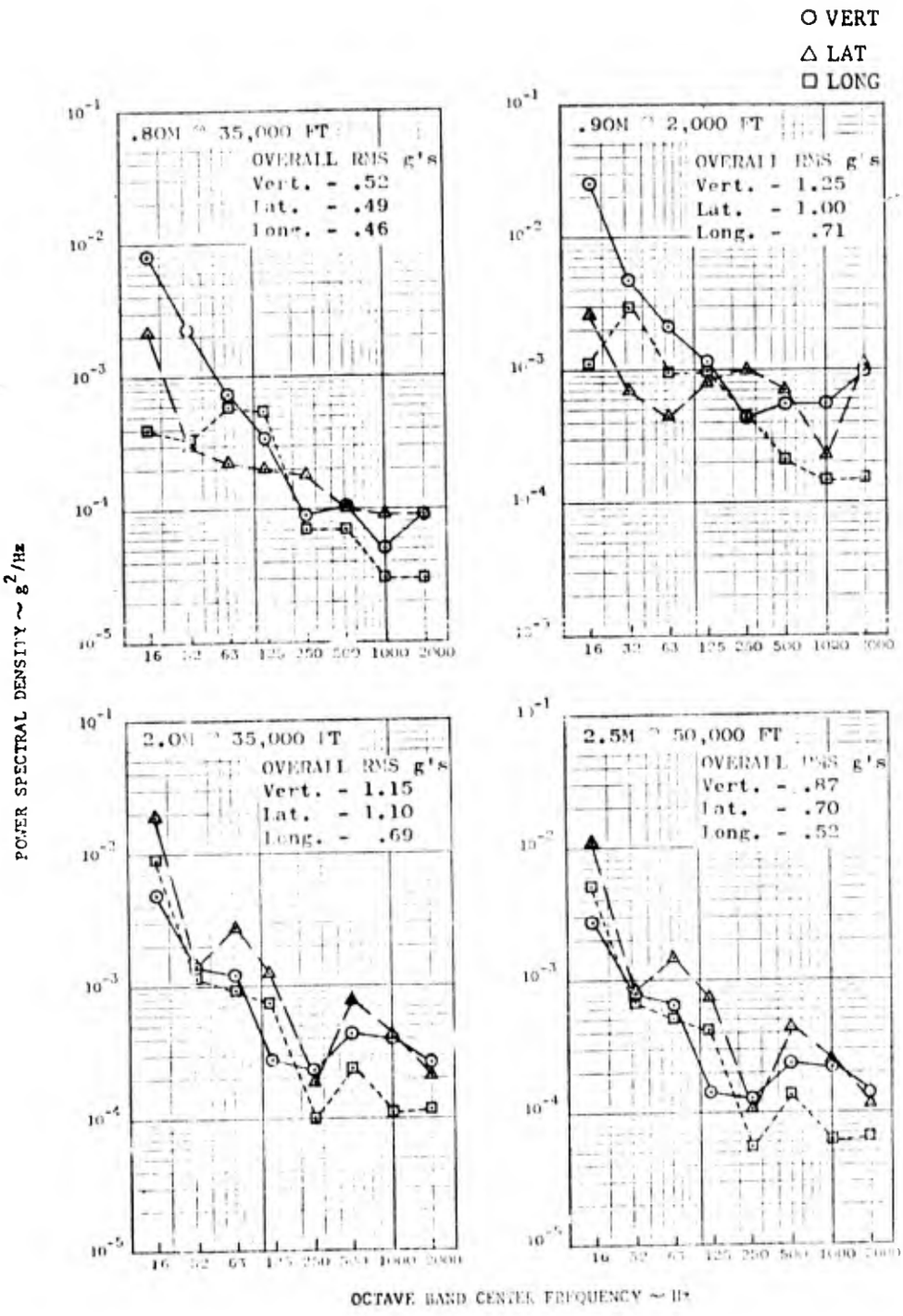

Figure 3-2. Predicted Vibration Levels for Test Store on F-111 Wing Pylon, Forward Hook

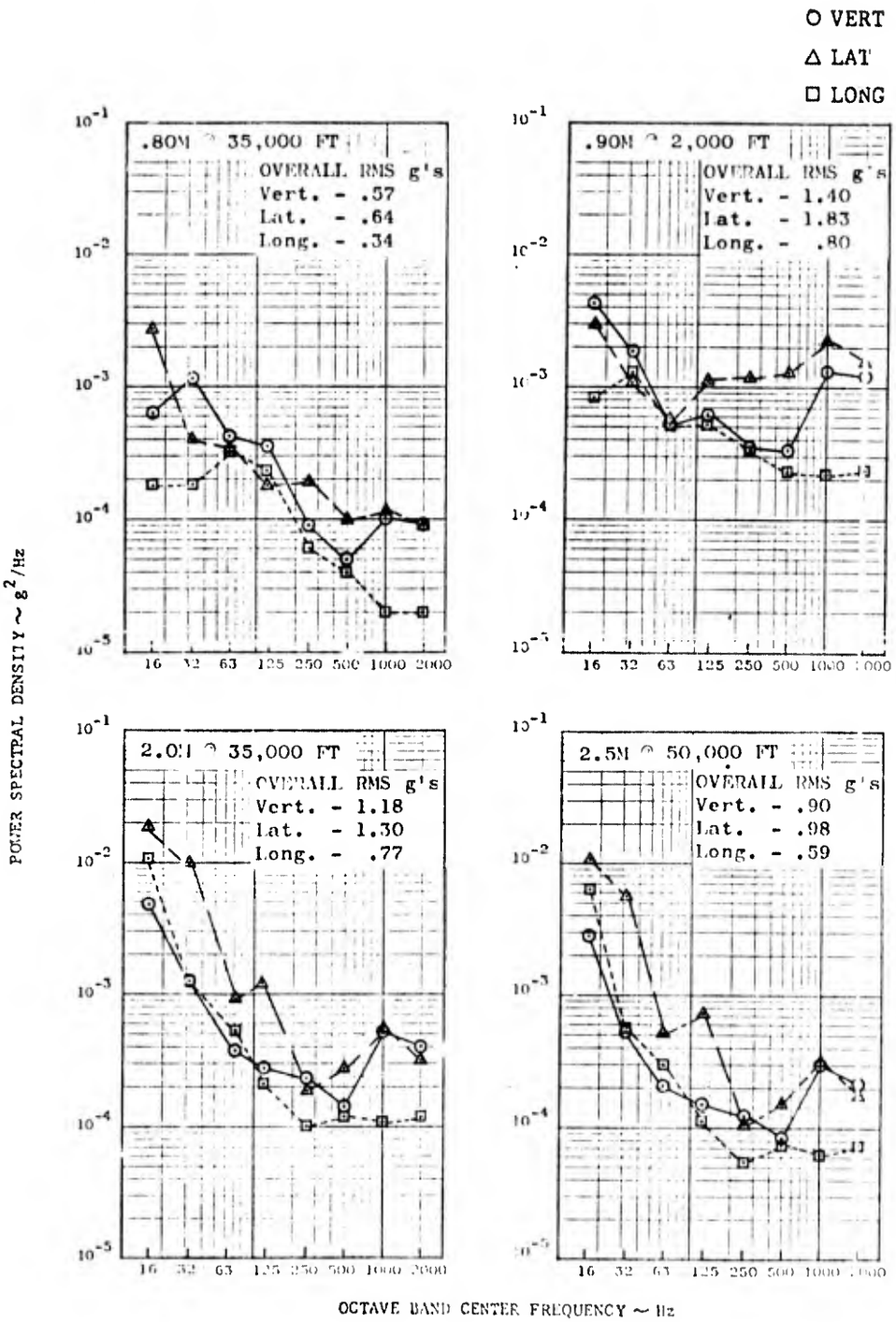

Figure 3-3. Predicted Vibration Levels for Test Store on F-111 Wing Pylon, Aft Hook

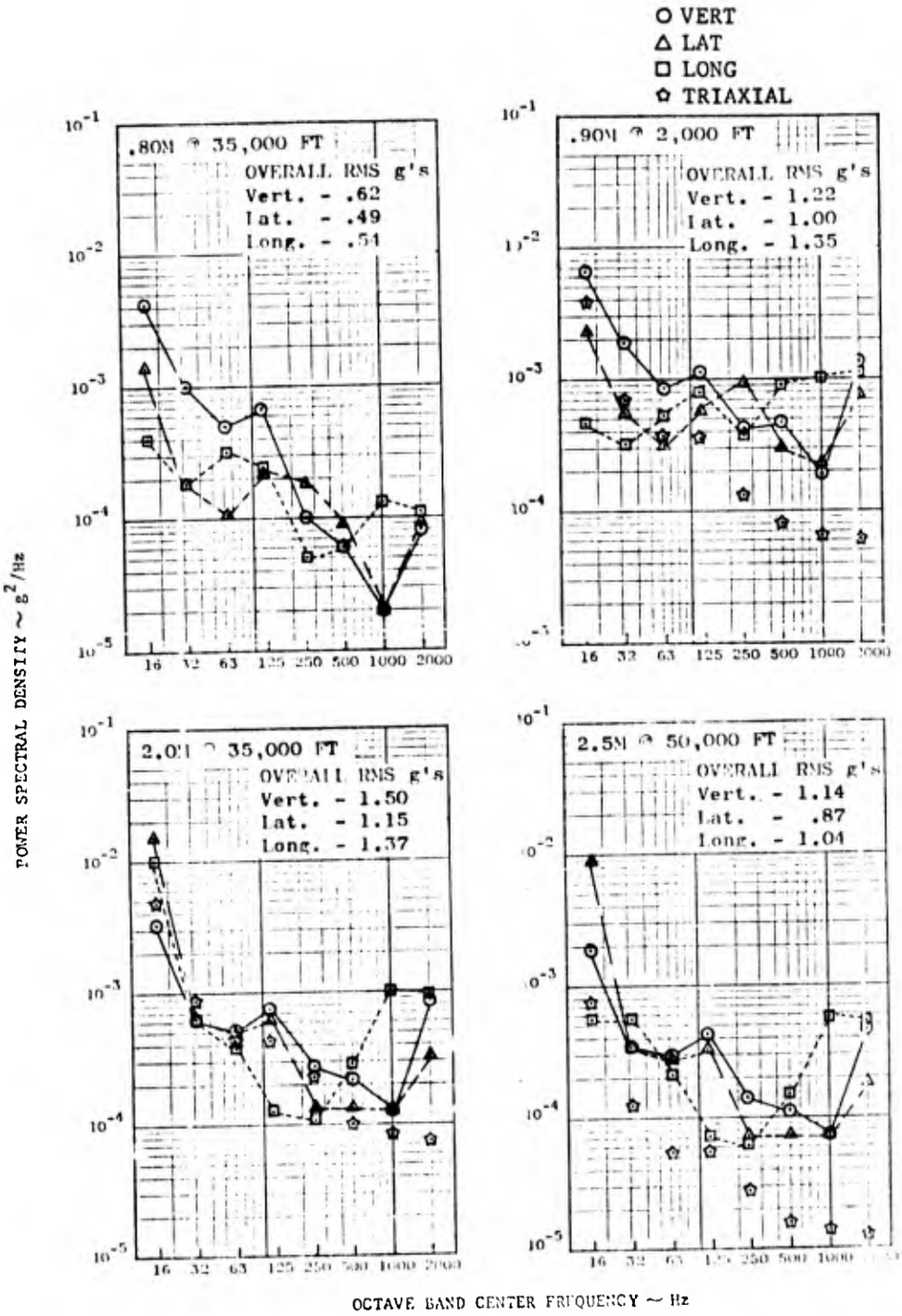

Figure 3-4. Predicted Vibration Levels for Test Store on F-111 Wing Pylon, Center of Gravity

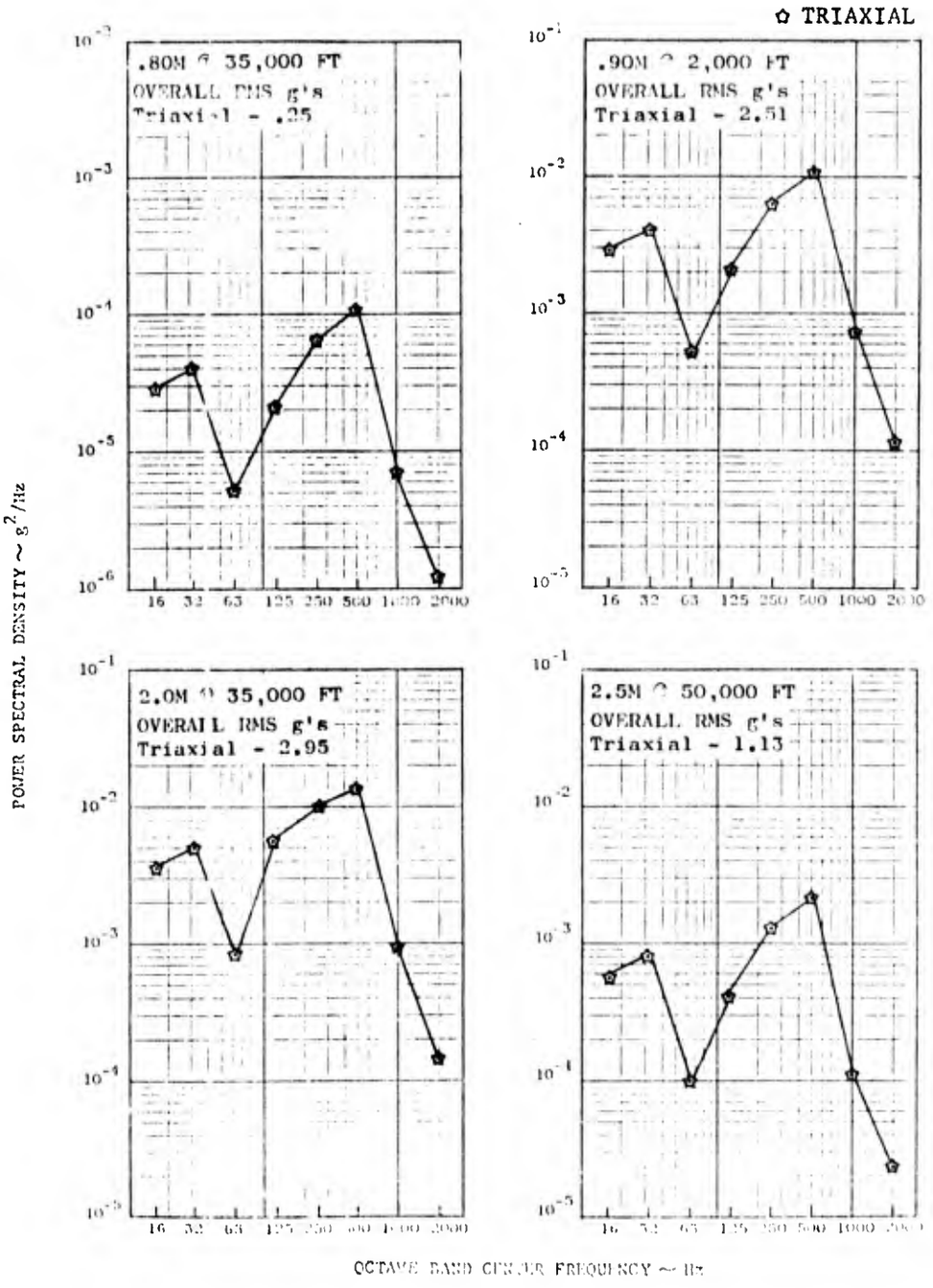

Figure 3-5. Predicted Vibration Levels for Test Store on F-111 Wing Pylons, Tail Section

THERMAL PREDICTION

A missile carried by an F-111 aircraft may be subjected to a wide variety of thermal environments that change rapidly during a given mission. This thermal environment controls the rate of heat transfer to (or from) the missile and thus influences the temperatures of the missile. The thermal environment of a typical missile carried on an F-111 has been predicted for each of the five profiles indicated previously. (The data for mission profiles and mounting conditions other than the preselected simulation profile are included in Attachment 1.) Three separate missile mounting conditions were considered:

1. Missile carried on external pylon
2. Missile carried in the weapons bay with weapons-bay doors closed
3. Missile carried in the weapons bay with weapons-bay doors open

The thermal data provided for the case of a pylon-carried missile for mission profile 3, Fig. 3-6, consisted of adiabatic wall temperatures, T_{aw}, and heat transfer coefficients, h, Fig. 3-7 and 3-8.

Heat transfer coefficients which are functions of the missile surface geometry and running length aft of the leading edge, were provided for three separate locations on the surface of the missile. These locations, as indicated in Fig. 3-9 have significance relative to the following internal equipment of the instrumented missile:

Position 1 - Approximate center of on-board recording and electrical conditioning equipment. Located 54.6 inches aft of leading edge.

Position 2 - Forward section of rocket-motor propellant. Located 75.5 inches aft of leading edge.

Position 3 - Aft section of rocket-motor propellant. Located 92.5 inches aft of leading edge.

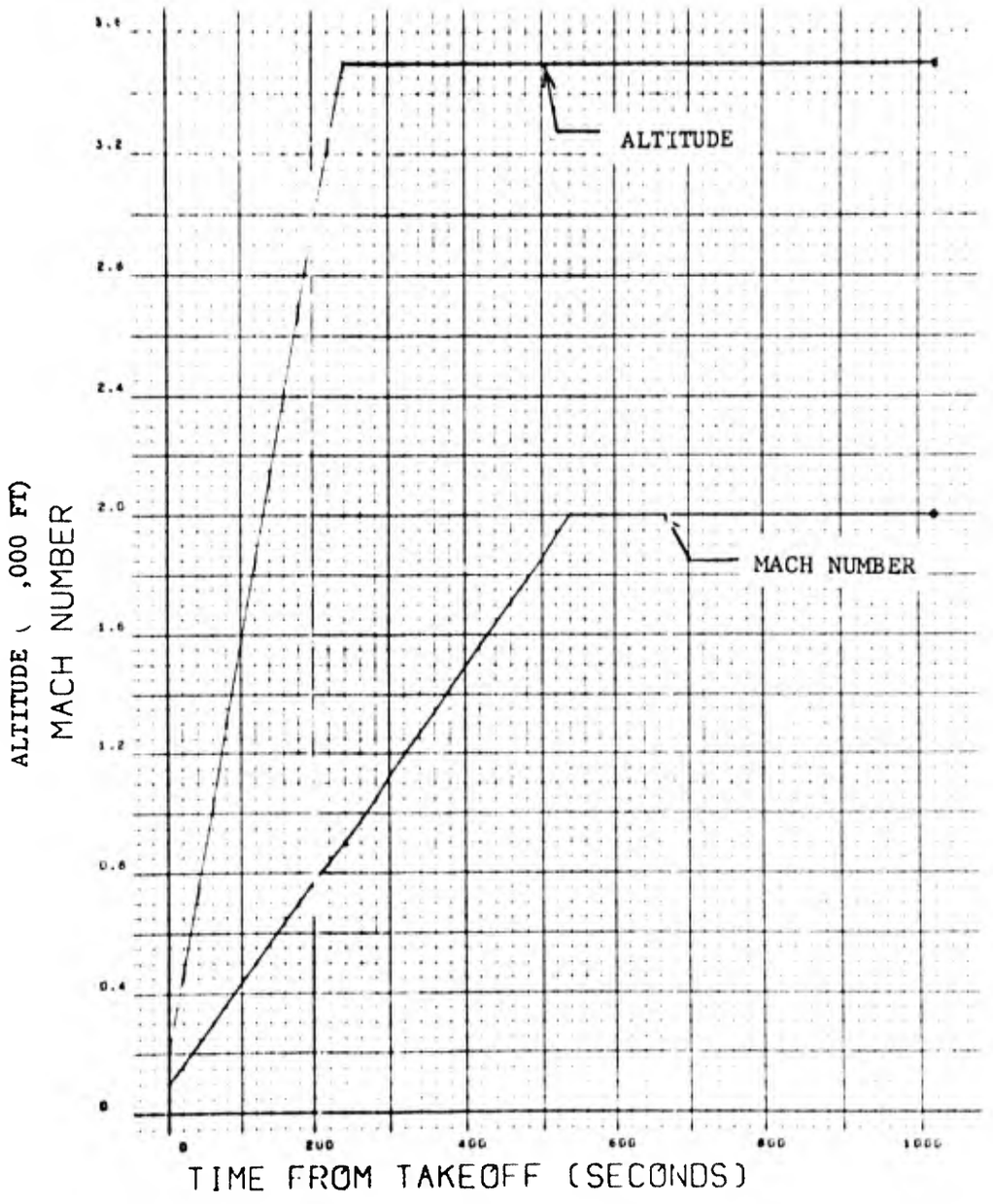

Figure 3-6. Altitude and Free Stream Mach Number for Mission Profile No. 3

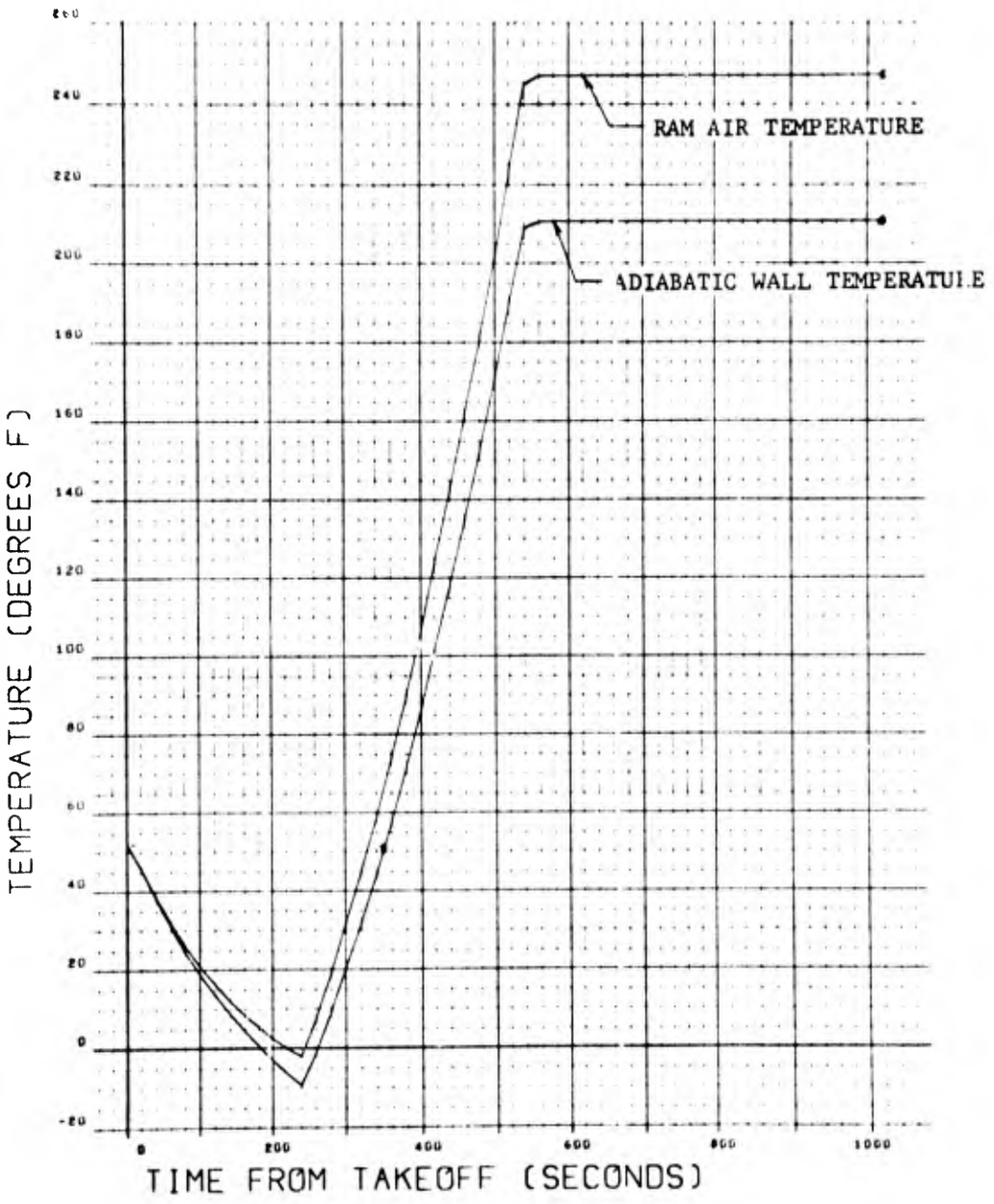

Figure 3-7. Ram Air and Adiabatic Wall Temperatures for a Pylon Mounted Store; Mission Profile No. 3

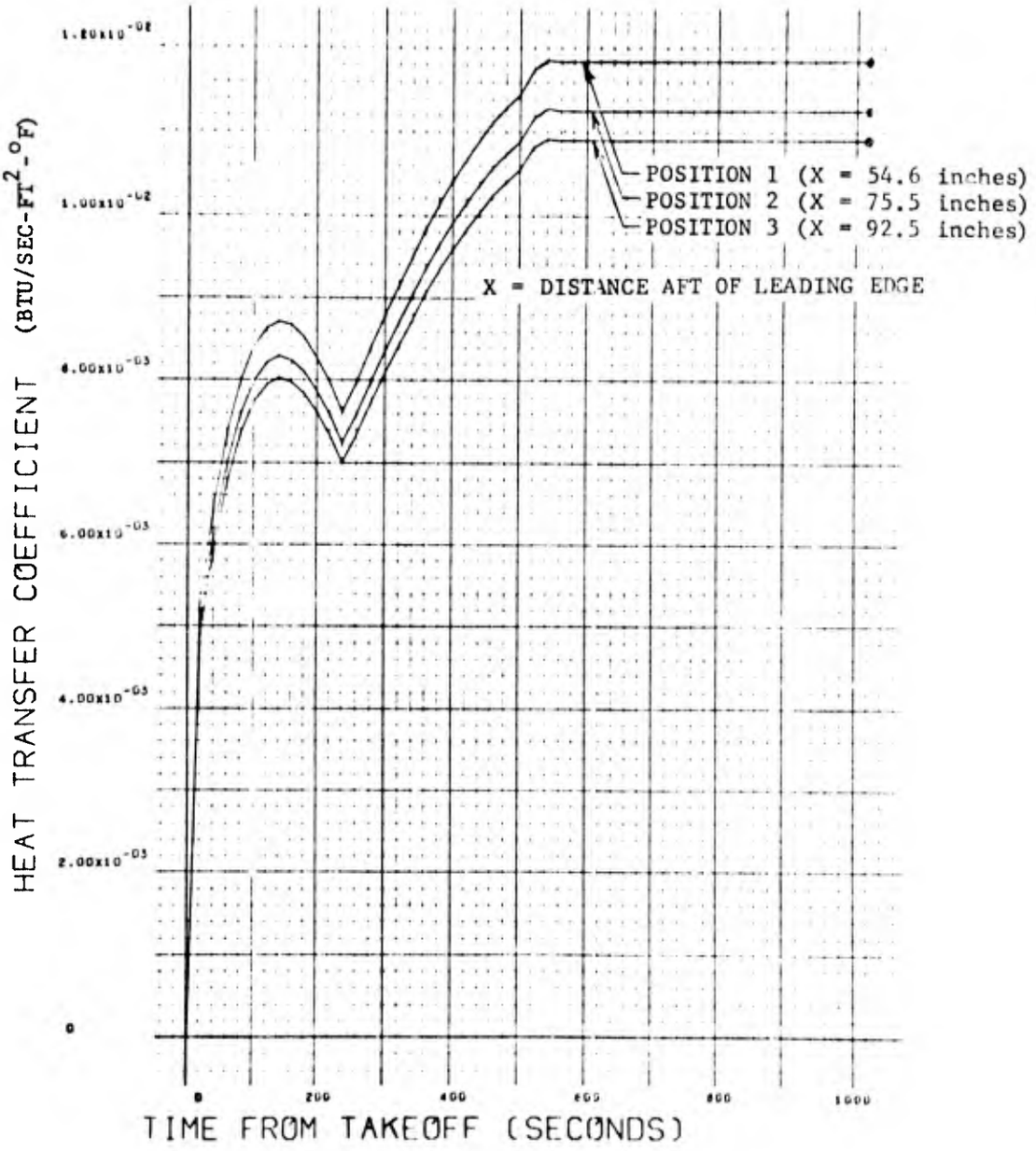

Figure 3-8. Heat Transfer Coefficients for a Pylon Mounted Store; Mission Profile No. 3

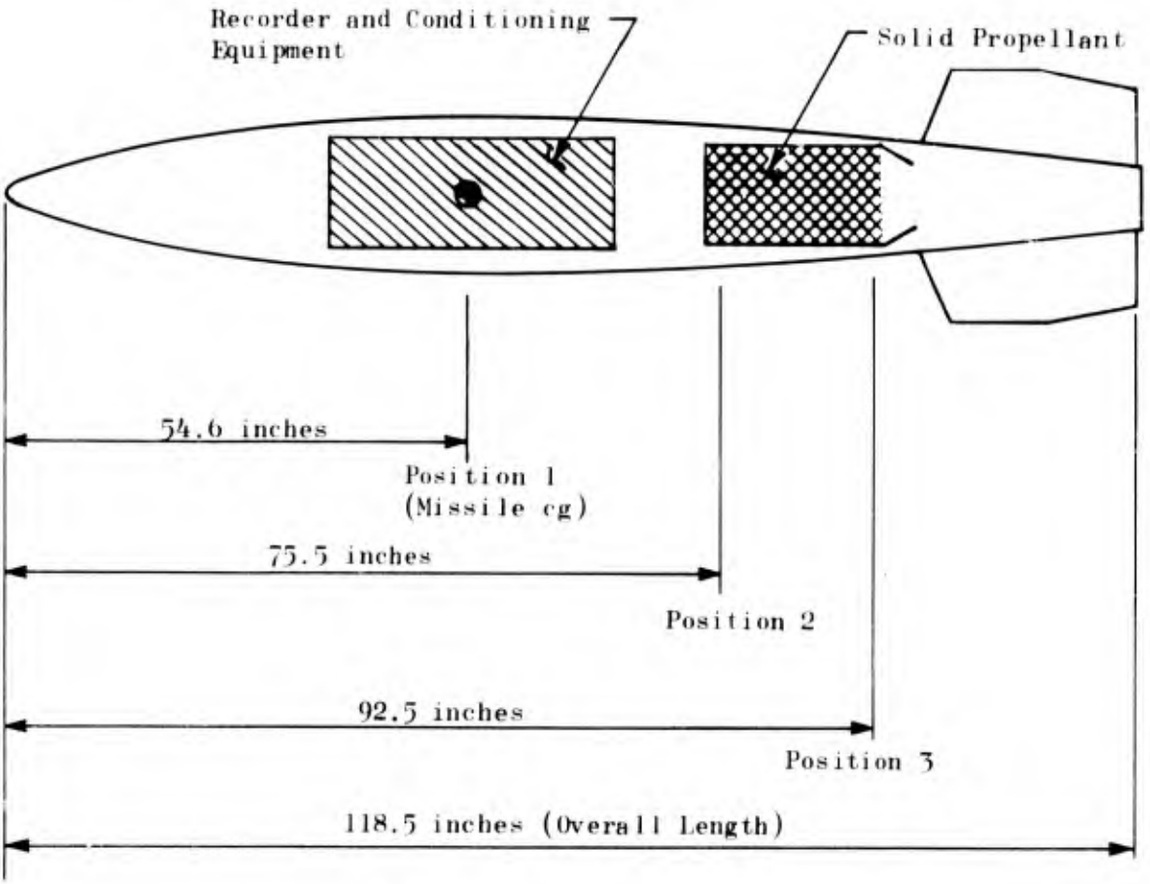

Figure 3-9. Points at which Heat Transfer Coefficients Were Determined

In addition, the unit Reynolds number (Re per foot) (Fig. 3-10), used in computing the heat transfer coefficient and the free stream stagnation air temperature (ram air temperature) has been provided.

The thermal simulation profile was generated using data for a position over the rocket-propellant section. This information is presented in the following section.

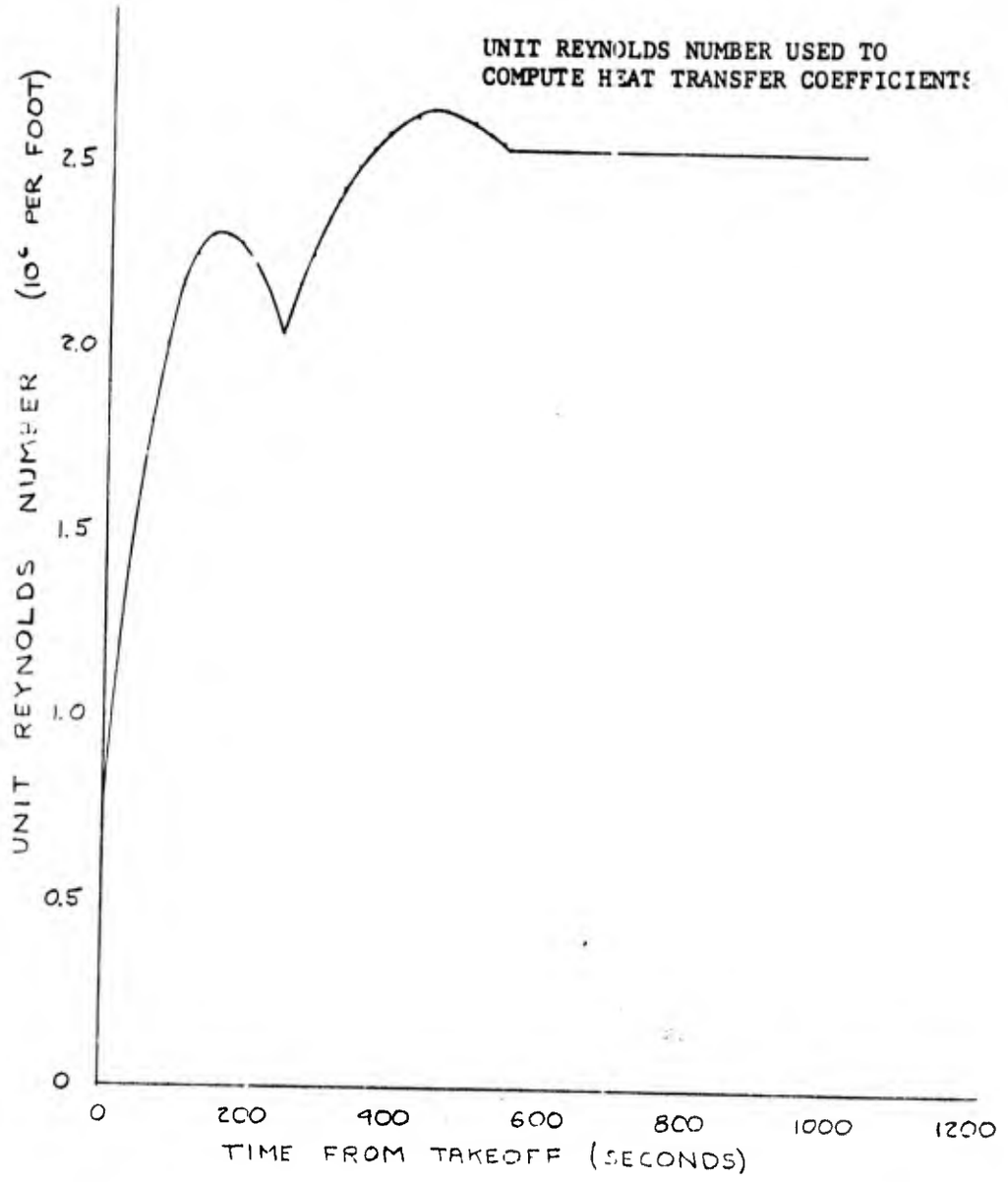

Figure 3-10. Unit Reynolds Number for a Pylon Mounted Store; Mission Profile No. 3

4. PHASE II - TEST SIMULATION

Phase II of the program consisted of defining the input levels of environmental vibration and aeroheat to be used during the pre-flight BDU checkout at Rocketdyne. These input requirements were based on the predicted environments supplied by GD during Phase I. The remainder of Phase II was devoted to designing and fabricating the required test equipment and conducting the actual test cycles that constituted the pre-flight BDU checkout.

DEFINITION OF ENVIRONMENT

Two test environments were established for the pre-flight checkout conducted at Rocketdyne. The first, vibration, input levels were defined after GD completed their vibration predictions for the test vehicle. Although the exact static vibration environment for the propellant section of the BDU is not known, the test simulation starting point was to encompass the flight prediction envelope supplied by GD for each axis of test. Figures 4-1 and -2 show the predicted envelopes for the vertical and lateral vibration axes and input spectra used in the subsequent random vibration test series.

The second environment, aeroheat, was more easily analyzed. A finite-element-type thermal analysis, programmed for the IBM 360-65, was used. This is a one-dimensional axisymmetric program that uses varying thermal properties with temperature and varying boundary conditions with time.

The first step was to determine case temperature due to aeroheating. Using the adiabatic wall temperature shown in Fig. 3-7, the heat transfer

coefficient in Fig. 3-8 corrected for the proper location on the case, and the following grain thermal data:

Temperature, deg F	70
Thermal Conductivity, k, Btu/ft/deg F-hr	0.57
Specific Heat, C, Btu/lb-deg F	0.32
Density, ρ, lb/cu in.	0.0634

the resulting case temperature, shown in Fig. 4-3 was derived. The analysis predicted that case temperature should reach a high of 190 F and a low of 28 F. Calculated case temperature for the motor enclosure is shown in Fig. 4-4. Since simulation tests were initiated at ambient temperature, it was not necessary to cool the motor. Therefore, aeroheat simulation tests could be started 420 seconds into the test (see Fig. 4-3). A 10-minute (1020 minus 420 seconds) aeroheat simulation test cycle duration was established.

During thermal analysis, the rate of temperature rise on the onboard flight recorder (magnetic tape, in particular) was deemed to merit consideration. Since the tape was limited to about 125 F, it appeared possible to induce damage, if not during flight, possibly during testing. Consequently, a thermocouple was attached to the tape recorder to monitor the temperature and a CO_2 cooling system was arranged to protect the tape during aeroheat simulation testing.

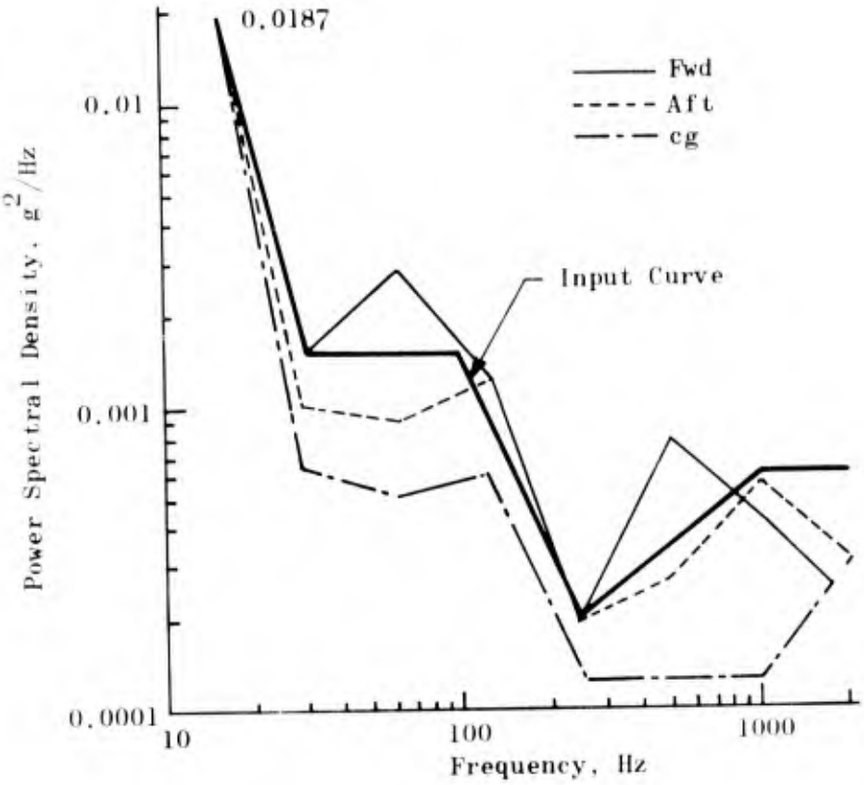

(U) Figure 4-1. Lateral Axis Data per General Dynamics

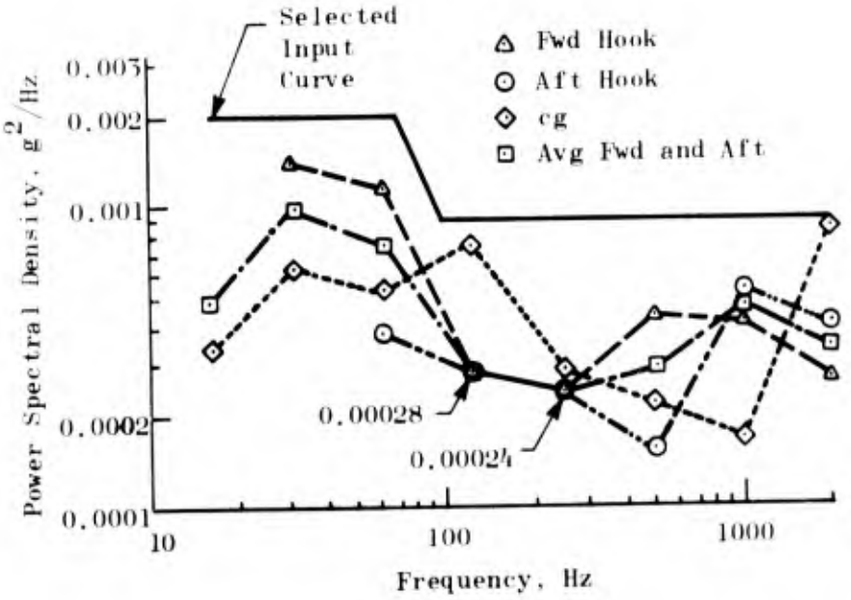

Figure 4-2. Vertical Axis, B-61 Data per GD

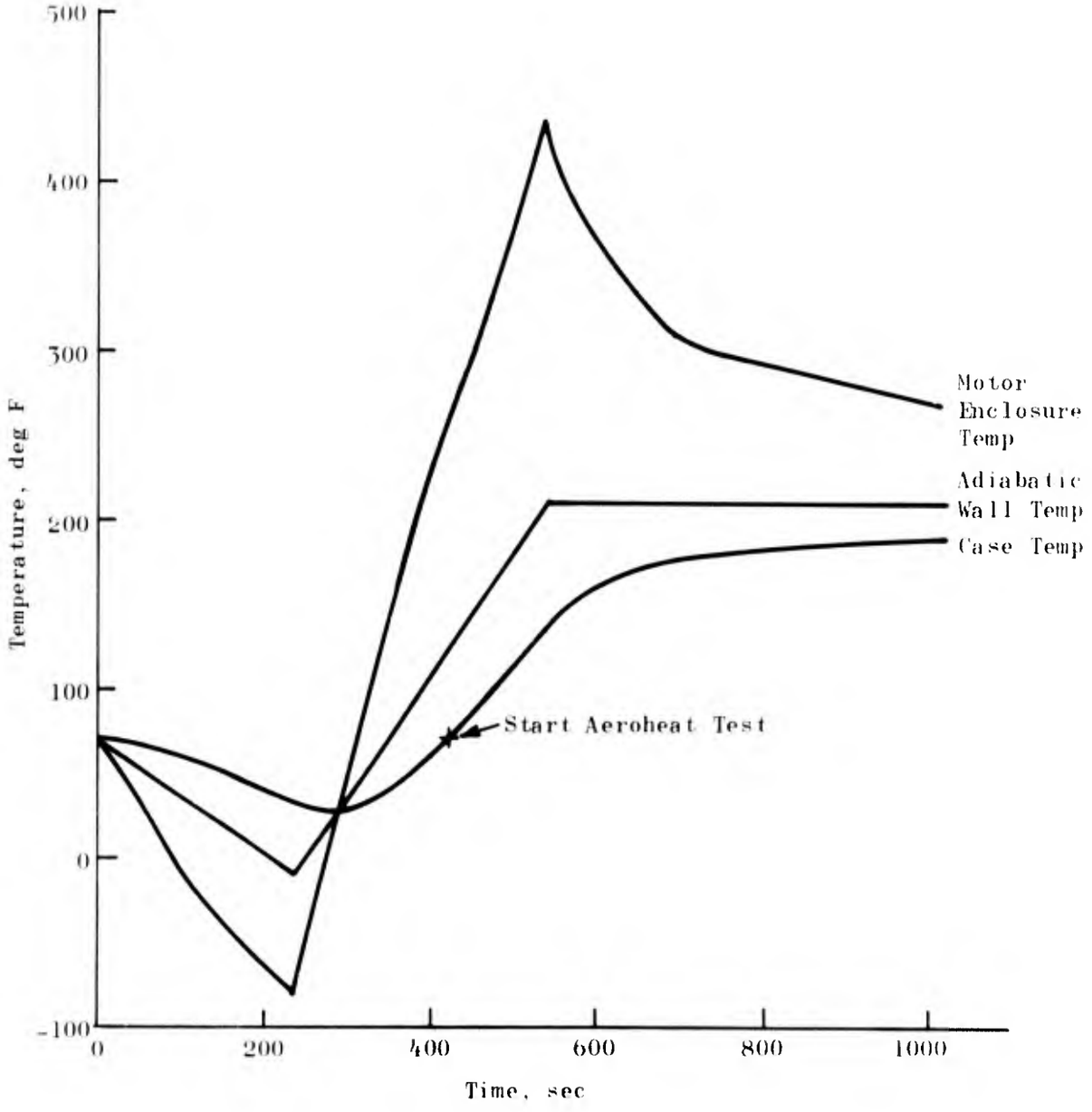

Figure 4-3. Calculated Case Temperature

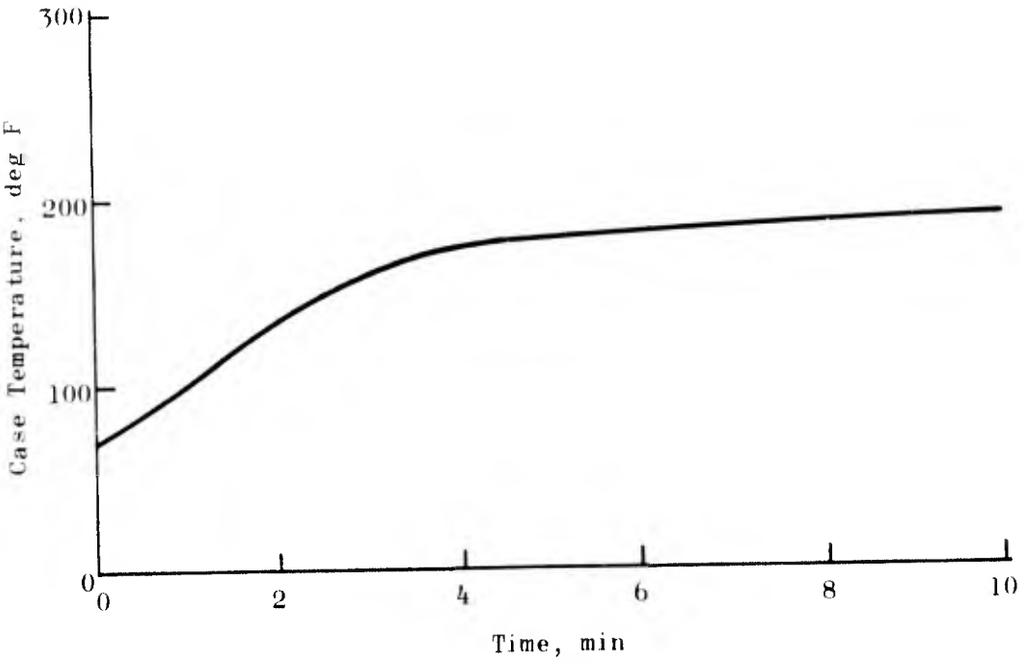

Figure 4-4. Calculated Case Temperature vs Time

TEST EQUIPMENT (TOOLING AND INSTRUMENTATION)

TOOLING

Maximum use was made of existing test tooling. The environmental test chamber from the AFRPL-sponsored Extended Environment contract was used; a new motor enclosure was the only modification required to accomplish the aeroheating tests. CONDOR vibration tooling was modified to support the BDU in a wing-support mode for the vertical axis, T_Z, Fig. 4-5 and 4-6.

The BDU was also in the wing-support mode for the transverse vibration axis, T_X (bell-ringer mode), Fig. 4-7, but the vibration input load was rotated 90 degrees from the T_Z axis.

The GFE MAU-12A/C ejector rack and BDU attachment fittings were used for the "soft" support system; while firm bolt and thread fittings into a solid welded frame replaced the ejector rack and "hook and eye" fittings on the BDU for the "hard" support system.

The motor aeroheat enclosure was tubular shaped and encapsulated the BDU with a minimal air passage between the shroud and BDU. Air entered the enclosure at the nose of the BDU and flowed down the unit through a small annular passage. A plenum chamber over the fin section enclosed the fins and served as a return outlet for the air line.

INSTRUMENTATION

The flight tape recorder held insufficient tape for continuous recording; therefore, it was operated intermittently to obtain the desired data. All channels of propellant sensors were recorded on the flight recorder. Data from selected sensors (Table 4-1) were redundantly recorded on Rocketdyne's ground test equipment during all vibration cycles. (Location of these instruments is shown in Fig. 4-8.) This

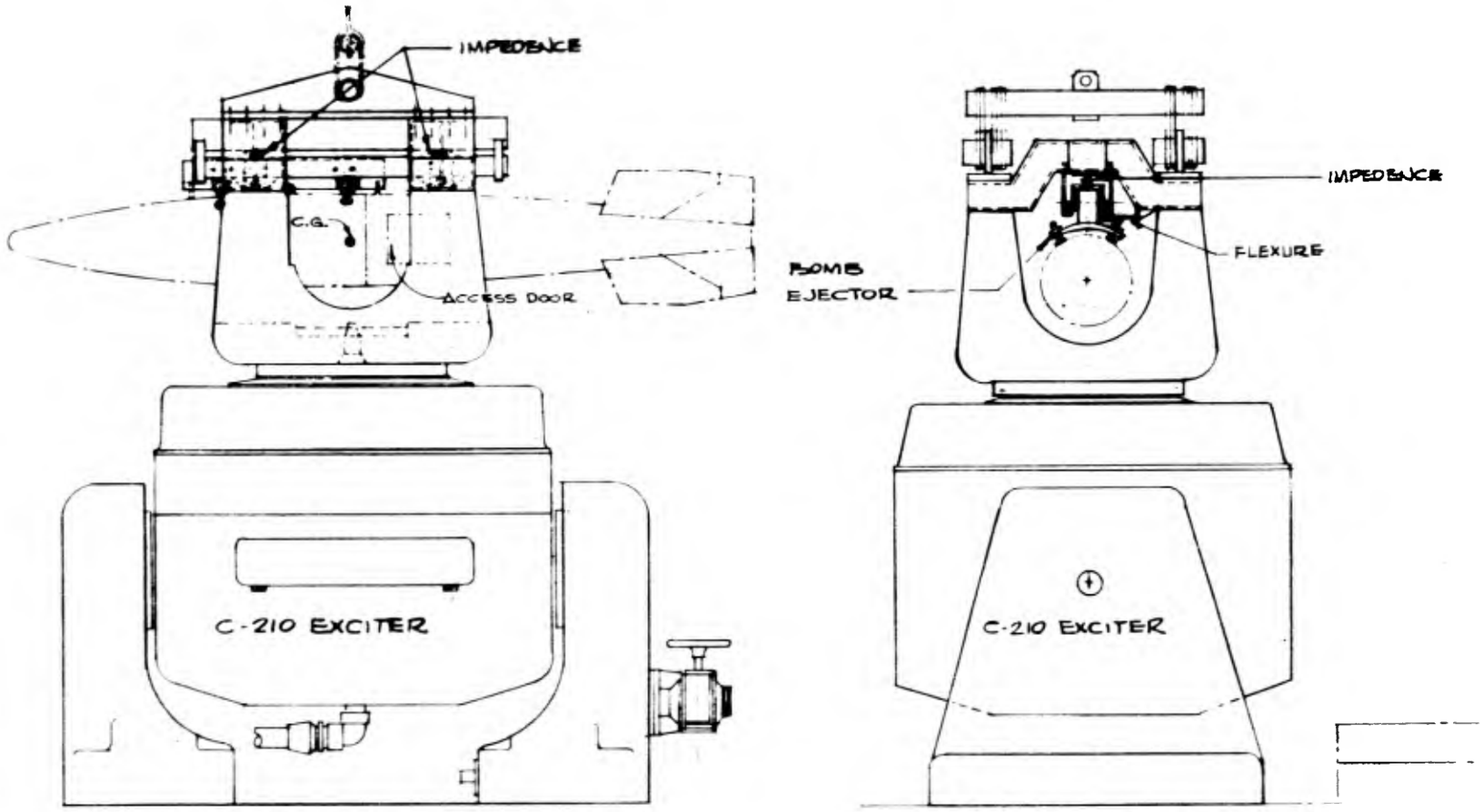

Figure 4-5. Vertical Vibration

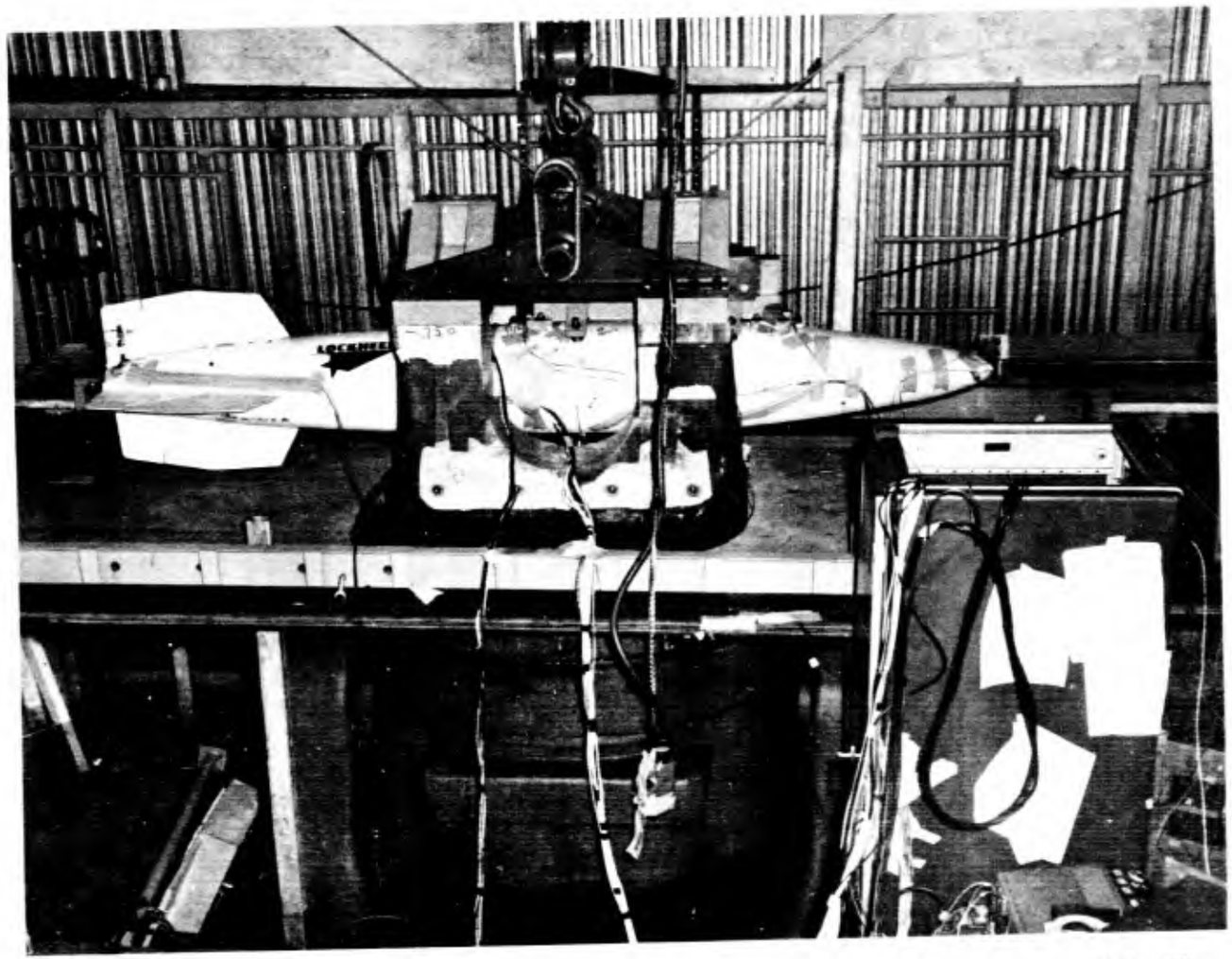

CN-2907

Figure 4-6. BDU in Vibration Fixture

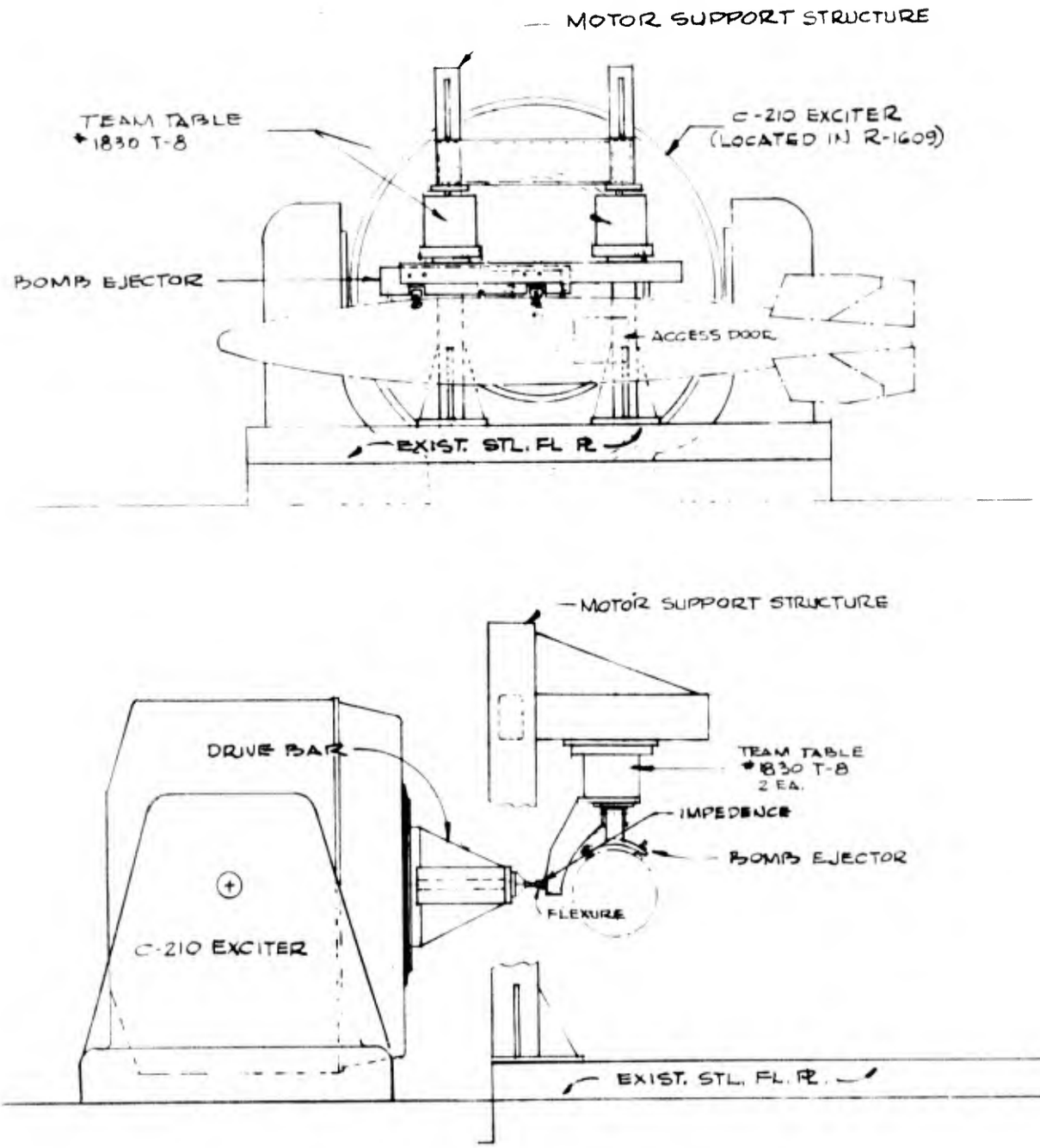

Figure 4-7. Transverse Vibration

TABLE 4-1

INSTRUMENTATION RECORD

Pin No.	Gage	Gage Major Active Axis	Adjacent Thermistor	Axis	
				Z	X
1 and 2	Stress #18	Z	5	X	X
5 and 6	Stress #22	Z	1	X	
7 and 8	Stress #23	X	6	X	X
11 and 12	Stress #26	X	2		X
16 and 17	Strain #17 (SWRI)	Hoop	15	X	X
18 and 19	Strain #17 (Clip)	Hoop	15	X	X
22 and 23	Strain A (Case) (Delete Requirement)	Hoop	--		
25 and 26	Shear #101 (Semi-conductor)	X	11		X
27 and 26	Shear #SH-2 (Semi-conductor)	Z	10	X	X
29 and 30	Shear #120A	Z	12	X	X
31 and 32	Shear #120B	X	13	X	X
33 and 34	Accelerometer (Propellant)	Y_2	--	X	X
36 and 52	Strain #1 (Lug #1 Fwd)		--	X	X
37 and 52	Strain #2 (Lug #2 Aft)		--	X	X
38 and 52	Strain #2B (Lug #2 Aft)		--	X	X
39 and 52	Accelerometer (cg)	X	--	X	X
40 and 52	Accelerometer (cg) Triaxial	Y	--	X	X
41 and 52	Accelerometer (cg)	Z	--	X	X
45 and 46	Accelerometer (Aft End)	X	--	X	X
47 and 48	Accelerometer (Aft End) Triaxial	Y	--	X	X
49 and 50	Accelerometer (Aft End)	Z	--	X	X
42 and 52	Accelerometer (Lug #1)	Z	--	X	X
43 and 52	Accelerometer (Lug #2)	Z	--	X	X
3 and 4	Stress #21	X	3		*B-up
9 and 10	Stress #24	Z	2	*B-up	
14 and 15	Strain #16 (SWRI) (Do not record)		15		
20 and 21	Strain #2 (Clip)	Hoop	15	XQ	X

*B-up: Recorded but data not reduced

Temperature outputs taken from the PAM system, decoded, and then recorded by Rocketdyne:

Thermistors:

(a) Adjacent to other gages:

#1, #2, #5, #6, #10, #11, #12, #13, and #15.

(b) Propellant grain profile:

#18, #19, #20, #21, and #23.

Thermocouples:

6 case

Additional temperature outputs recorded by Rocketdyne:

Thermistors:

#16 - Forward face of grain
#17 - Forward face of grain
A - Case thermistor (propellant/case)
B - Case thermistor (propellant/case)
D - Case thermistor (propellant/case)

Thermocouples: 15 total

3 in tail section
7 in fore body section
1 in electronic package
4 locations to be defined later

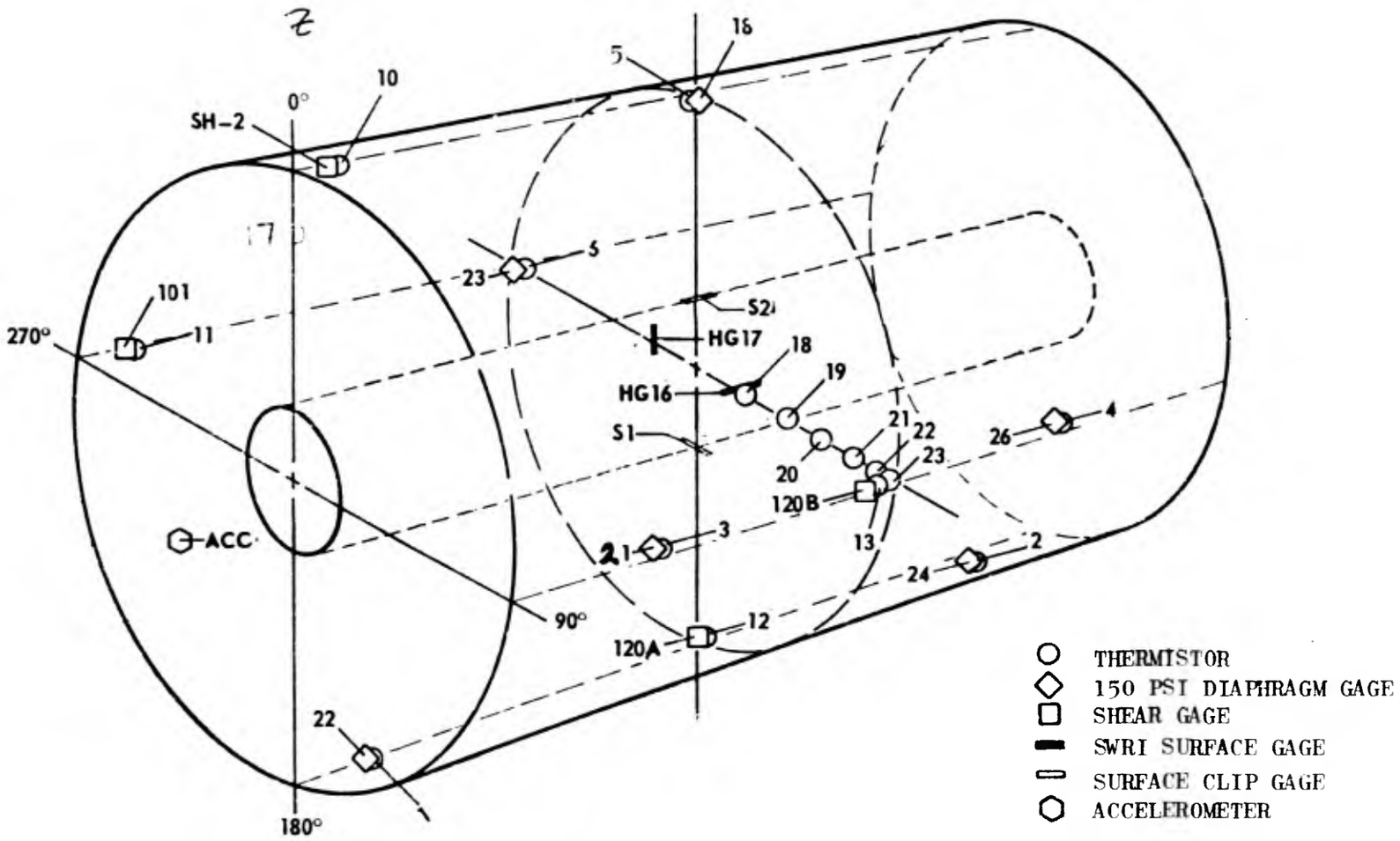

Figure 4-8. Propellant Gage Location

parallel recording was as independent of the flight equipment as possible to provide as complete redundancy as could be achieved while using the same sensor. In addition to the BDU propellant gages, accelerometers were installed for definition of total test vehicle response.

Ground instrumentation tie-in points were directly on the output of the sensor on all strain gages and directly on the output of the charge amplifiers of crystal accelerometers. It was believed that switching transients from the commutator used on the temperature sensors would make it inadvisable to parallel record from these units; therefore temperature stations recorded on ground station equipment were derived from a de-com unit furnished by NWC.

Since the test specimen is an inert unit, the connecting instrumentation cables for all gages, thermistors, and internal thermocouples were less than 20 feet long. The instrument take-off point, signal conditioning, and recording equipment are shown in Fig. 4-9.

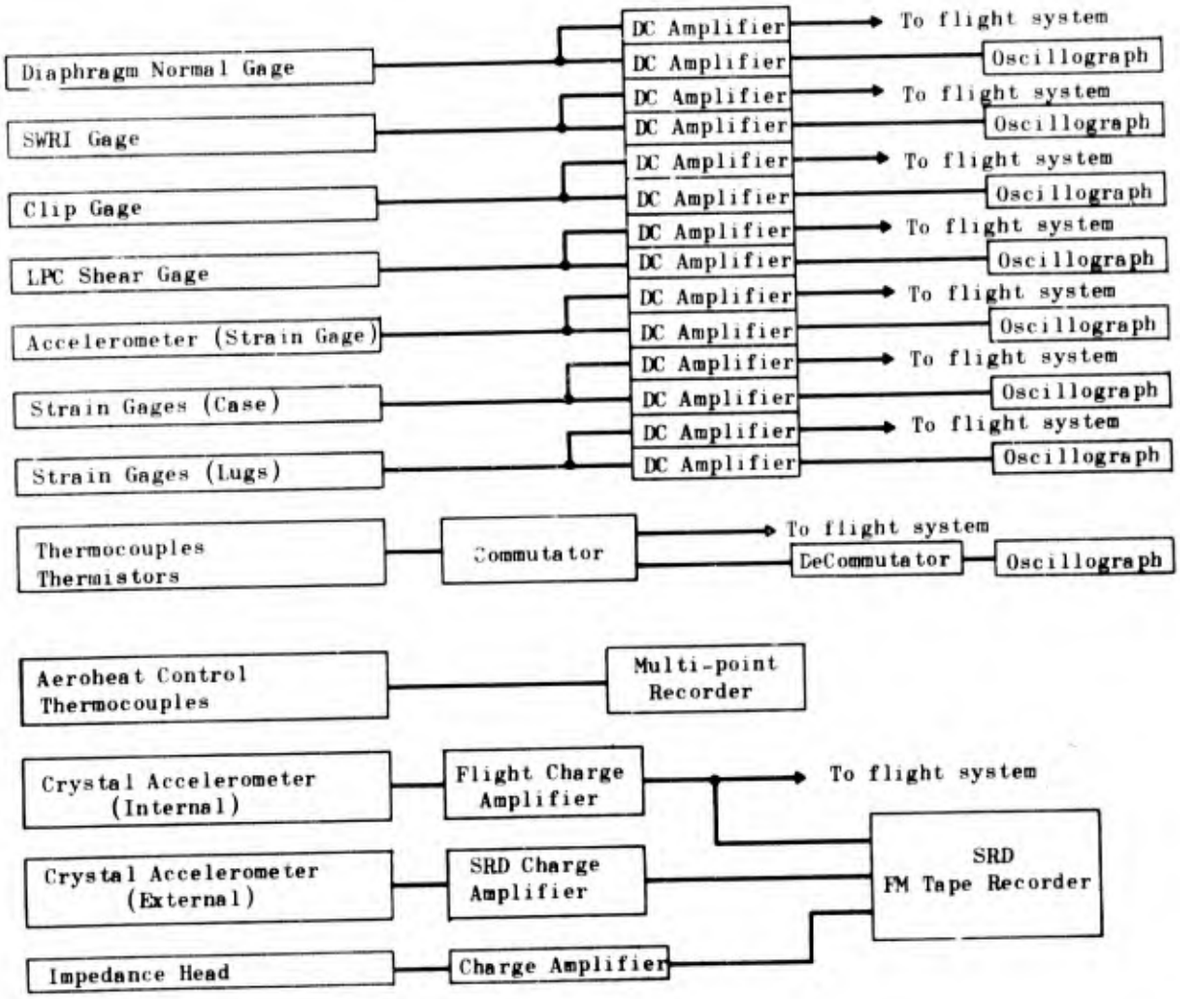

Figure 4-9. Recording Equipment Layout

TEST SEQUENCE

A preliminary test plan was established and approved before testing was begun. However, flexibility was maintained to ensure the ability to change the plan as requirements were changed during the program. One such change resulted in the recording of data from the instrumented launcher and in repeating the sine vibration test cycles. The final test plan is discussed in the following paragraphs with a brief discussion of each test cycle and data recorded during the cycle. Interpretation of the data is presented in Section 5 of this report.

TEST PLAN

The test plan was based on the work statement requirements for sinusoidal and random vibration in two transverse axes, combined aeroheat and random vibration in two transverse axes, and aeroheating only in one axis. Random vibration and aeroheat requirements were based on the flight prediction environments.

Other prerequisites used in developing the testing sequence were: (1) minimize number of difficult and hazardous BDU handling operations, (2) delay the aeroheating cycles until last, and (3) provide maximum possibility of data gathering at both ground and flight recording stations. Minimal handling of the BDU reduced the chances of damaging instrumentation. By holding all aeroheat cycles until near the end of the checkout test cycle, the maximum data were obtained before the BDU was subjected to potential heating damage. The actual sequence of tests were as follows.

1. Initial Functional Checks
   a. Pressure check 10 and 20 psig
   b. Thermal check
      (1) 70 F stability
      (2) 20 F stability check
      (3) 20--100 F gradient and stability check

c. Low level vibration instrument and recording system check, hard-mount Z axis with impedance head.

2. Z Axis (Vertical)

a. Hard-mount sine sweep vibration with impedance head

(1) Calibrate system

(2) Perform 10 to 2000 Hz sinusoidal survey

(3) Make X-Y plots of all specified channels

(4) Process oscillograph records

b. Hard-mount random vibration with impedance head

(1) Multiple random vibrations with increasing power input were run until either the impedance head load limit was reached or the required random vibration level was achieved. If the impedance head limit was reached first the impedance heads were to have been replaced with steel blocks. The impedance head load limit (5000 pounds max) was not reached during this test step; therefore, the impedance heads were used in all vibration tests.

(2) Reload flight recorder

(3) Perform random vibration

(4) Make PSD plots as specified

(5) Process oscillograph records

c. Replace hard-mount with launcher and reload flight recorder

d. Soft-mount sine vibration with impedance heads

(1) Calibrate system

(2) Perform 10 to 2000 Hz sinusoidal survey

(3) Make X-Y plots of all specified channels

3. X Axis

a. Soft-mount sine sweep vibration with impedance heads

(1) Calibrate system

(2) Perform 10 to 2000 Hz sinusoidal survey

(3) Make X-Y plots of specified data channels

b. Replace launcher with hard back and reload flight recorder

c. Hard-mount sine sweep vibration with impedance heads

(1) Calibrate system

(2) Perform 10 to 2000 Hz sinusoidal survey

(3) Make X-Y plots of specified data channels and process oscillograph records

d. Hard-mount with impedance heads (random)

(1) Perform random vibration

(2) Make PSD plots as specified

(3) Process oscillograph records

(4) Continue making any X-Y plots from previous tests as specified

(5) Reload flight recorder

4. Thermal soak unit for flight recorder system checkout

5. Instrument sway braces and lugs

6. Thermal calibration

7. Static load calibrate Z, X, and Y axes

8. X Axis

a. Calibrate system

b. Perform 10 to 2000 Hz sinusoidal survey

c. Make X-Y plots of specified channels and process oscillograph record

d. Set up and conduct aeroheat only

(1) Record temperature vs time as specified

(2) Reload flight recorder

e. Soft-mount with impedance heads

(1) Perform random vibration in conjunction with aeroheat

(2) Process oscillograph records

(3) Make PSD plots as specified

(4) Reload flight recorder

9. Z Axis (Vertical)

a. Calibrate system

b. Perform 10 to 2000 Hz sinusoidal survey

c. Make X-Y plots of specified channels and process oscillograph record

d. Soft-mount with impedance heads

(1) Perform random vibration in conjunction with aeroheat

(2) Process oscillograph records

(3) Make PSD plots as specified

10. Ship BDU to AFRPL for flight test preparation

TEST CYCLES, DATA, AND DISCUSSION

FUNCTIONAL CHECKS

The initial tests were conducted to perform three types of functional checks on the instrumentation. The first was to record the response of the instruments to existing internal pressure, 10 psig, then to 20 psig and compare the two sets of data. The second check was to record selected responses to three different temperature levels, 20, 75, and 100 F. The third test was conducted on the vibrator to verify that the instruments and recording system were functioning.

Pressure Check. Static pressure was not checked because of a low-level pressure leak around the bulkhead electrical connectors. As a substitute, pressure was held at 10 and 20 psig by regulating the pressure source. Resulting data are shown in Tables 4-2 and -3.

TABLE 4-2

PRESSURE CHECK AT 20 F UNIT TEMPERATURE

Gage No.	Gage Readings, mv		
	0 psig	10 psig	20 psig
Stress #18	- 46	- 38	- 28
Stress #21	- 4	+ 4	+ 12
Stress #22	- 20	- 11	- 1
Stress #23	- 35	- 27	- 19
Stress #24	+ 23	+ 14	+ 6
Stress #26	- 7	+ 1	+ 9
Strain #17	- 22	- 22	- 22
Strain #1	+ 13	+ 12	+ 12
Strain #2	+ 75	+ 73	+ 72
Shear #101	+109	+109	+112
Shear #SH-2	+158	+161	+169
Shear #120A	- 6	- 8	- 8
Shear #120B	+ 1	0	0

TABLE 4-3

PRESSURE CHECK AT 75 F UNIT TEMPERATURE

Gage No.	Gage Readings, mv		
	0 psig	10 psig	20 psig
Stress #18	- 30	- 19	- 9
Stress #21	- 5	+ 4	+ 13
Stress #22	- 13	- 3	+ 7
Stress #23	- 23	- 14	- 4
Stress #24	+ 8	0	- 9
Stress #26	- 5	+ 4	+ 13
Strain #17	- 17	- 17	- 16
Strain #1	- 4	- 4	- 3
Strain #2	+127	+125	+124
Shear #101	+ 46	+ 48	+ 50
Shear #SH-2	+ 64	+ 71	+ 77
Shear #120A	- 1	- 2	- 3
Shear #120B	- 7	- 6	- 5

Thermal Check. A static pressure thermal check was not made because of the existing pressure leak. However, pressure and thermal conditions were checked. Resulting calibration and gage response data are shown in Fig. 4-10. A gradient check verified pin connector nomenclature and gage locations.

Z Axis (Vertical)

One of the initial concerns was transmissibility and control of the BDU during vibration with what was thought to be a very soft mounting system when using the MAU-12A/C launcher. For this reason a hard mounting system was included in the test program. The first vibration test was with the hard mounting system.

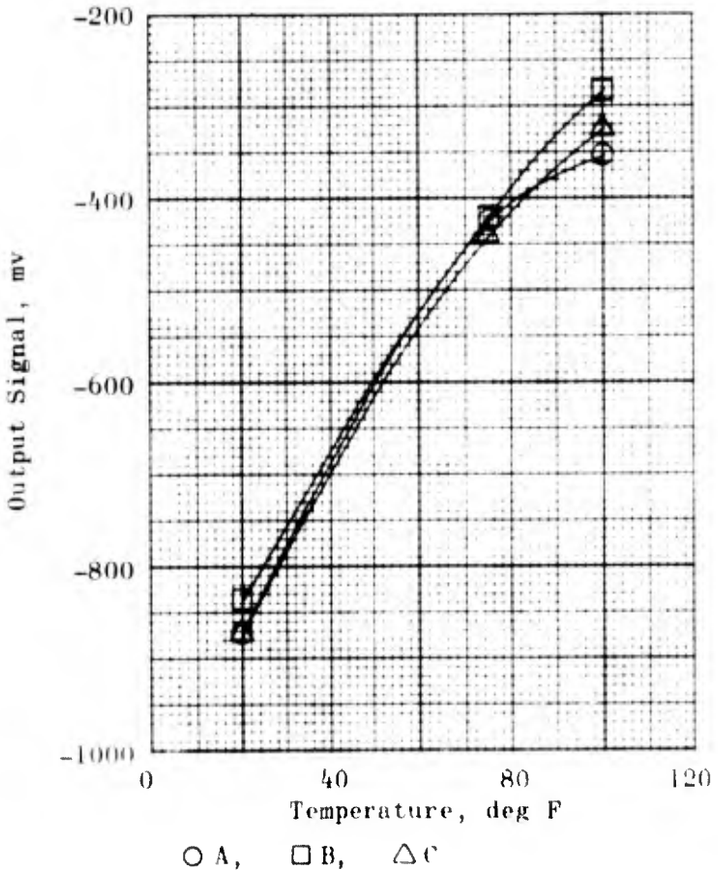

Figure 4-10. Thermistor Data from Propellant Grain

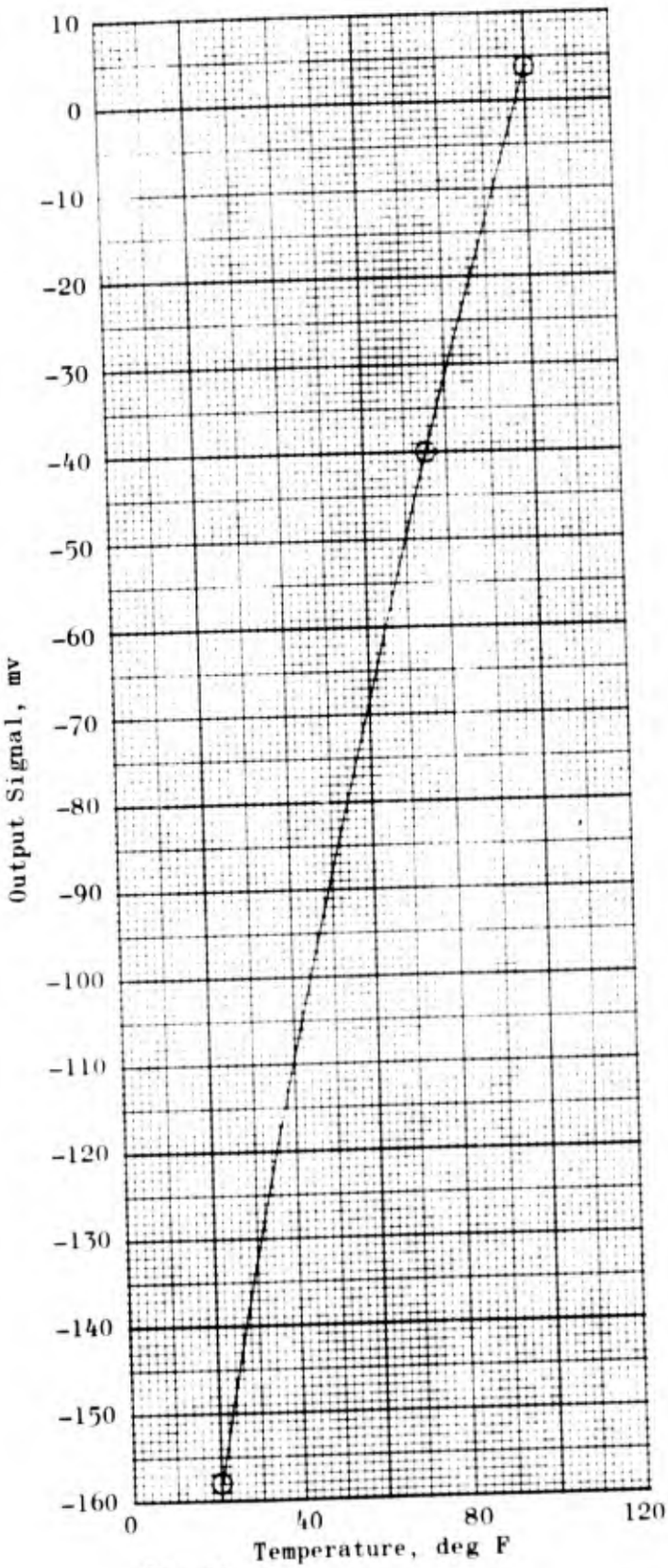

Figure 4-10. Continued

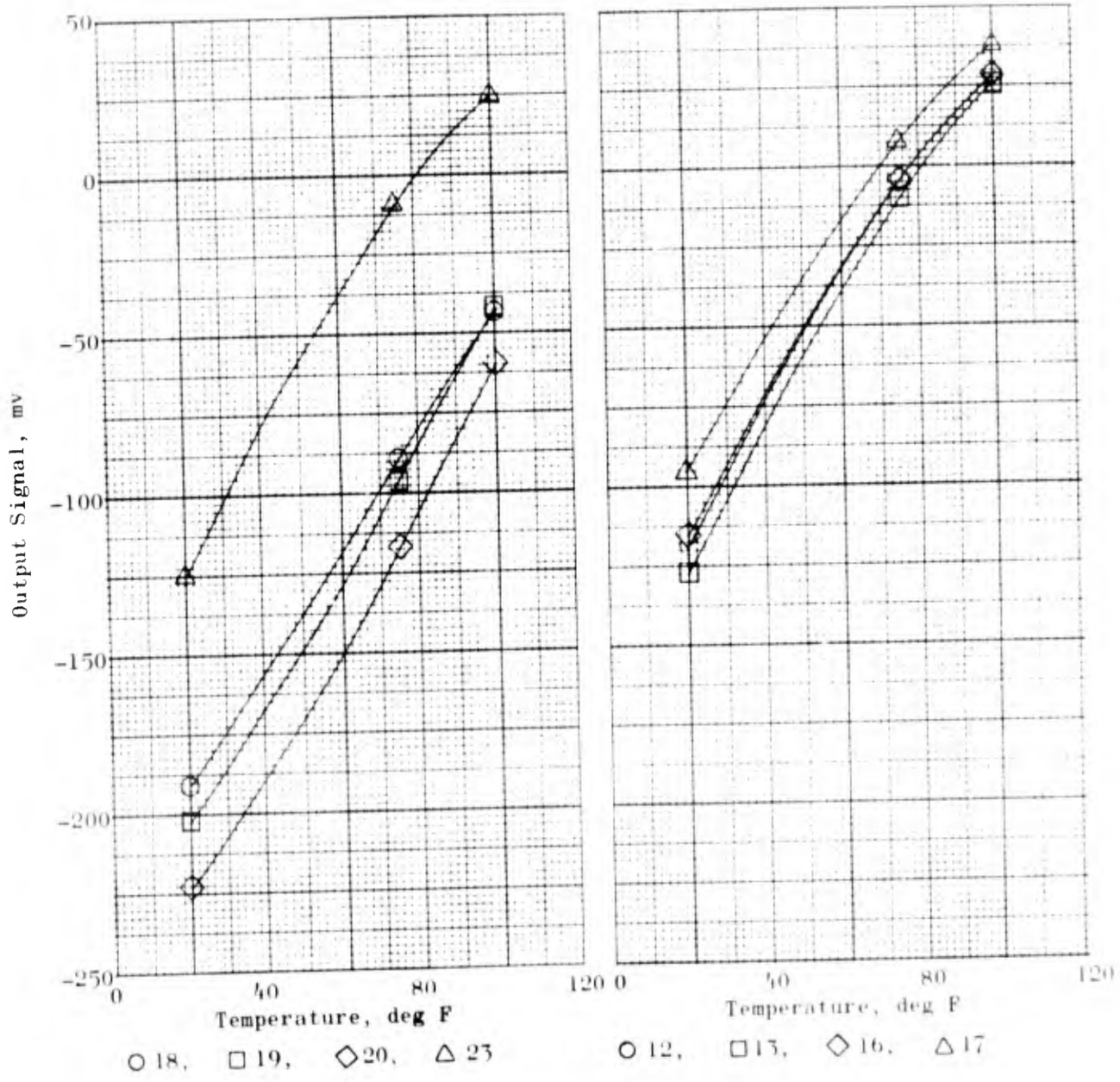

Figure 4-10. Continued

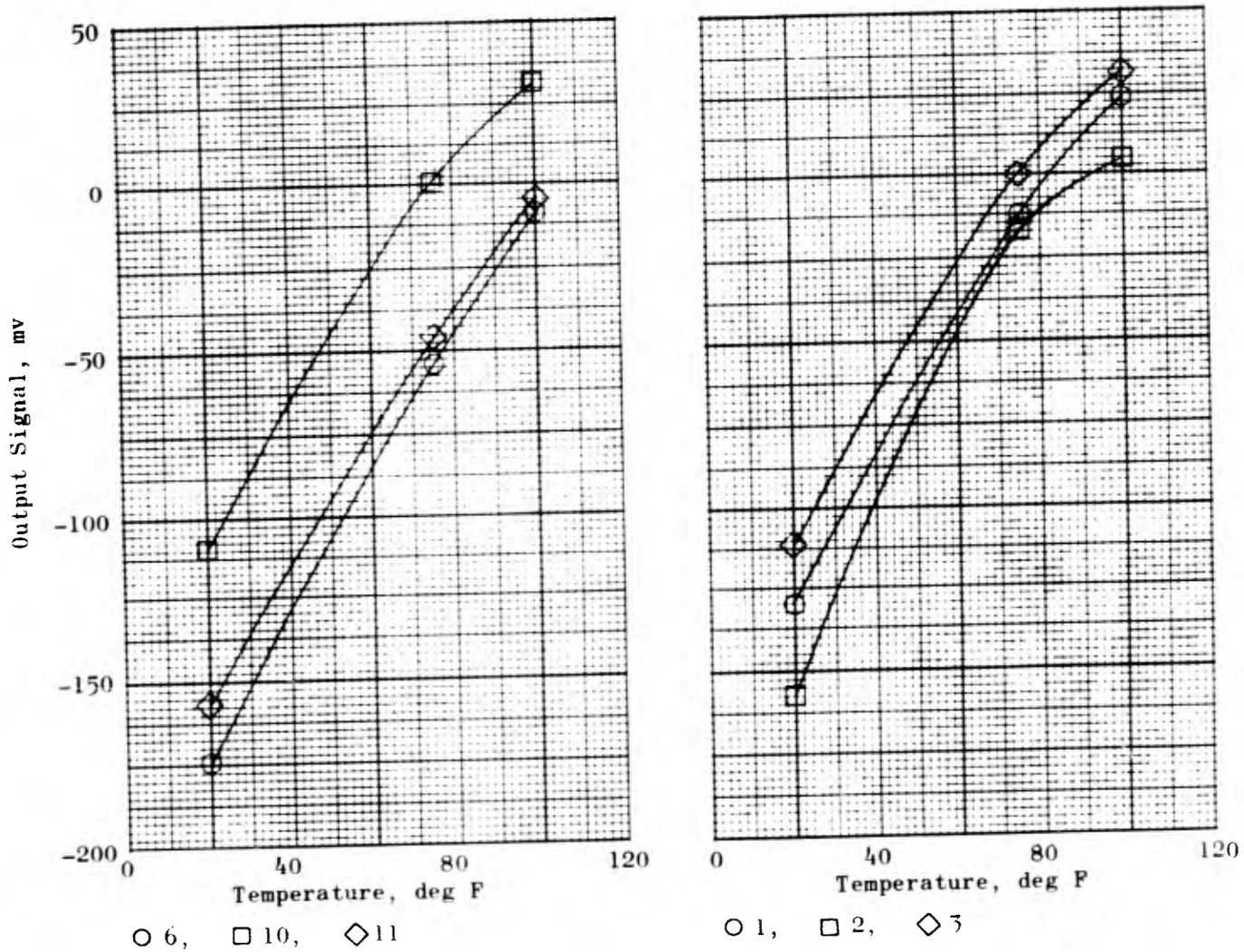

Figure 4-10. Continued

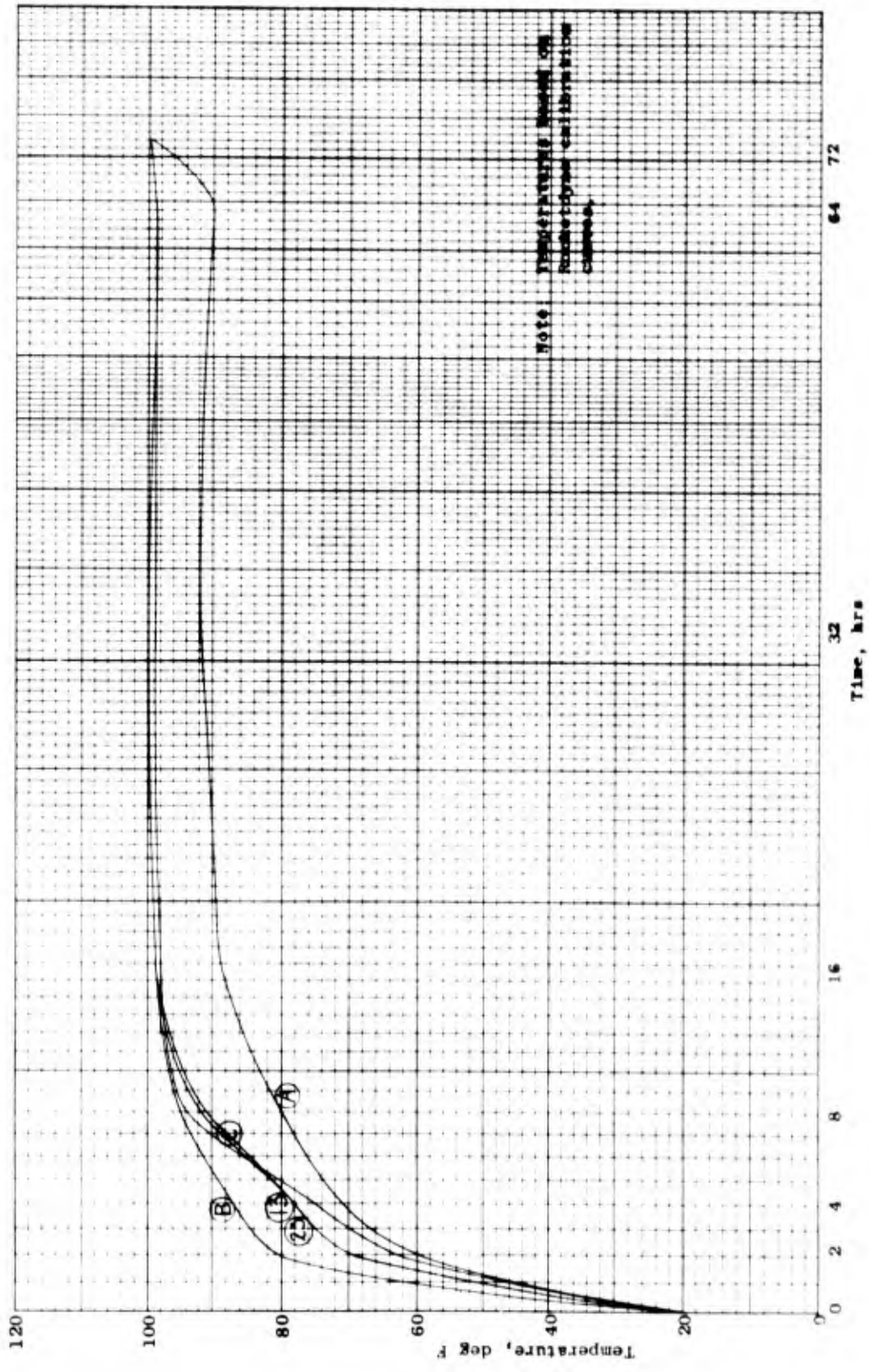

Figure 4-10. Continued

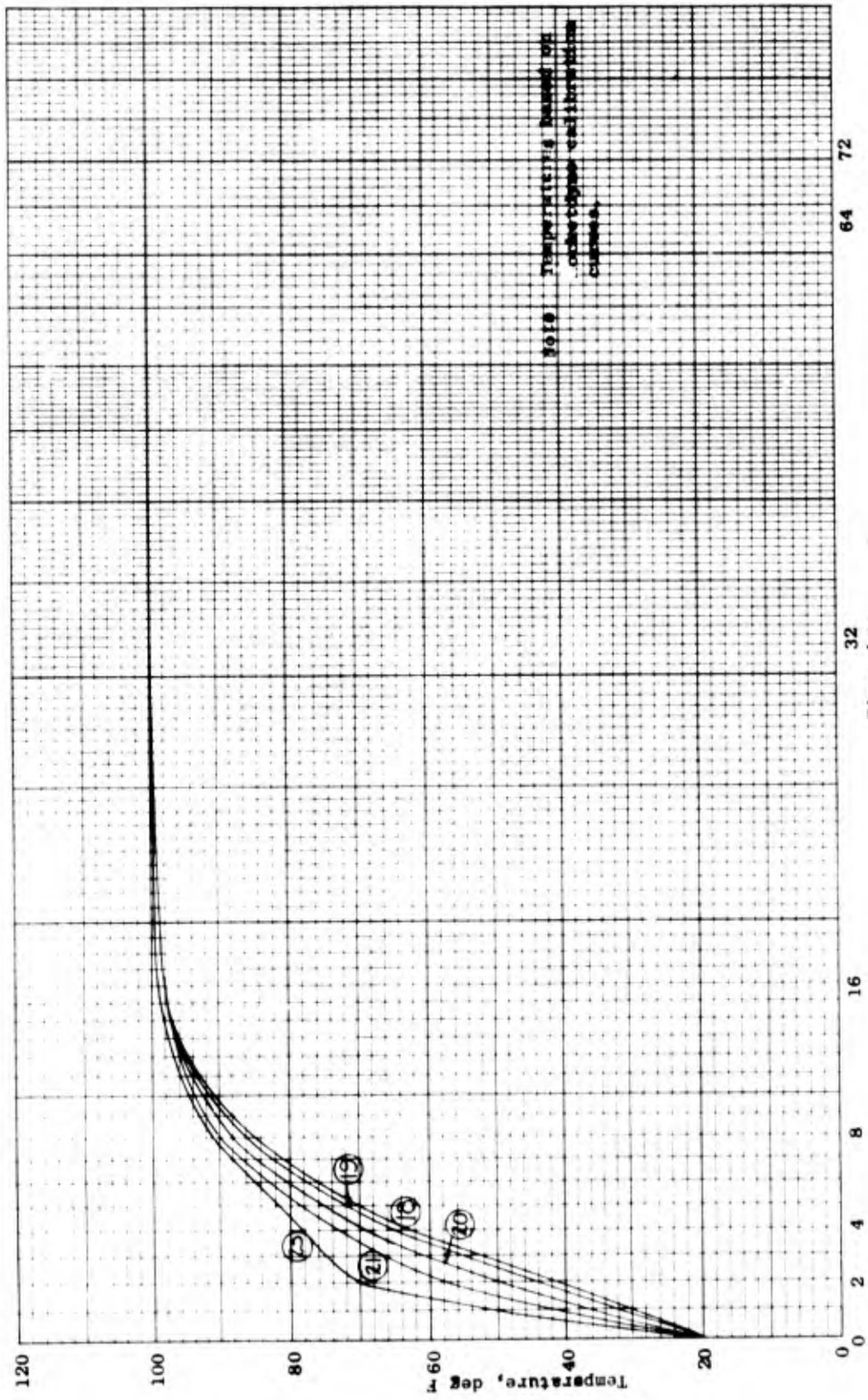

Figure 4-10. Continued

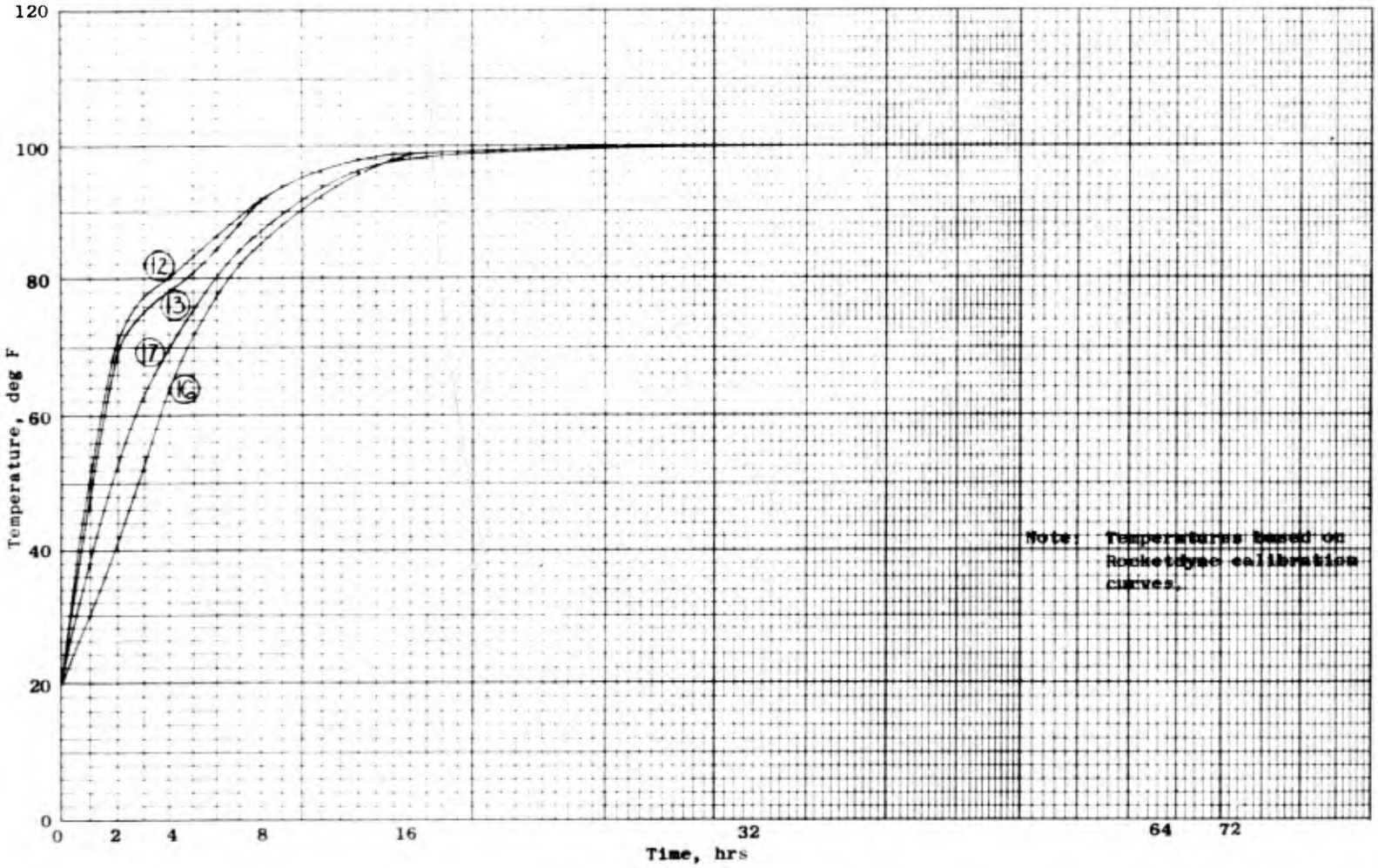

Figure 4-10. Continued

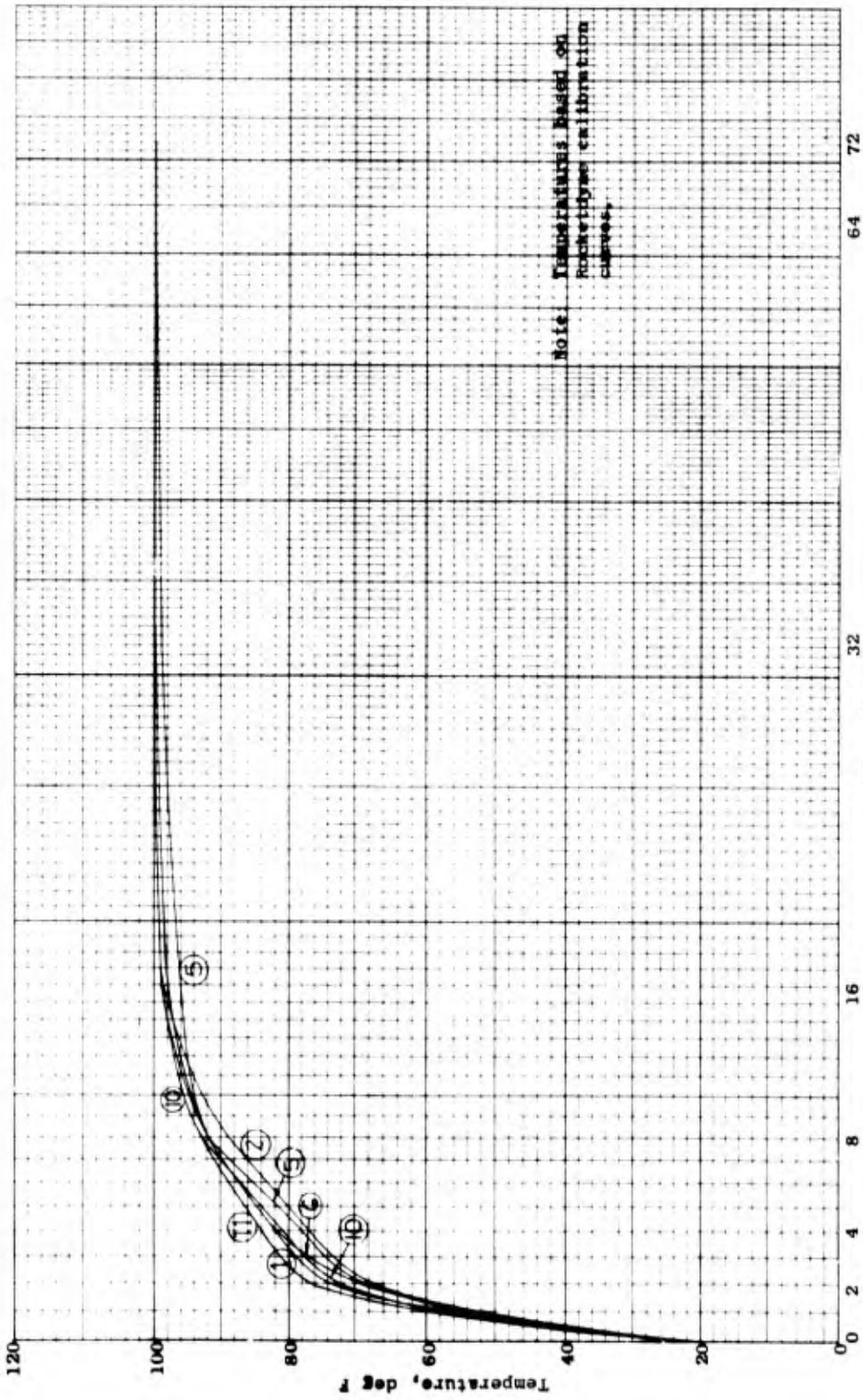

Figure 4-10. Continued

Besides the instrumentation shown earlier in the propellant grain section, additional accelerometers, Fig. 4-11, were placed on the unit to define the vibration mode(s) of the total test vehicle. These accelerometer locations were maintained for all vibration tests in the Z axis.

Hard-Mount Sine Sweep with Impedance Head, 30 June 1971. A 1-g input level was maintained during the sweep from 10 to 2000 Hz at 0.63 octaves/minute. Accelerometer channels 5 and 8 were used as dual controls during the sweep. Replots of these two channels are shown in Fig. 4-12 and -13. Reduced data for this test cycle are reported in Appendix A.

Data revealed that some of the internal instruments were showing impacting between components. The on-board flight recorder was also running intermittently. During coordination discussions it was decided to conduct subsequent testing at 0.5-g input. NWC also modified the attachment of the tape recorder to minimize vibration chattering within its carriage.

Hard-Mount Random Vibration, 1 July 1971. Random vibration was conducted at ambient temperature with the scheduled input shown in Fig. 4-14. However, the BDU was generating sufficient energy from shaker input below about 1000 Hz that no additional shaker energy was required above this frequency to complete the total spectrum. The duration of the test was determined by the time necessary to obtain both ground-station and on-board recording systems data, about 3 minutes. Complete ground-station reduced data are reported in Appendix B.

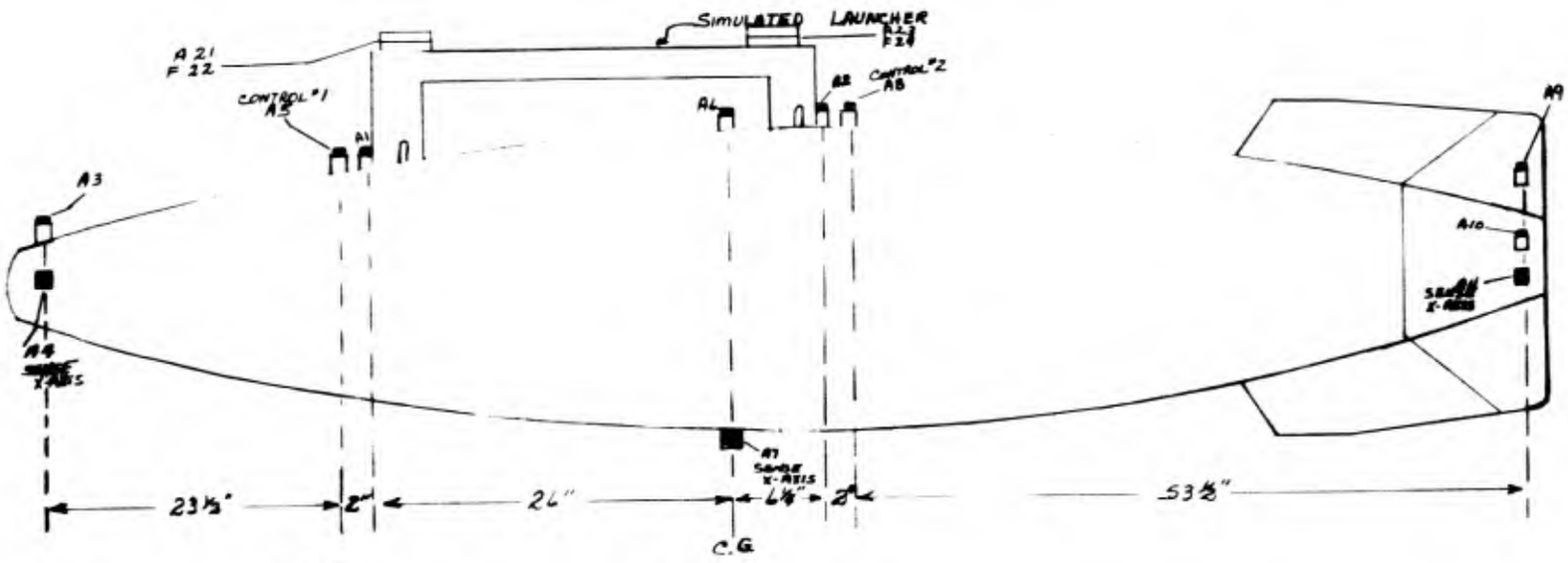

Ch No.	Axis — Range	Axis
A-1	Accelerometer Location	
A-2	Accelerometer Location	
A-3	Accelerometer Location	
A-4	Accelerometer Location	
A-5	Accelerometer Location	
A-6	Accelerometer Location	
A-7	Accelerometer Location	
A-8	Accelerometer Location	
A-9	Accelerometer Location	
A-10	Accelerometer Location	
A-11	Accelerometer Location	
A-12	Accelerometer Triax - Axis	
A-13	Accelerometer Triax - Axis	
A-14	Accelerometer Triax - Axis	
A-15	Accelerometer Triax Aft -	
A-16	Accelerometer Triax Aft -	
A-17	Accelerometer Triax Aft -	
A-18	Accelerometer Location #1	
A-19	Accelerometer Location #	
A-20	Accelerometer Location	
A-21	Accelerometer Location (Mounted on Left Fin)	
A-22	Force Location - Head Aft	

Figure 4-11. Location of External Instrumentation

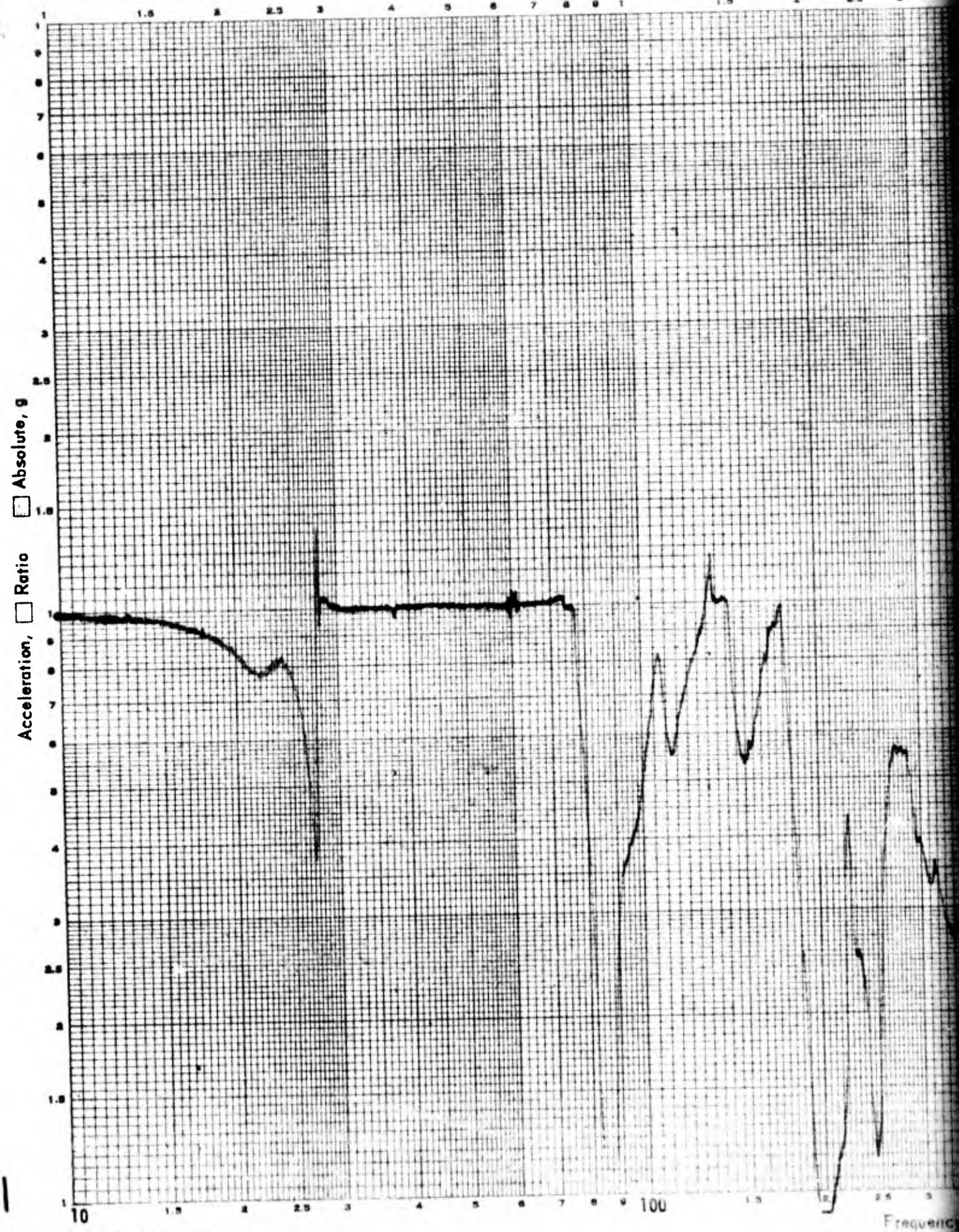

FORM 626-J-6 Nov 4-67

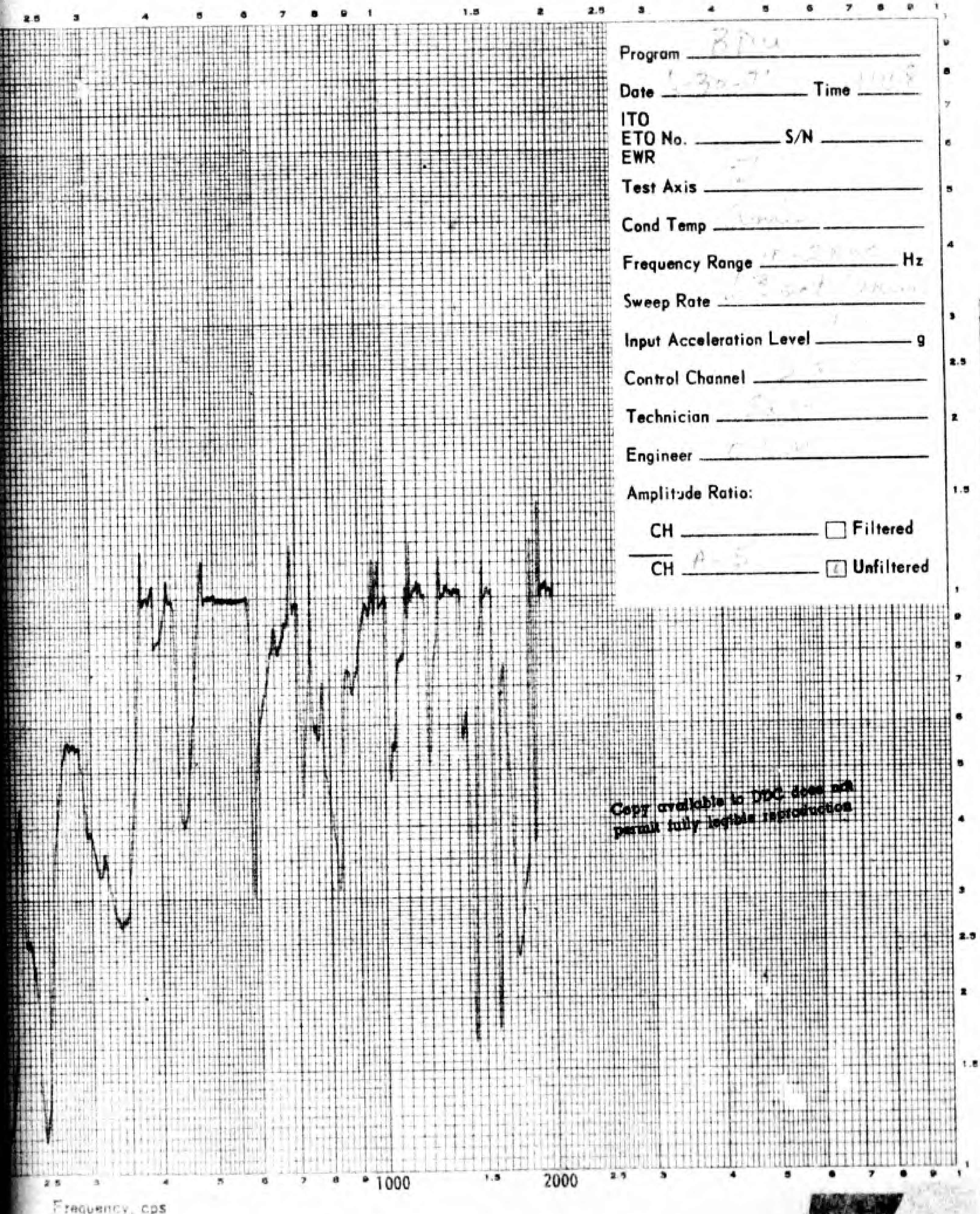

(U) Figure 4-12. Replot of Data from Control Channel 5, Measurement Sine Sweep, 30 June 1977

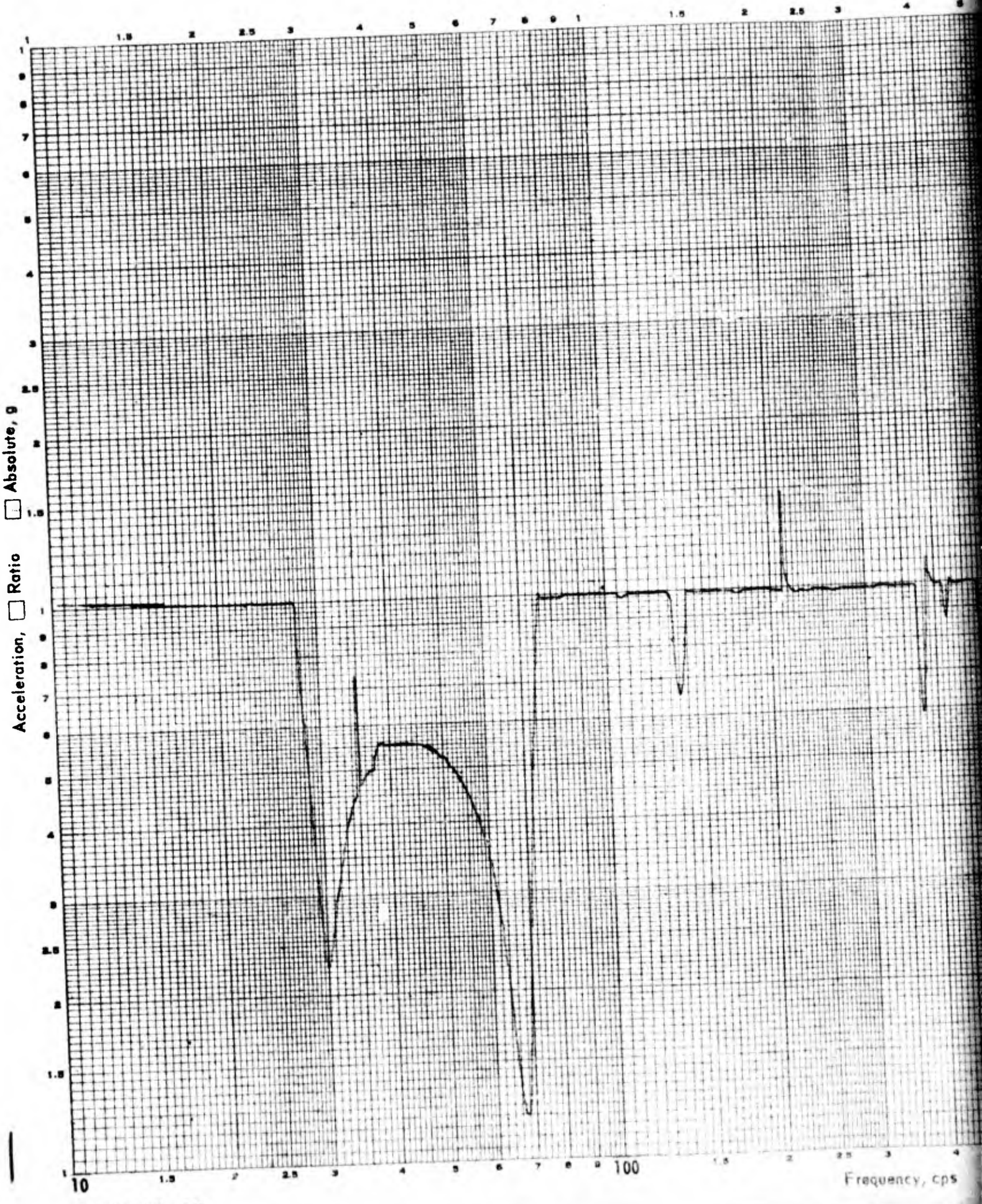

FORM 626-J-6 New 4-67

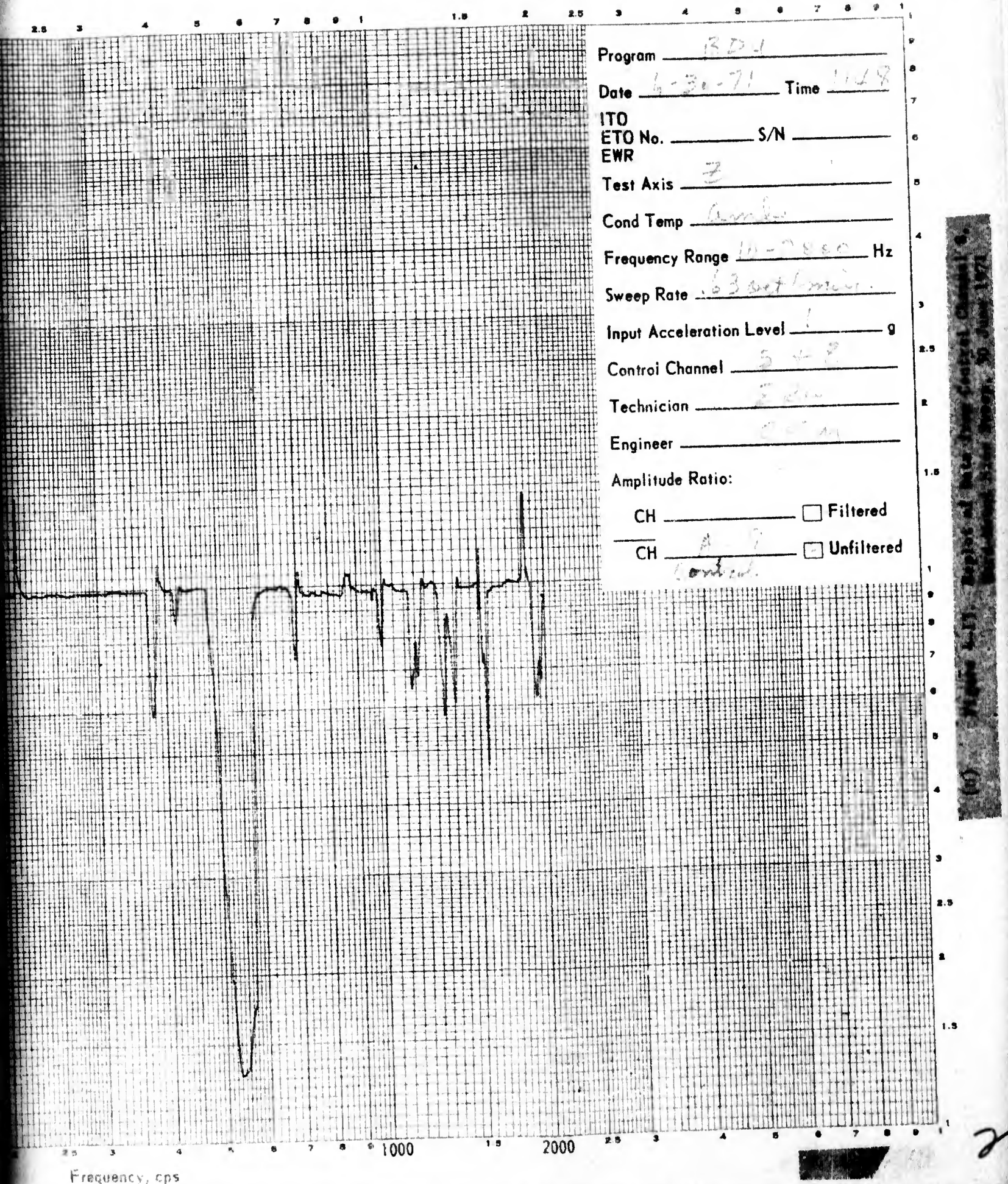
Program BD-1
Date 6-30-71 Time 1148
ITO
ETO No. S/N
EWR
Test Axis Z
Cond Temp Amb.
Frequency Range 10-2000 Hz
Sweep Rate 4 Oct/min.
Input Acceleration Level 1 g
Control Channel 3 + 8
Technician
Engineer
Amplitude Ratio:
CH Filtered
CH A 1 Control Unfiltered
1000
2000
Frequency, cps

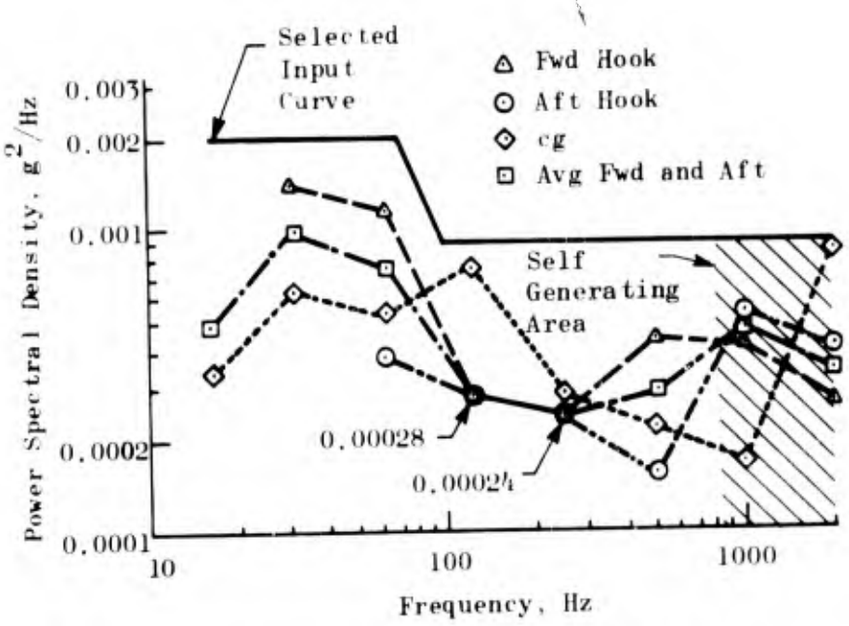

(U) Figure 4-14. Hard-Mount Random Vibration Input, Z Axis

Random data were reduced in analogue form through an ASD-80 spectral analyzer. These data revealed high responses between 1250 and 1750 Hz. Since all shaker excitation power at frequencies above 1000 Hz had already been filtered out, the response was clearly resulting from sympathetic harmonics that are a characteristic of the mechanical system. The amplitudes of these harmonics were reducible by lowering the power density at certain frequencies (such as 300 Hz), but it appears the harmonics cannot be eliminated without mechanical rearrangement.

Soft-Mount 0.5-g Sine Sweep Vibration, 6 July 1971. The soft-mount 0.5-g sine sweep vibration more closely simulated the actual flight test due to the use of the launcher. Dual control channels were used during this test also. One difference between this test and the other sine tests was the input g level, Fig. 4-15, and -16. Because of the loading amplification on the previous 1-g test and difficulties with the on-flight recorder at this loading level, a 0.5-g loading level was used on this test. However, problems still existed with the on-board recorder, and it was returned to the manufacturer for a quick check before the next test. Reduced data from this test cycle are presented in Appendix C.

X Axis Tests (Transverse)

Soft-Mount 0.5-g Sine Sweep Vibration, 13 July 1971. The reduced g level input load was maintained for X-axis sine vibration sweeps. The instrumentation in the propellant section remained the same due to lack of access; however, the externally applied instrumentation was relocated in accordance with Fig. 4-17. Only one impedance head was used in this axis since the vibrator input to the tooling was positioned to coincide with the center of gravity of the BDU, Fig. 4-7. Control was again accomplished through dual use of accelerometers 5 and 8. These were located on the case adjacent to the BDU/launcher (or hard-mount) interface. Input channel data are shown in Fig. 4-18 and -19. Reduced data from this test are presented in Appendix D.

Hard-Mount 0.5-g Sine Sweep Vibration, 14 July 1971. Instrumentation locations were not changed for the hard-mount sine sweep vibration. Input control accelerometer replots are shown in Fig. 4-20 and -21. Reduced data are shown in Appendix E.

Hard-Mount Random Vibration, 14 July 1971. Instrumentation data channels and the actual test set-up were not changed for hard-mount random vibration. The shaker input was changed from sine to random, Fig. 4-22. BDU self generation again negated required input from the shaker above 1000 Hz. Reduced data from this cycle are contained in Appendix F.

BDU Thermal Soak

Up to this time the test program had been conducted at ambient temperature. However, the next set of tests were to be conducted at elevated temperatures. Since one of the objectives in this preflight testing was to establish proper grain levels for the on-board recording system, the BDU was placed in a 200 F oven for 2 hours and the flight recording system was activated to verify and/or change the gain settings

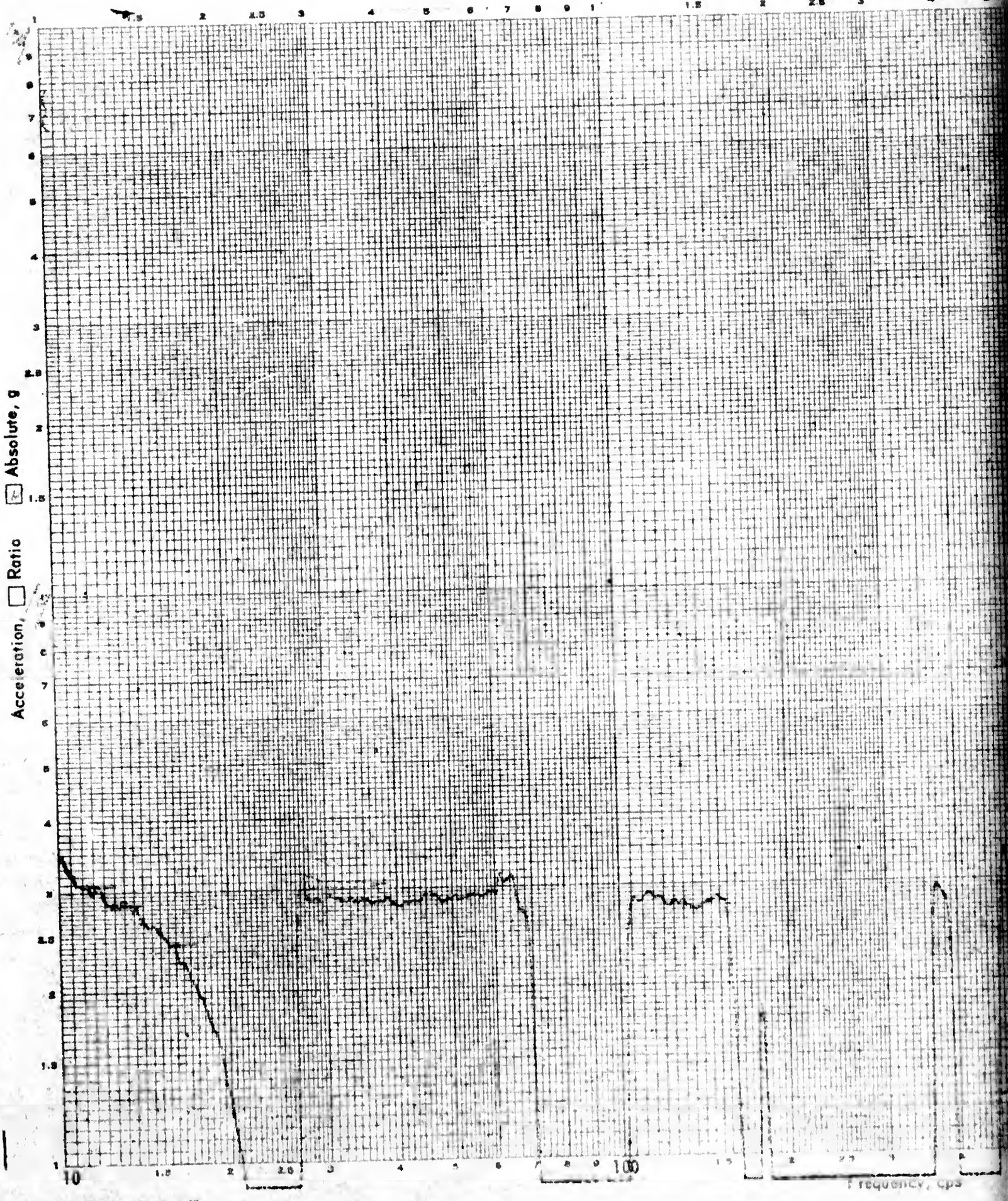

FORM 626-J-6 Nov 4-67

Program EDU

Date 2-6-71 Time 1125

ITO

ETO No. _____ S/N _____

EWR

Test Axis Z

Cond Temp Room

Frequency Range 10-2000 Hz

Sweep Rate 4 oct/min

Input Acceleration Level 5 g

Control Channel 5 & 8

Technician [illegible]

Engineer [illegible]

Amplitude Ratio:

CH A-5 ☐ Filtered

CH _____ ☒ Unfiltered

1000

2000

Frequency, cps

Z

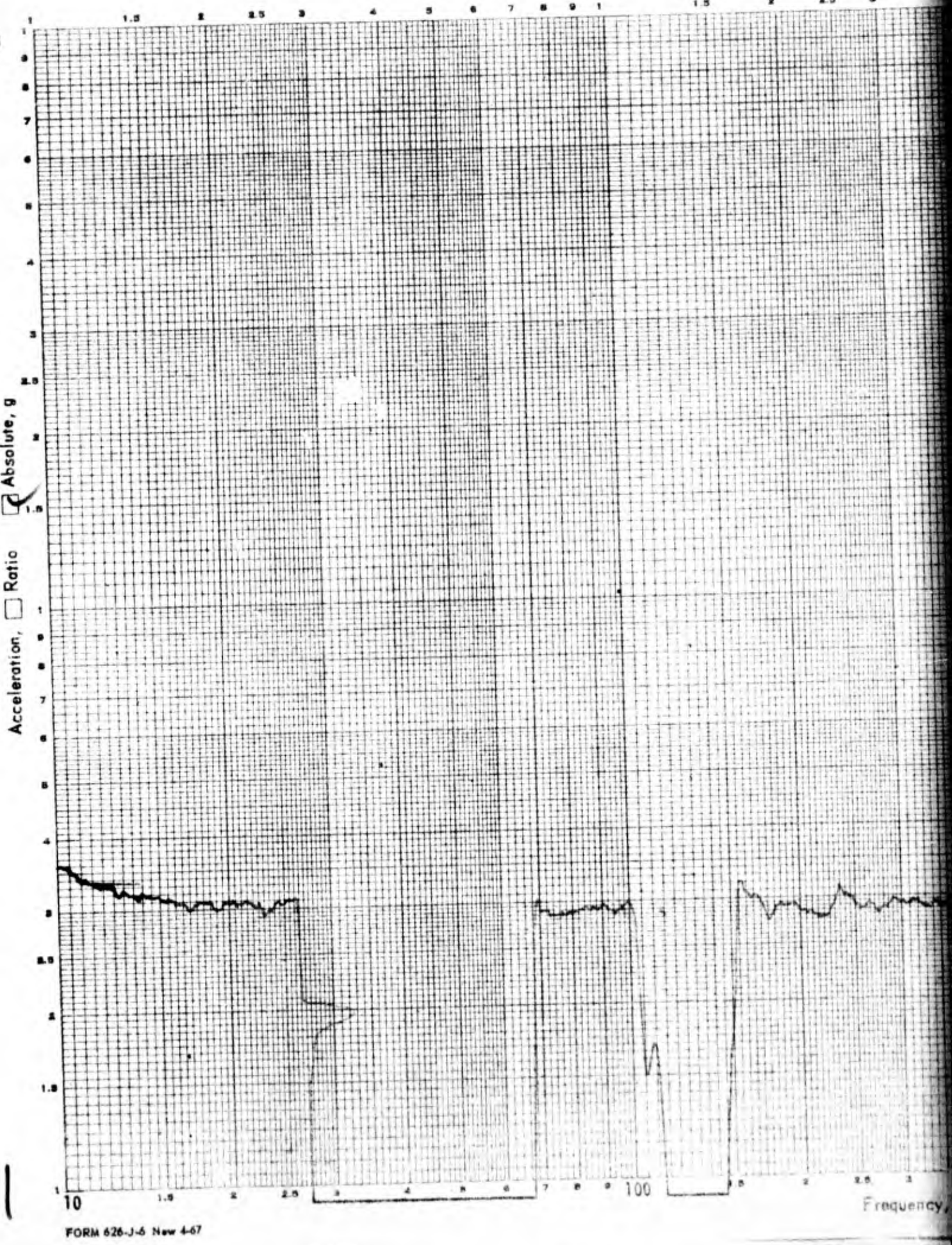

FORM 626-J-5 New 4-67

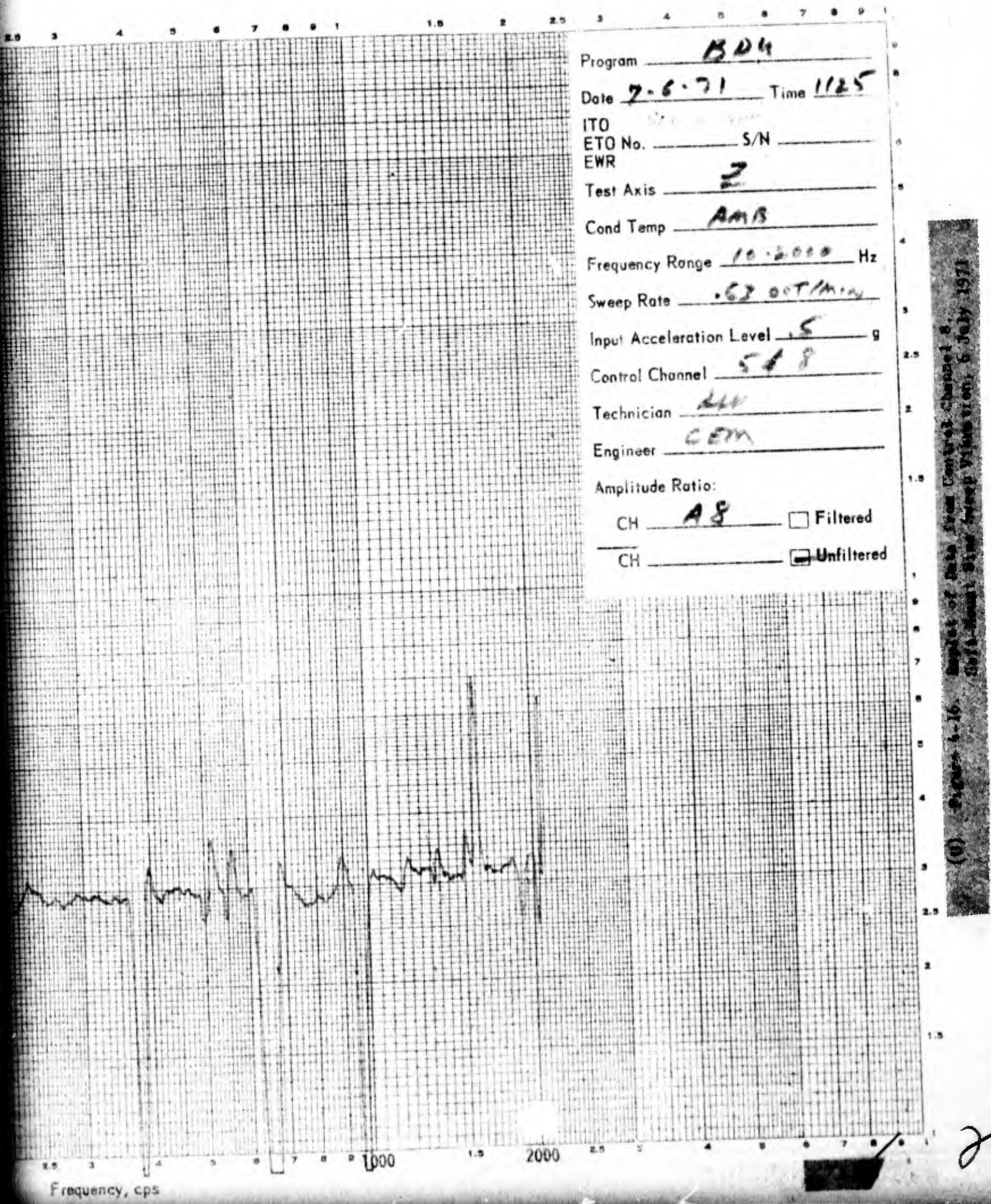
Program BD4
Date 7-6-71 Time 1125
ITO
ETO No. S/N
EWR
Test Axis Z
Cond Temp AMB
Frequency Range 10-2000 Hz
Sweep Rate .63 OCT/MIN
Input Acceleration Level .5 g
Control Channel 5 & 8
Technician AH
Engineer CEM
Amplitude Ratio:
CH A8 Filtered
CH Unfiltered
1000
2000
Frequency, cps

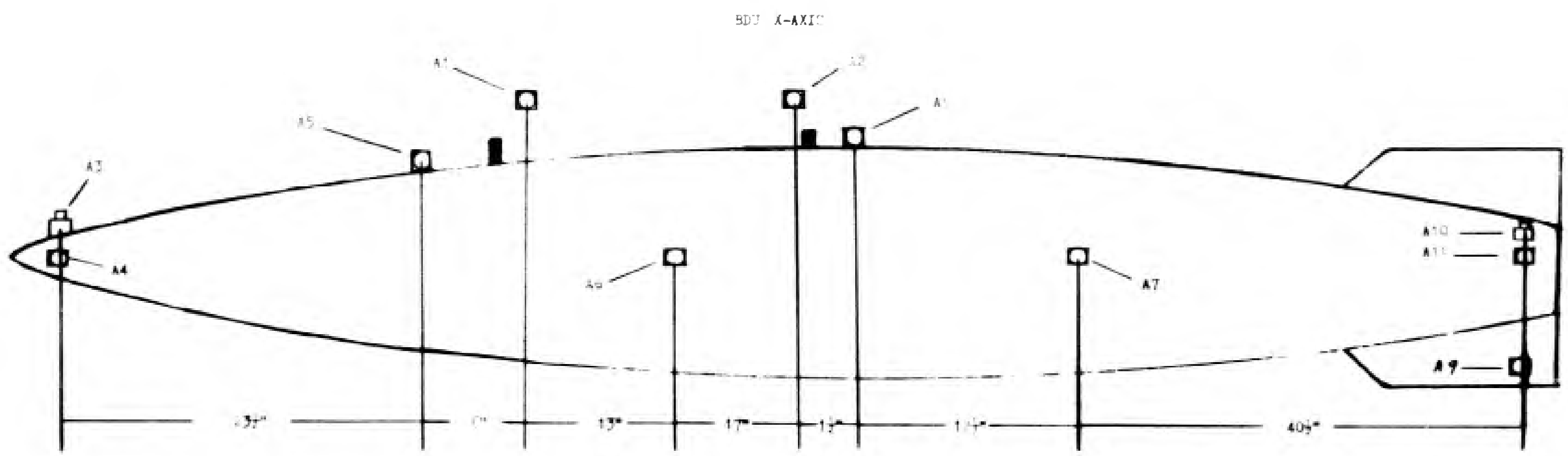

CH NO.	GAGE	[illegible]	ACTIVE AXIS
A1	Accel. (Contr 1)		X
A2	Accel. (Contr 1)		X
A3	Accel. (Case)		
A4	Accel. (Case)		X
A5	Accel. (Case)		X
A6	Accel. (Case)		X
A7	Accel. (Case)		X
A8	Accel. (Case)		X
A9	Accel. (Case)		X
A10	Accel. (Case)		[illegible]
A11	Accel. (Case)		X
A12	Accel. Triax C.G.	[illegible]	X
A13	Accel. Triax C.G.	[illegible]	Y
A14	Accel. Triax C.G.	[illegible]	[illegible]
A15	Accel. Triax Aft End	[illegible]	X
A16	Accel. Triax Aft End	[illegible]	[illegible]
A17	Accel. Triax Aft End	[illegible]	[illegible]
A18	Accel. [illegible] #1	[illegible]	
A19	Accel. [illegible]	[illegible]	
A20	Accel. [illegible]	[illegible]	
A21	Accel. Impedance Head #1		X
F22	Force Impedance Head #1		X

Figure 4-17. Relocated External Insulation

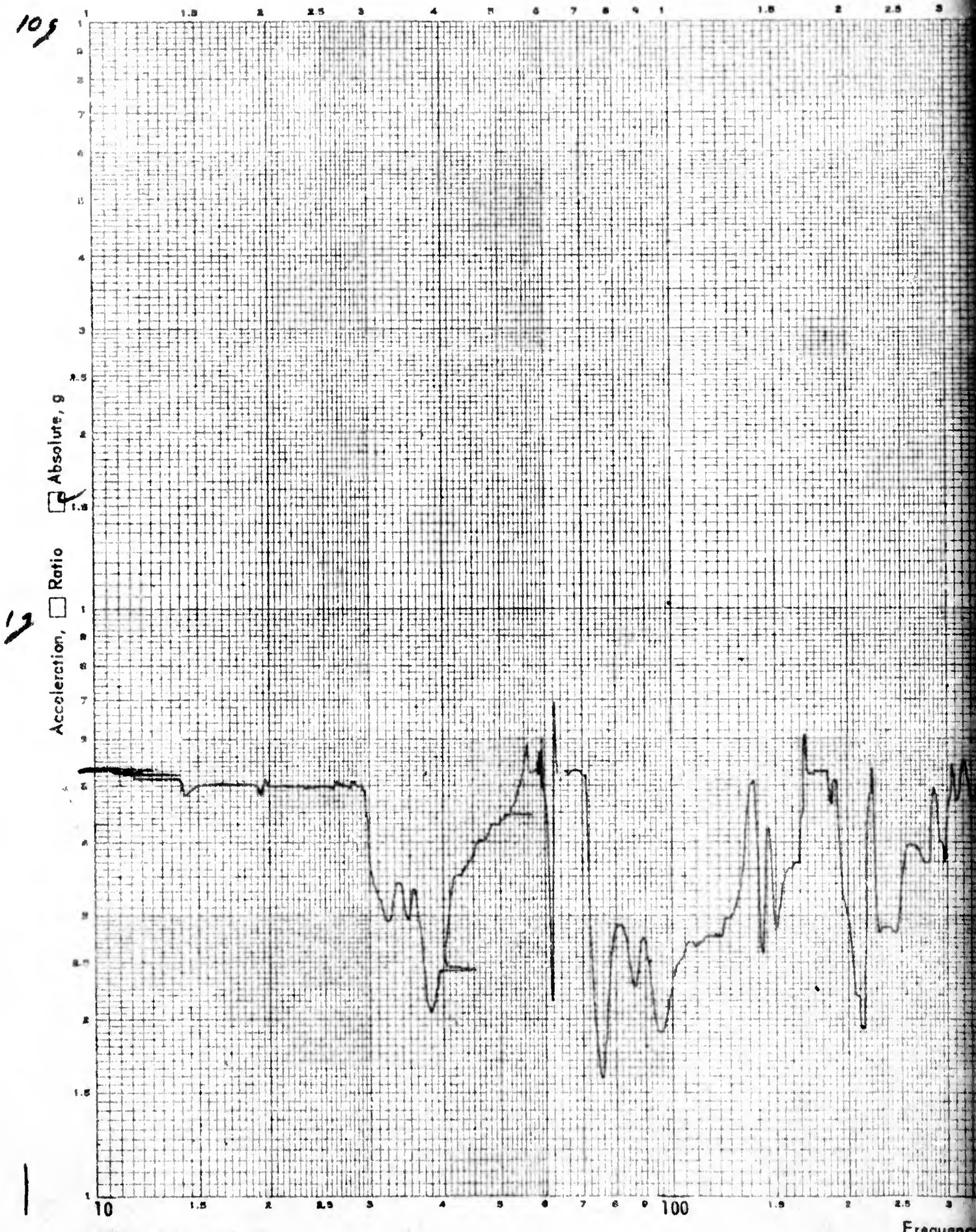

FORM 626-J-6 Nov 4-67

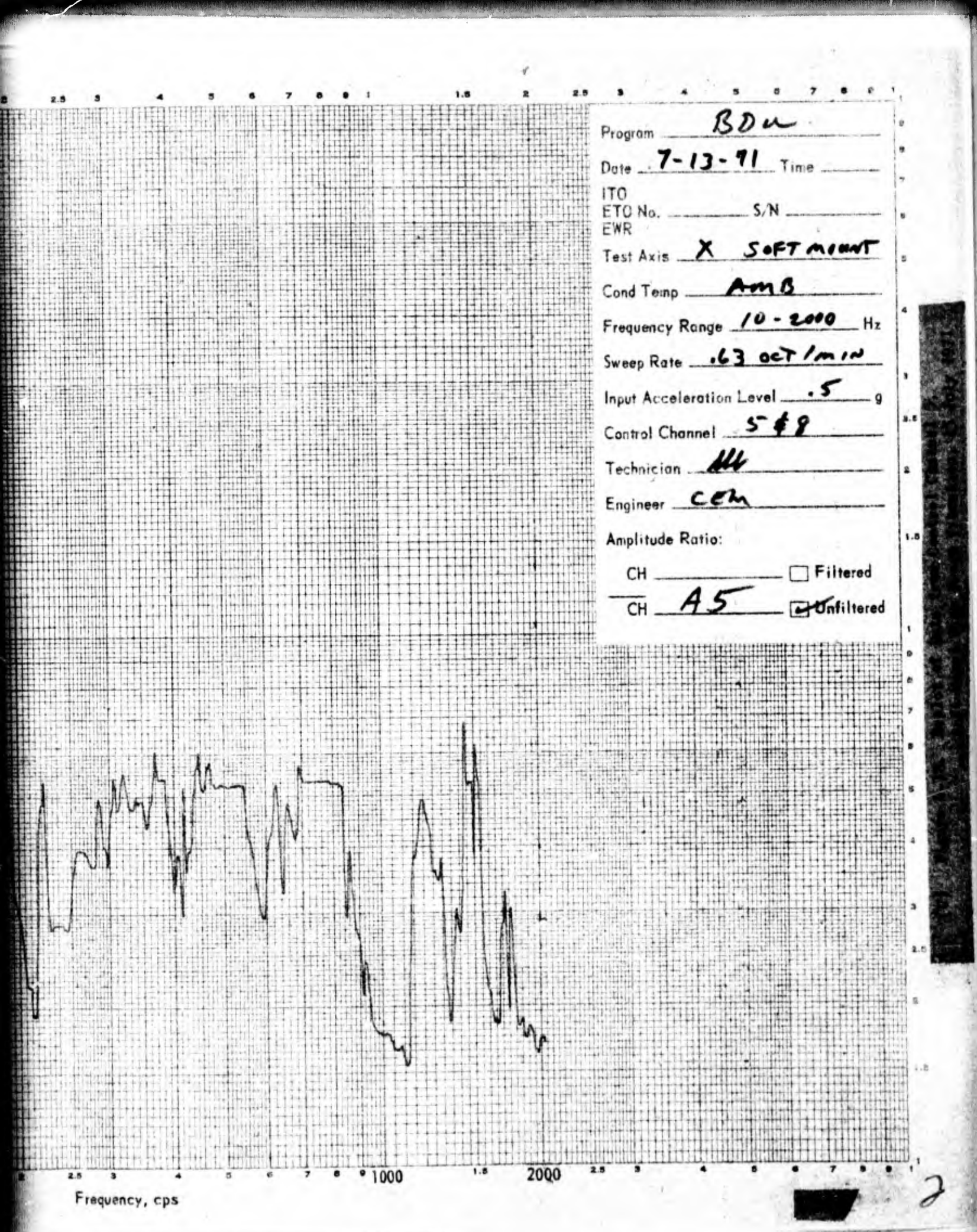
Program BDU
Date 7-13-91 Time
ITO
ETO No. S/N
EWR
Test Axis X SOFT MOUNT
Cond Temp AMB
Frequency Range 10 - 2000 Hz
Sweep Rate .63 oct/min
Input Acceleration Level .5 g
Control Channel 5 #9
Technician MH
Engineer CEM
Amplitude Ratio:
CH Filtered
CH A5 Unfiltered
1000
2000
Frequency, cps

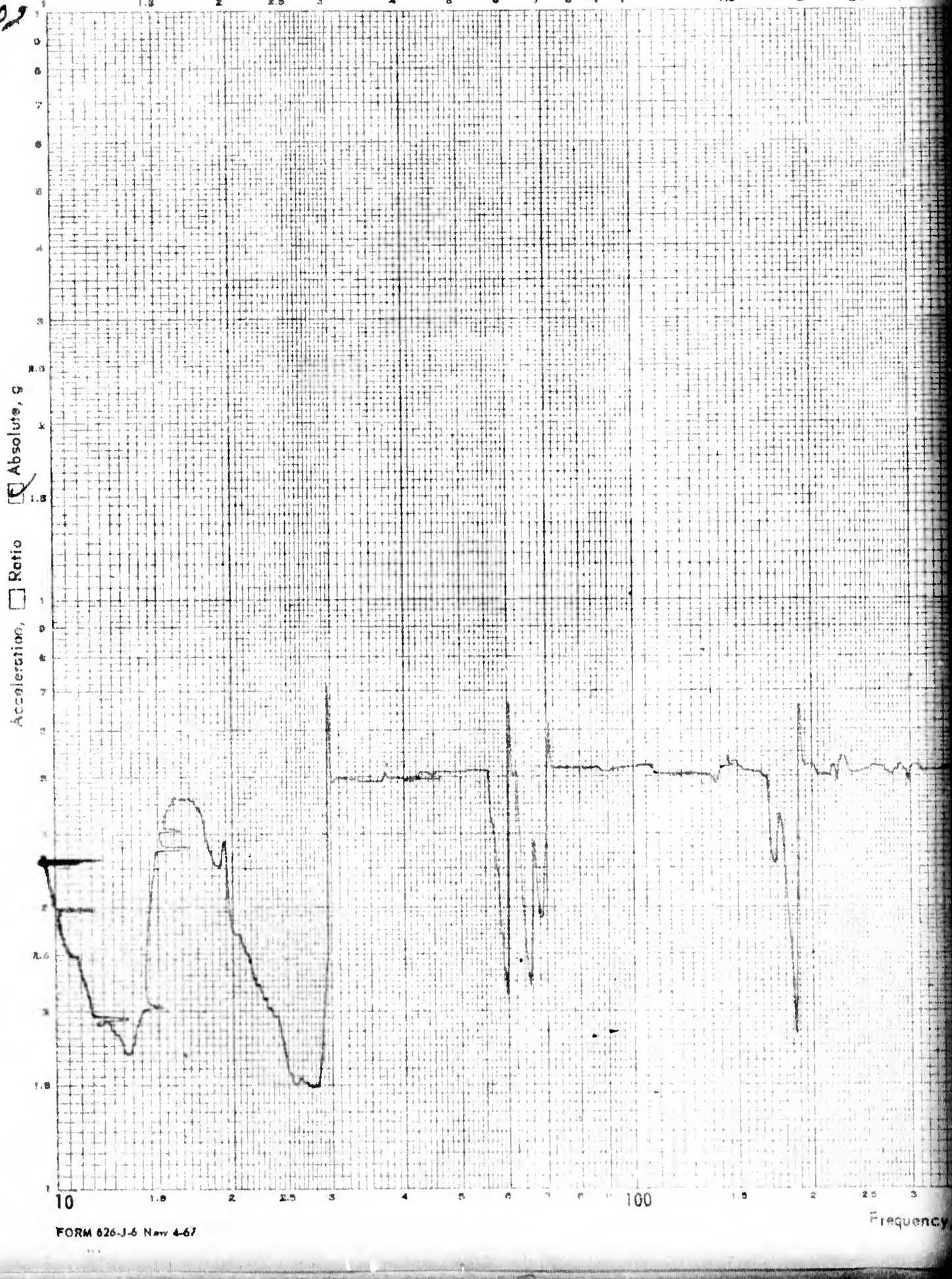

FORM 626-J-6 Nov 4-67

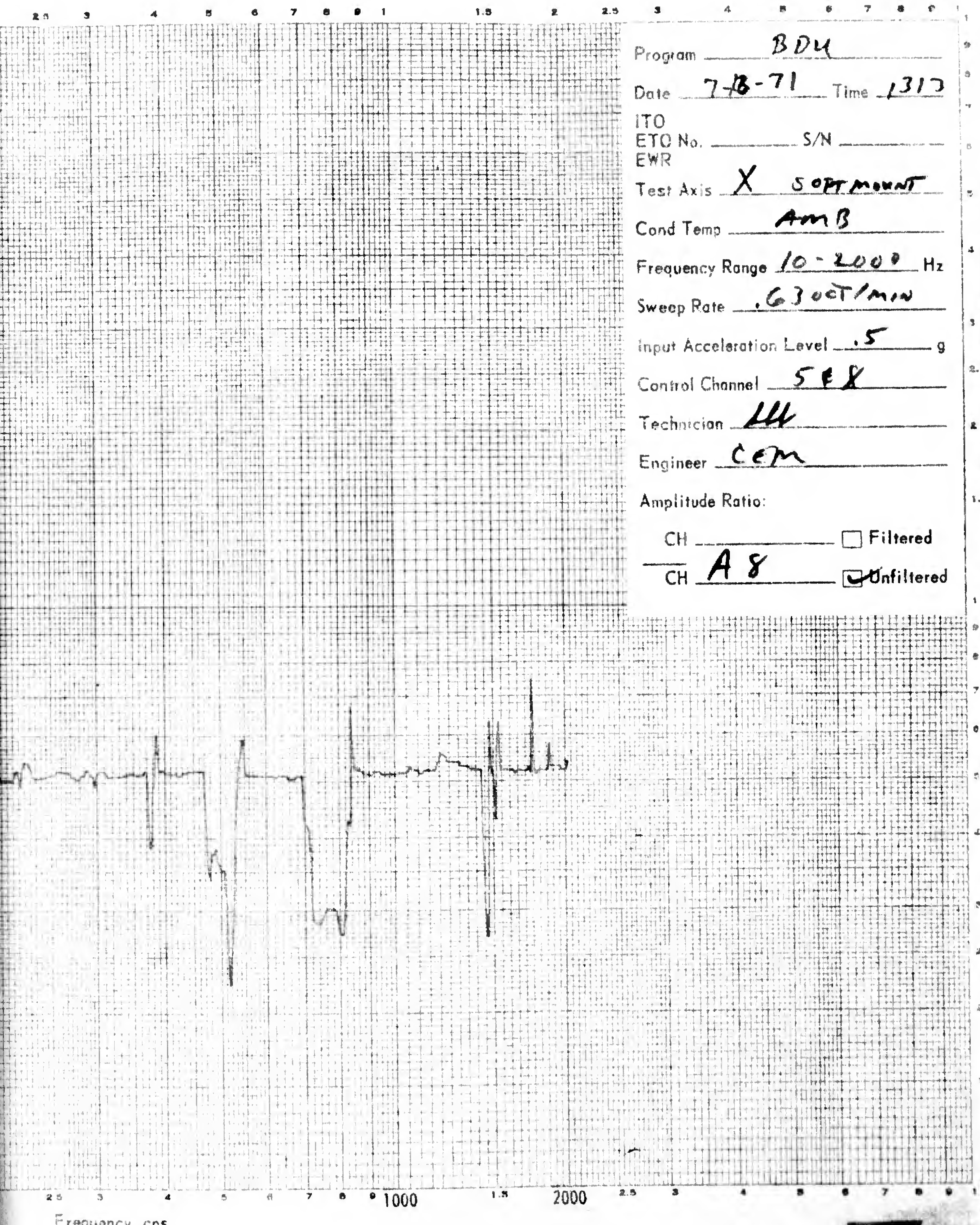

Figure 4.19. Replot of Data from Control Channel 8, Soft-Mount Sine Sweep Vibration, 13 July 1971 (d)

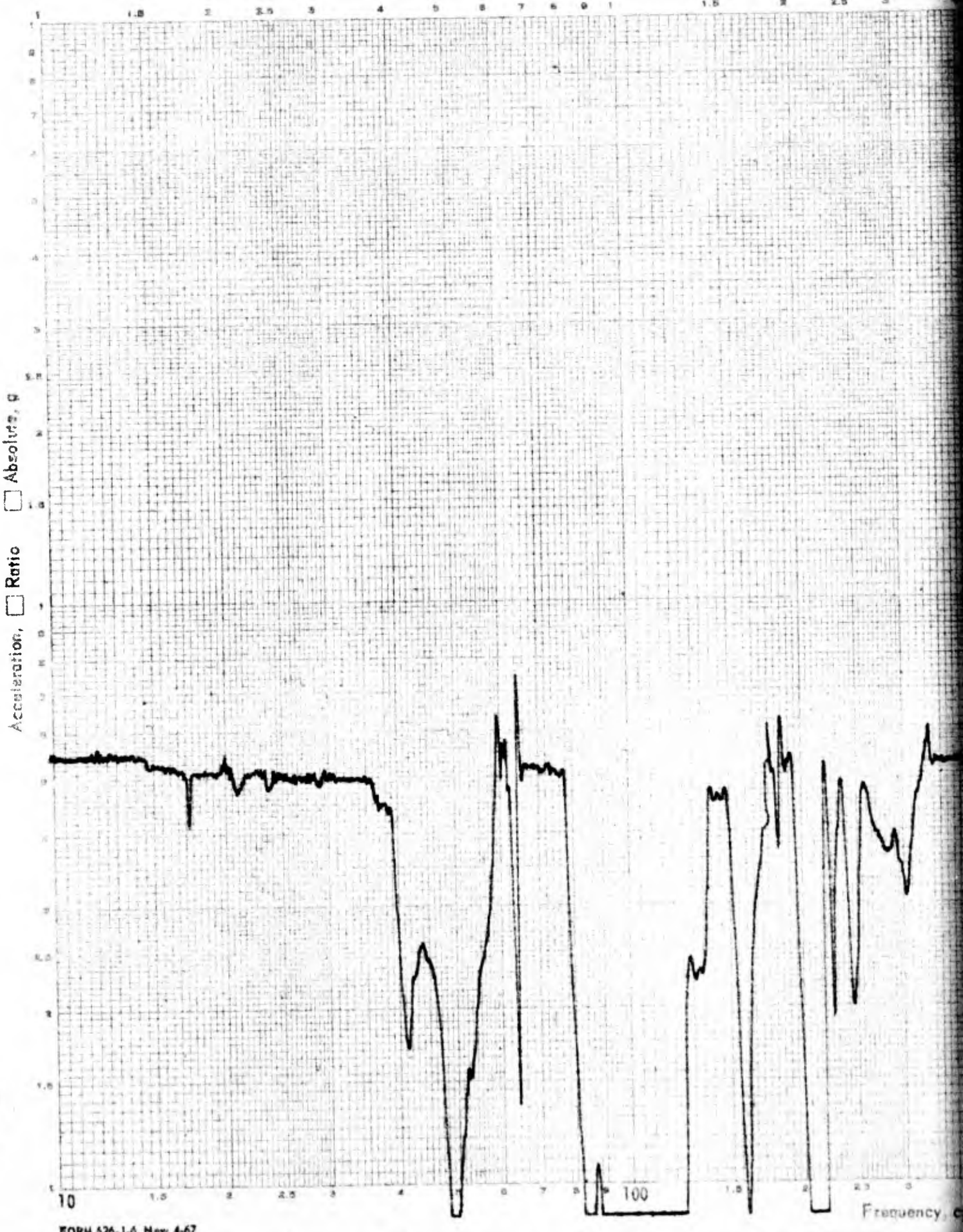

FORM 526-J-6 Nov 4-67

Program BDU

Date 7-14-71 Time 1049

ITO
ETO No _____ S/N _____
EWR

Test Axis X HARD MOUNT

Cond Temp AMB

Frequency Range 10-2000 Hz

Sweep Rate .63 oct/min

Input Acceleration Level .5 g

Control Channel A5 + A8

Technician EXW

Engineer CEM

Amplitude Ratio:

CH _____ ☐ Filtered

CH A-5 ☑ Unfiltered

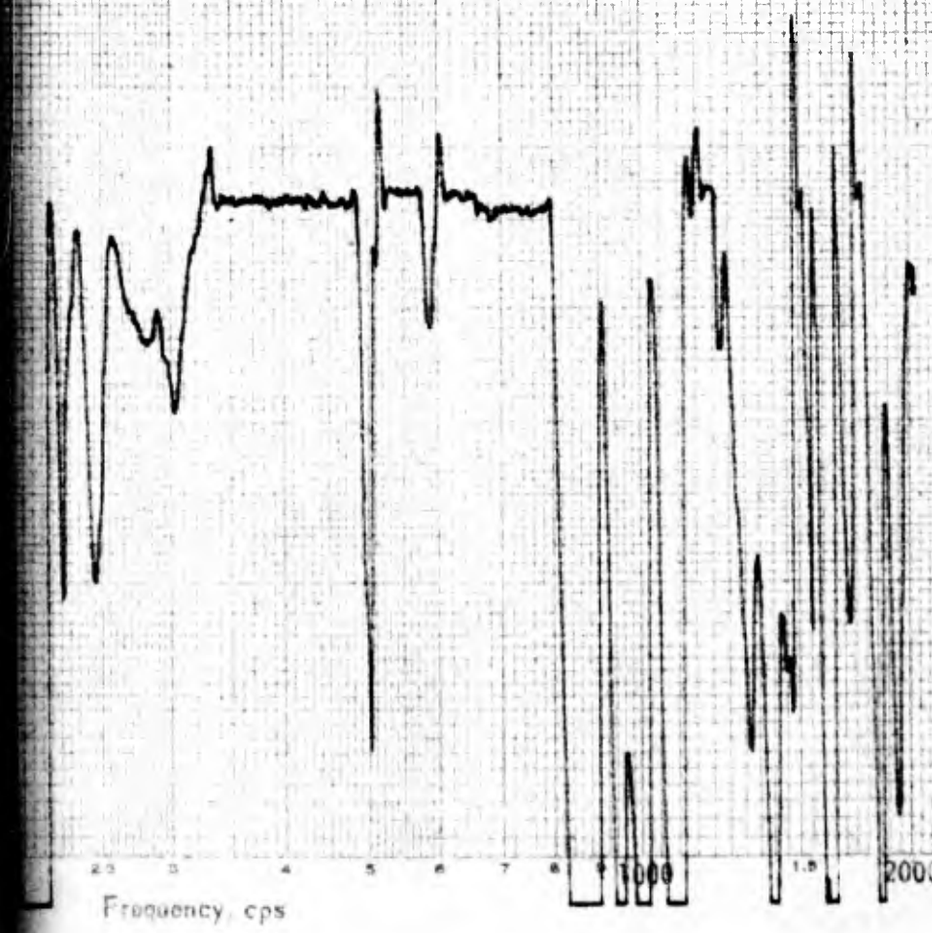

Frequency, cps

2

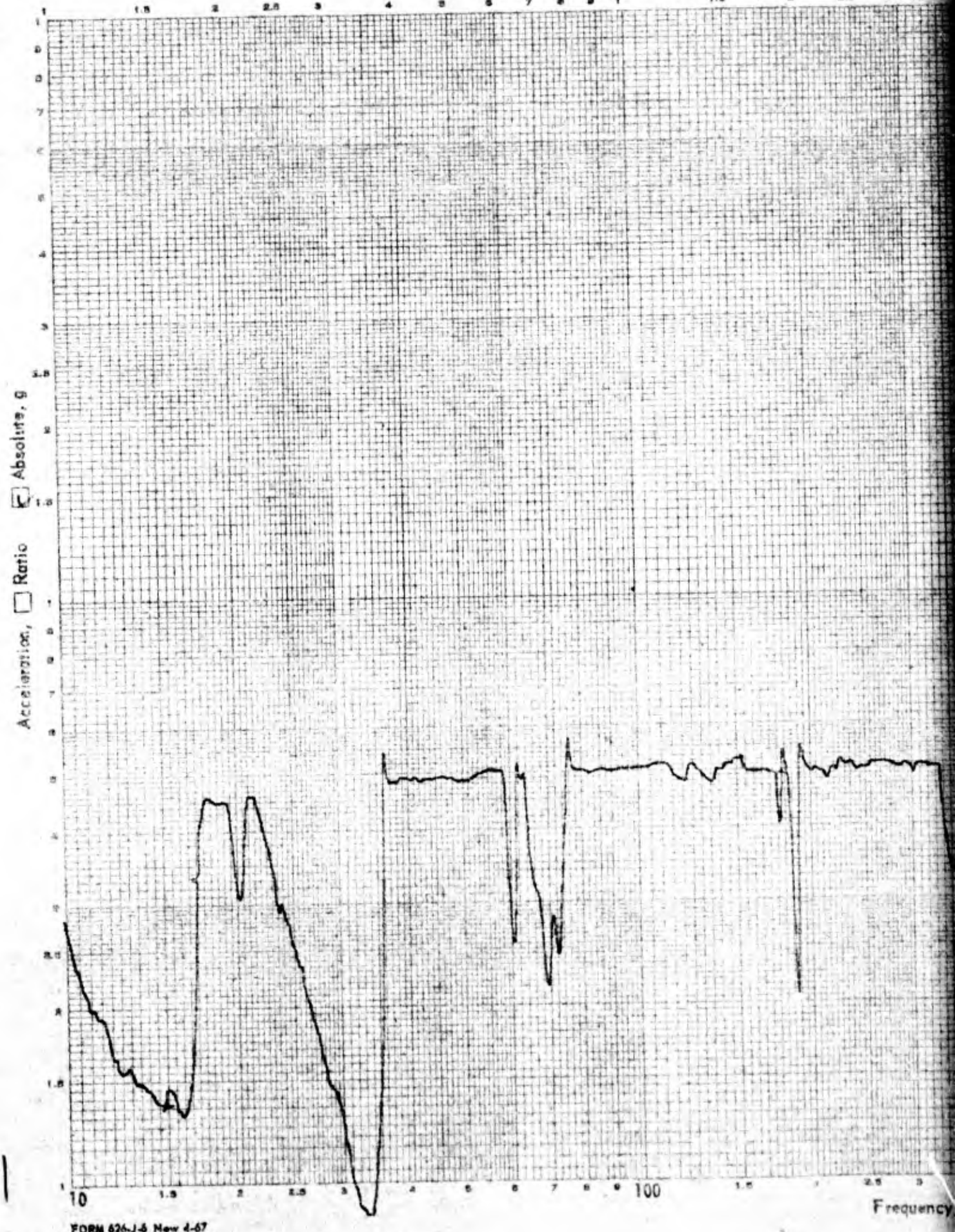

FORM 626-J-6 Nov 4-67

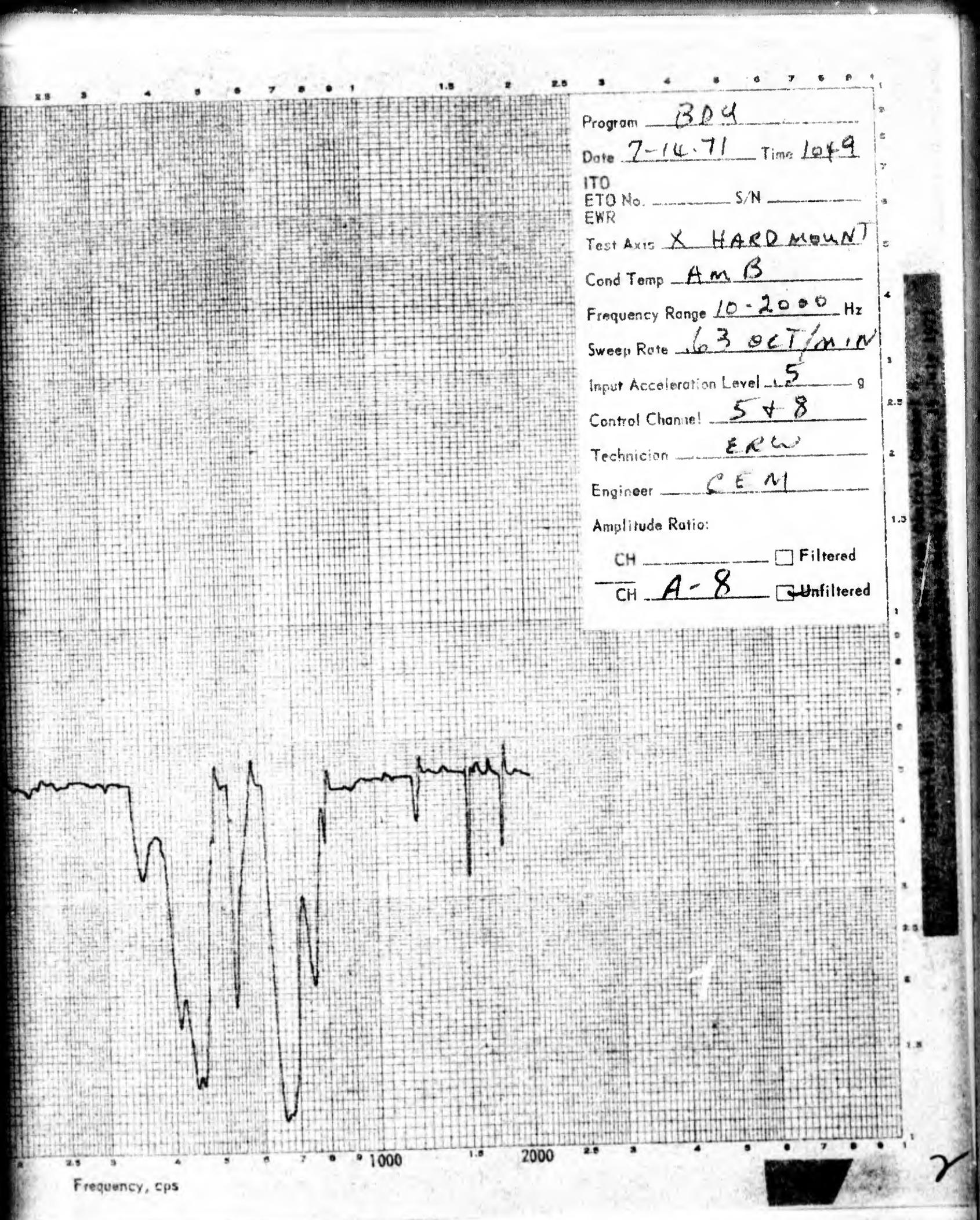
Program BD4
Date 7-14-71 Time 1049
ITO
ETO No. S/N
EWR
Test Axis X HARD MOUNT
Cond Temp AMB
Frequency Range 10-2000 Hz
Sweep Rate .63 OCT/MIN
Input Acceleration Level .5 g
Control Channel 5 + 8
Technician ERW
Engineer CEM
Amplitude Ratio:
CH Filtered
CH A-8 Unfiltered
1000
2000
Frequency, cps

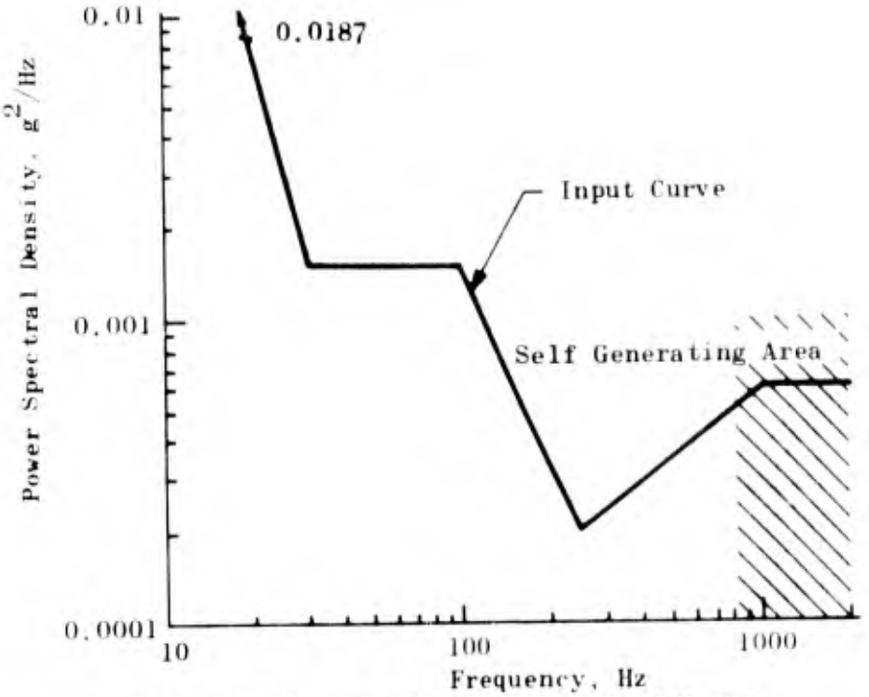

Figure 4-22. Shaker Input for Hard-Mount Random Vibration

on those elements sensitive to temperature change. This test was scheduled at this time because gain level changes required extensive breakdown of the total BDU and the next 2 months could be used for both gain level changes and replacement of instrumentation on the launcher sway braces and lugs.

The thermal soak test indicated some desired gain-level changes for the on-board recording system. Data from this test were recorded on the on-board data acquisition system and were not totally available at the printing of this report. However, some data are shown in Fig. 4-23.

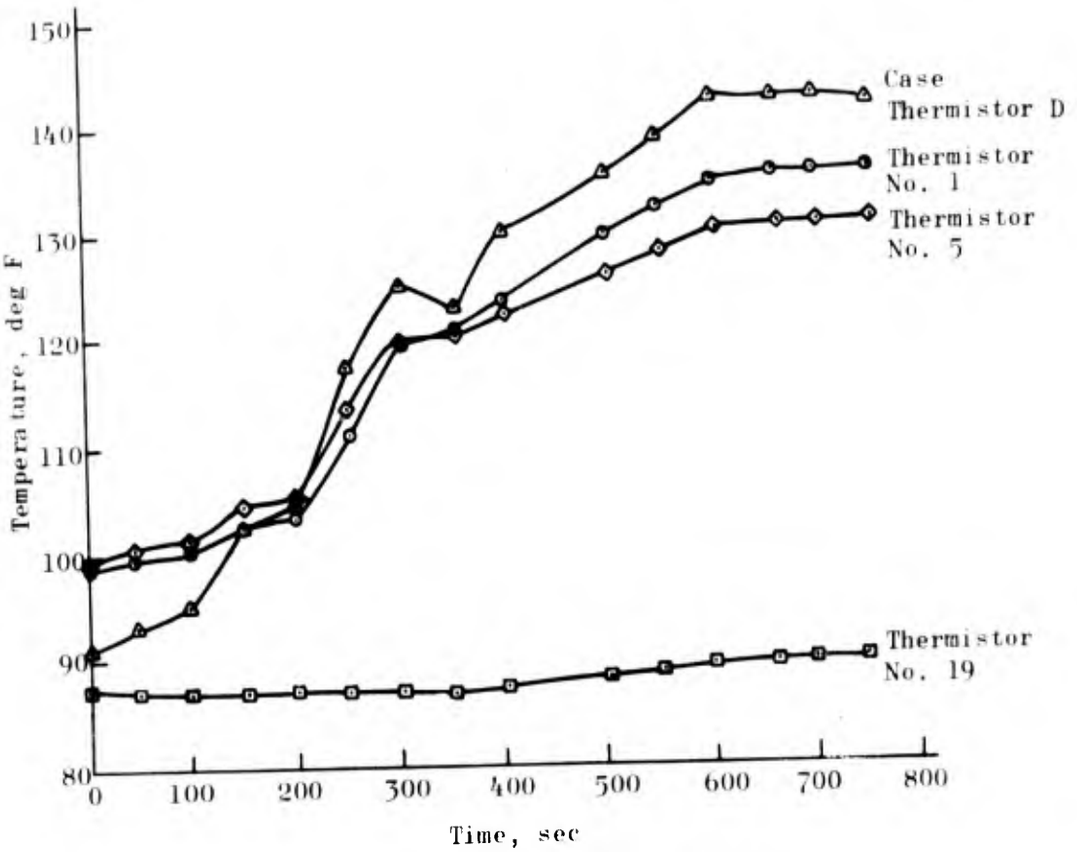

Figure 4-23. Thermistor Data from 200 F Soak Test

Instrumented Launcher--Flight Load Measuring System

In addition to the numerous propellant transducers and accelerometers on the Bomb Dummy Unit it was deemed advantageous for flight testing subsequent to this program to install additional devices capable of indicating the load interchange between the aircraft and externally carried store (the BDU). In order not to alter the structural capability of components previously qualified for flight testing, it appeared the load measuring system could be best implemented by the application of strain gages to strategic points on the MAU-12A/C launcher and on the BDU launch lugs. Metal foil strain gages had previously been installed (by the Navy, China Lake) on the launch lugs,

but the circuit sensitivity was such that the output signal/noise ratio was deemed too low during vibration testing. Consequently, the foil strain gages were replaced with more seusitive semiconductor gages; and additional gages were applied to the launcher. Flight load measuring instrumentation and calibration are described in the following section.

Launch Lugs. The BDU is retained by the launcher solely by a stiff aft lug and a hinged forward lug (see Fig. 4-23A). While the BDU is attached, the lugs will be preloaded in a tensile sense by the launcher sway brace set screws. Due to the preload, an instrumented lug response on the system level will appear stiffer than the lug element alone. Therefore, as will be later discussed, the lugs were calibrated by applying known force vectors to the launcher/BDU assembly.

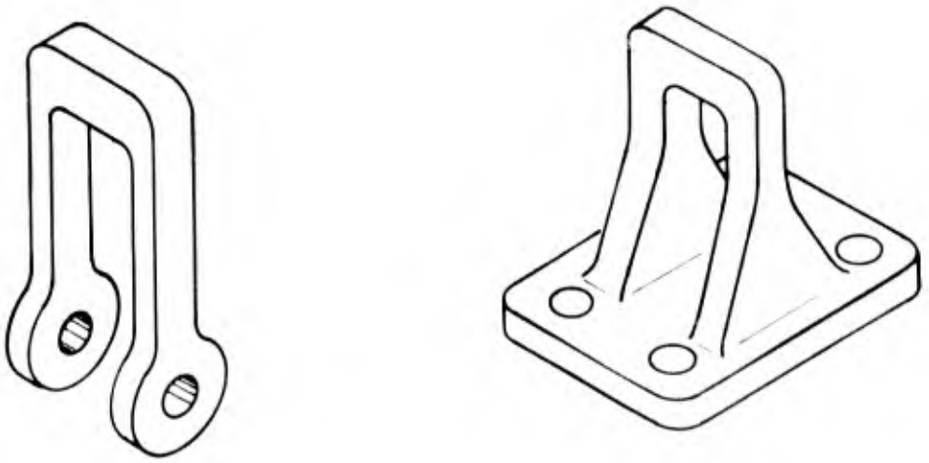

(a) Forward Lug (b) Aft Lug

Figure 4-23A. BDU Launch Lugs

Semiconductor strain gages were applied to both launch lugs and arranged in a bridge circuit to sense tensile loads in the forward lug and tensile and fore-to-aft bending loads in the aft lug.

Bridge circuit for measuring tensile loads in the forward launch lug is shown in Fig. 4-24.

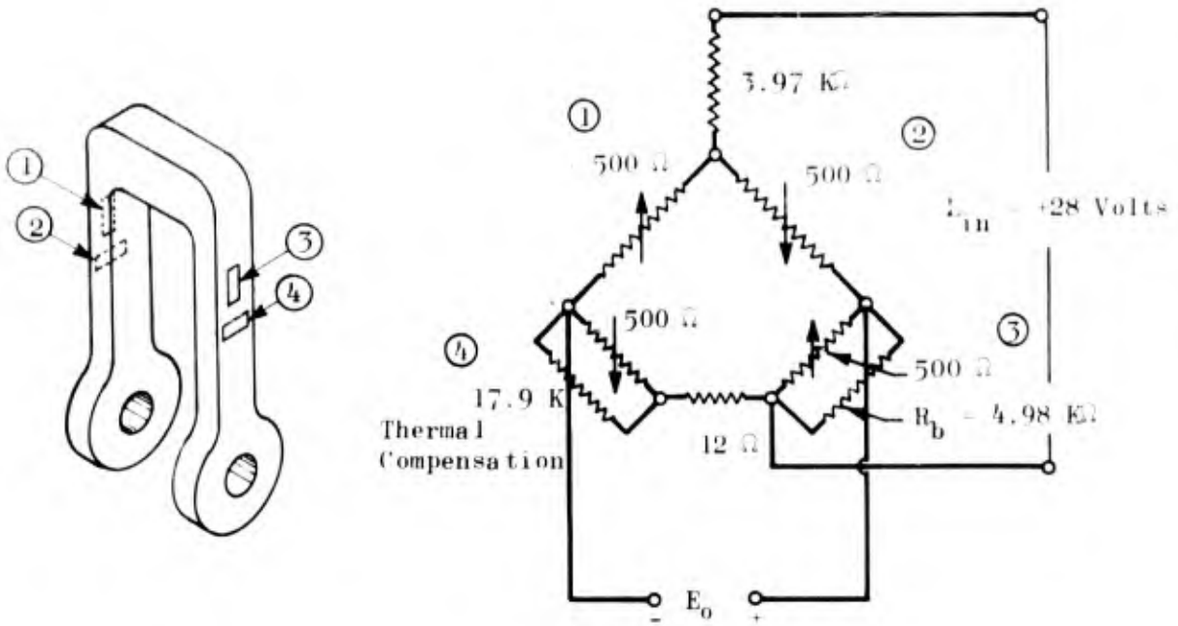

Figure 4-24. Mechanical and Electrical Circuit Schematic for Forward Lug Tensile Load Measuring Elements

The cross axis, or Poisson's effect, (gages ② and ④, Fig. 4-24) are arranged in the bridge to increase tensile load sensitivity and to cancel the undesirable influences of bending. Additional resistors, R_b (Fig. 4-24 and -25), were added to balance the sway brace tightening load and improve the accuracy of the calibration procedure. Figure 4-25 shows the final circuit thermal calibration factors.

The aft launch lug is rigidly bolted to the BDU and can sustain bending induced by longitudinal (Y axis) loads. Semiconductor strain gages were applied to the aft lug and arranged in an electrical bridge circuit as shown in Fig. 4-26.

In the bridge arrangement shown, the strains are summed while the tensile strains are cancelled. Refer to Fig. 4-24 for final thermal calibration factor.

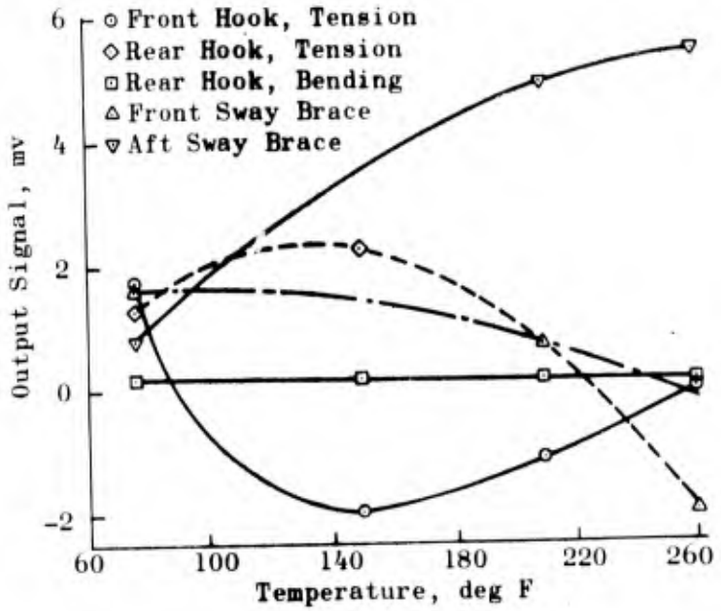

Figure 4-25. Zero Load Gage Circuit Readings vs Temperature

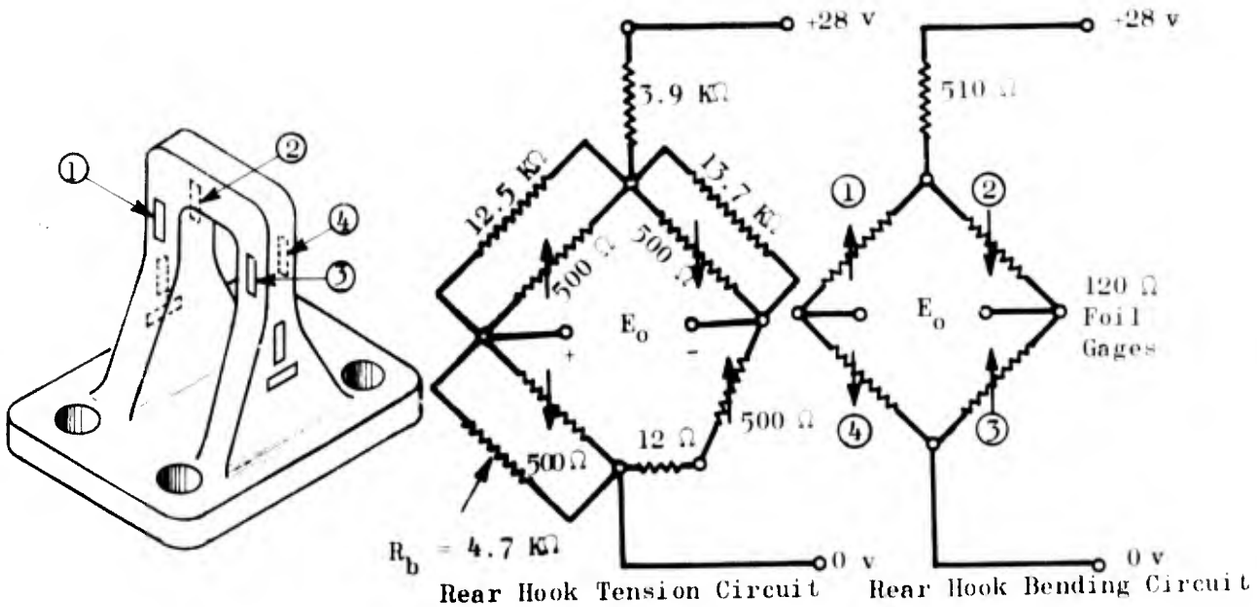

Figure 4-26. Schematic of Aft Lug Circuits

Launcher Sway Braces. The launcher sway braces were instrumented in a full bridge arrangement sensitive to differential bending as shown in Fig. 4-27. With strain gages mounted on the top and bottom each sway brace "cantilever," lateral movement could be sensed as one cantilever flexed upward and the opposing one flexed downward. The forward and aft sway brace pairs were instrumented identically using semiconductor gages; but during test, one of the strain gages on a forward sway brace was inadvertently damaged. Consequently, the damaged gage (and its counterpart in the bridge) was replaced and the bridge voltage was increased so the forward and aft sway brace bridges had the same sensitivity. These bridge arrangements are somewhat temperature compensating with the final calibration factor shown in Fig. 4-24.

After completion of instrumenting the launch lugs and the launcher sway braces, the circuits were checked out and the launcher was assembled with the BDU for loads calibration.

Static Load Calibration. The BDU/launcher assembly was mounted into a portion of the vibration jig (Fig. 4-28) for static calibration of the flight loads measuring system. Load vectors were then applied through the center of gravity. The resulting sensing element response data are shown in Fig. 4-29 through 4-31. Data shown in Fig. 4-32 indicate a cross-axis response displayed by the launch lugs in tension to a load applied in the transverse or X axis. This cross sensitivity is relatively low, but should be accounted for in a precise analysis. Cross sensitivity of the other sensing elements is substantially less.

Calibration factors were determined through a combination of a statics analysis and the relation between bridge sensitivities. Dimensions used for the statics analysis are shown in Fig. 4-33, which also shows location of the Z-axis impedance heads used in dynamic testing. These factors are shown in Table 4-4.

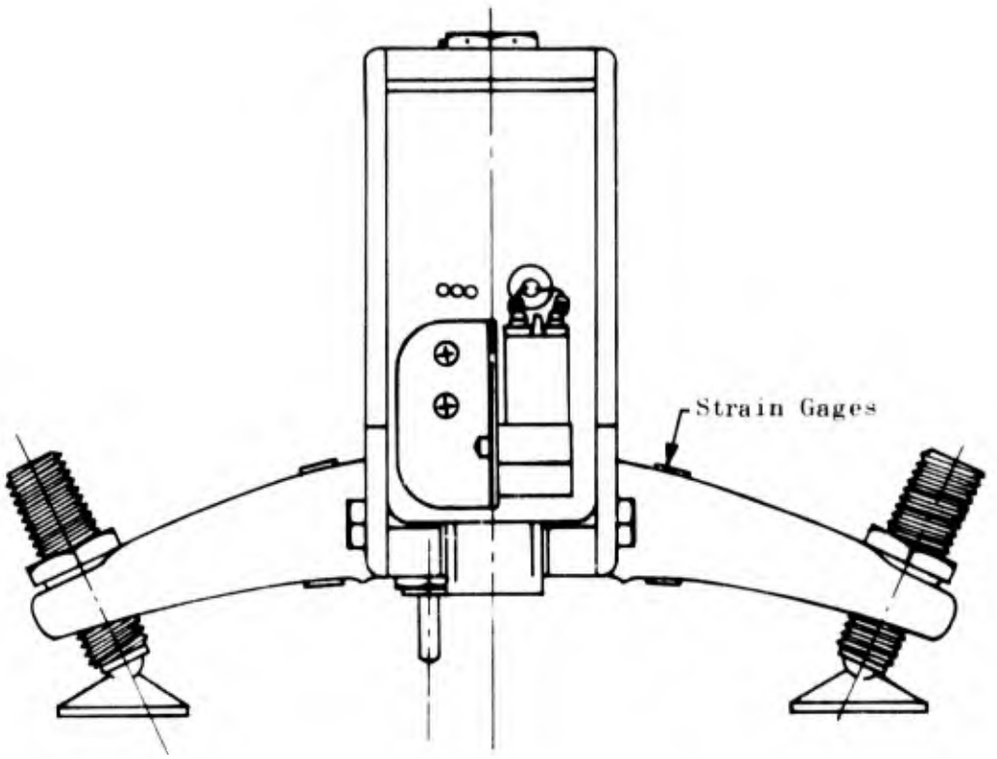

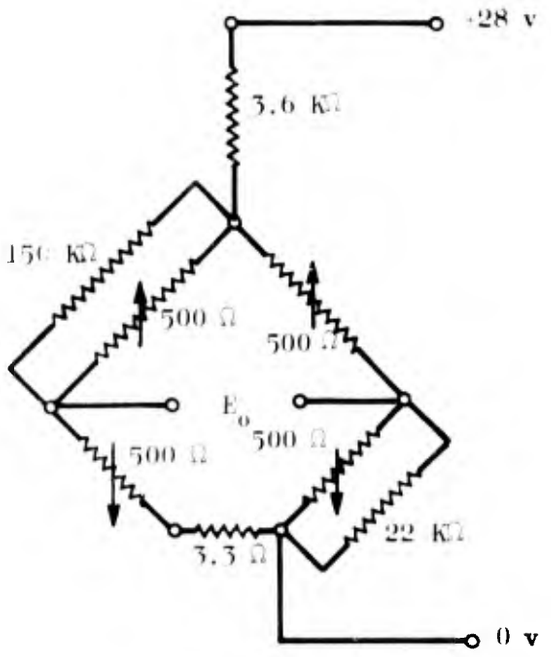

(a) Aft Sway Brace Circuit

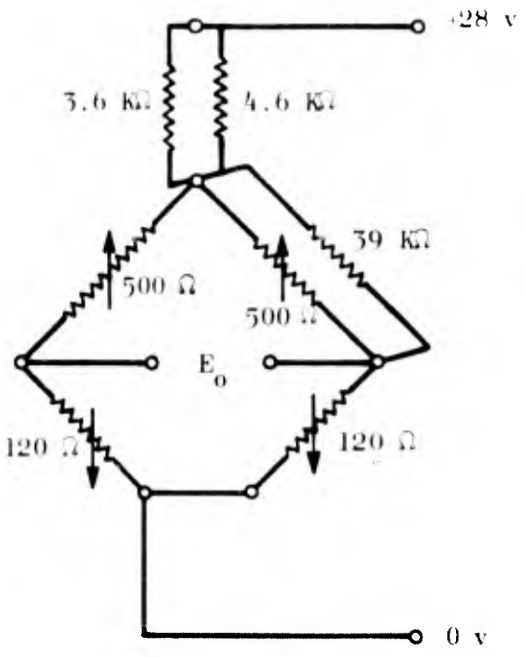

(b) Front Sway Brace Circuit

Figure 4-27. Schematic of Sway Brace Strain Gages and Bridge Circuit

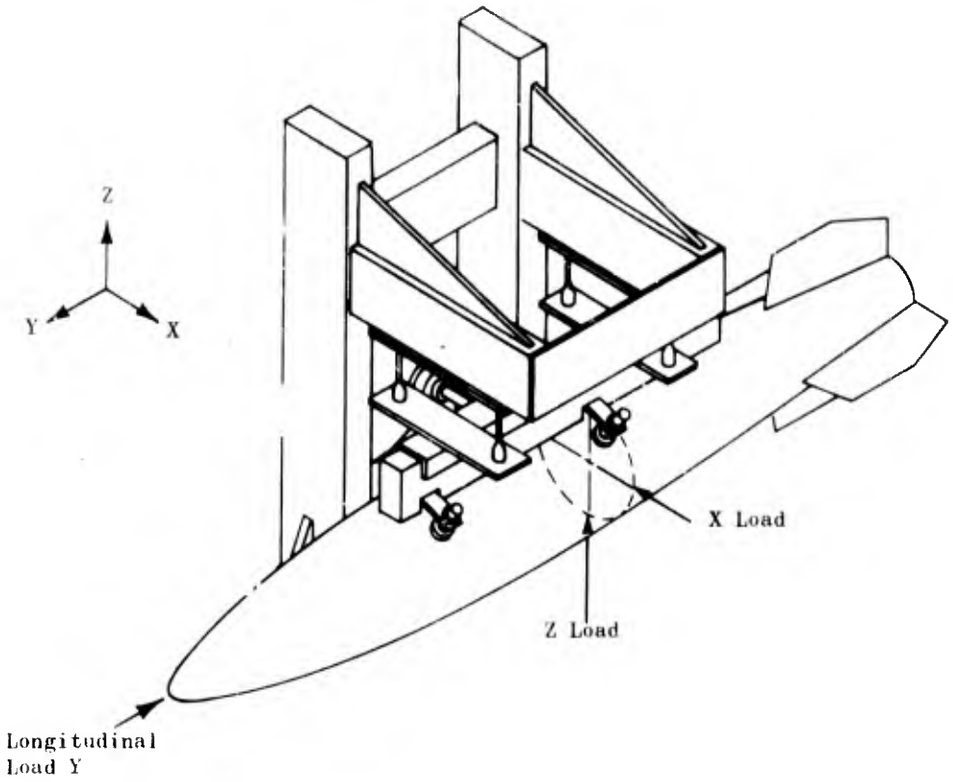

(U) Figure 4-28. Loads System Calibration

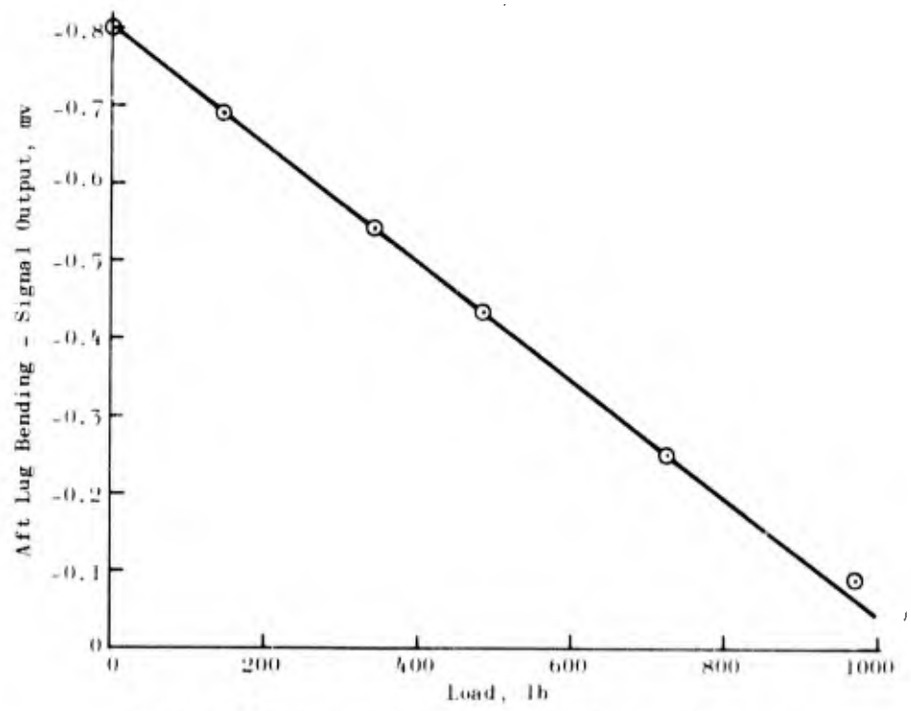

Figure 4-29. Static Load Calibration, Y Axis

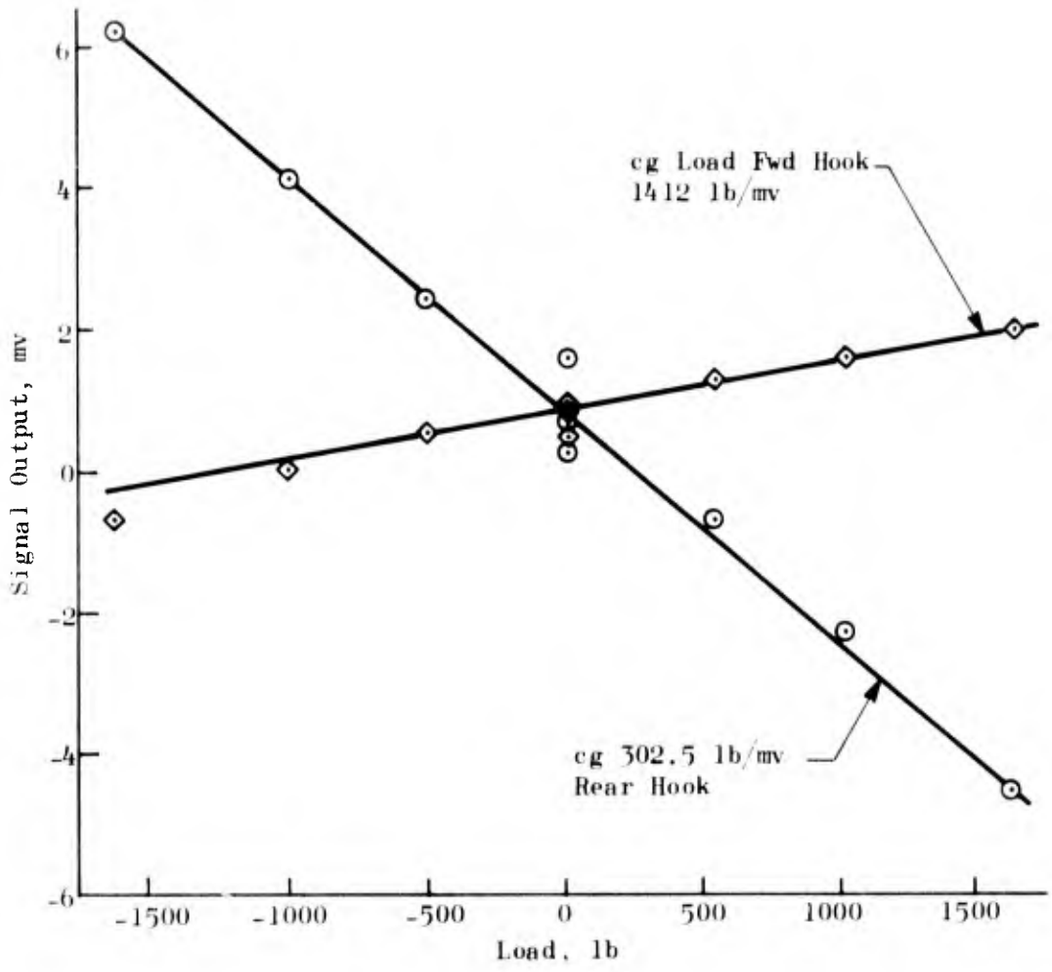

Figure 4-30. Static Load Calibration, Z-Axis

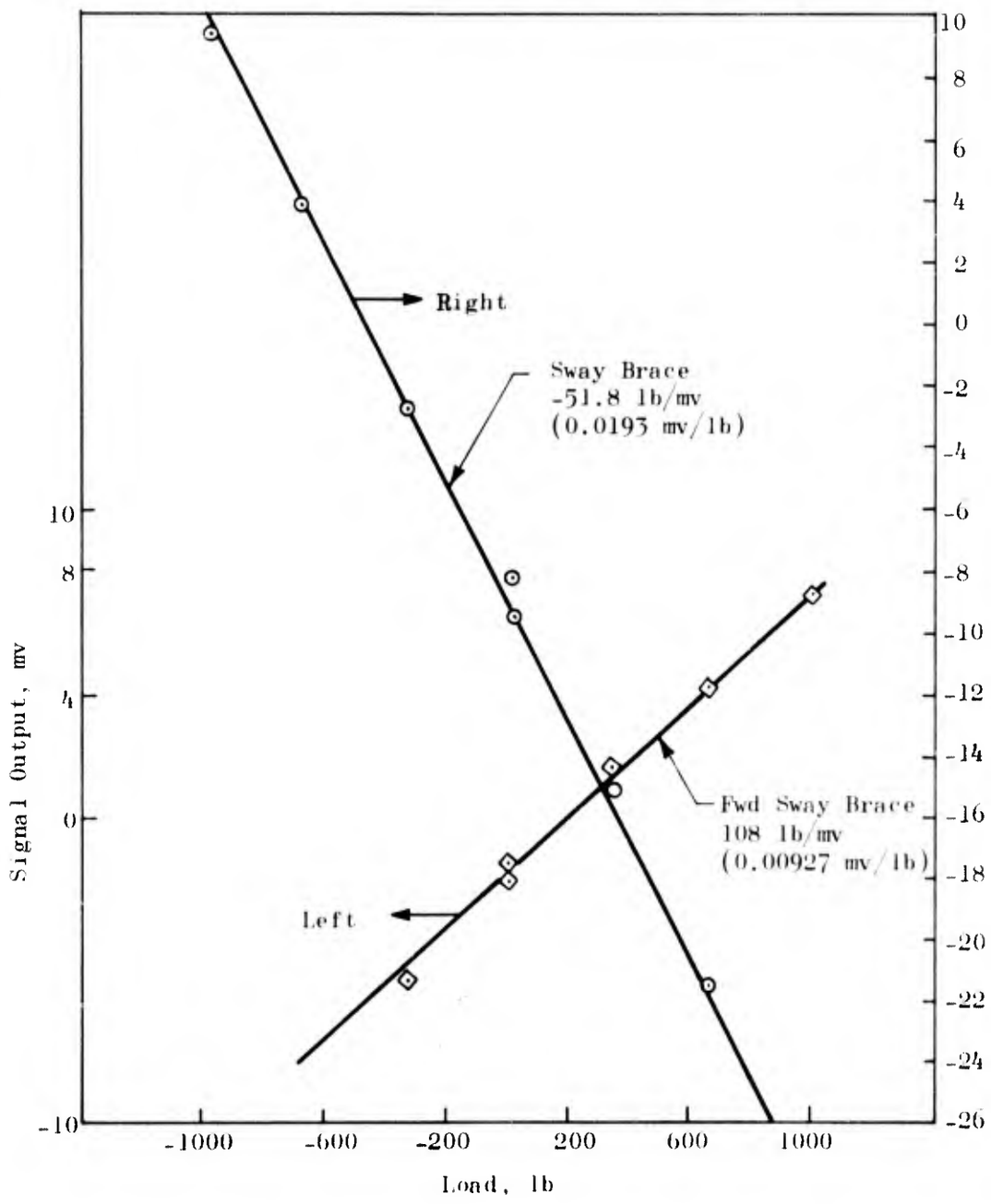

Figure 4-31. Static Load Calibration, X-Axis

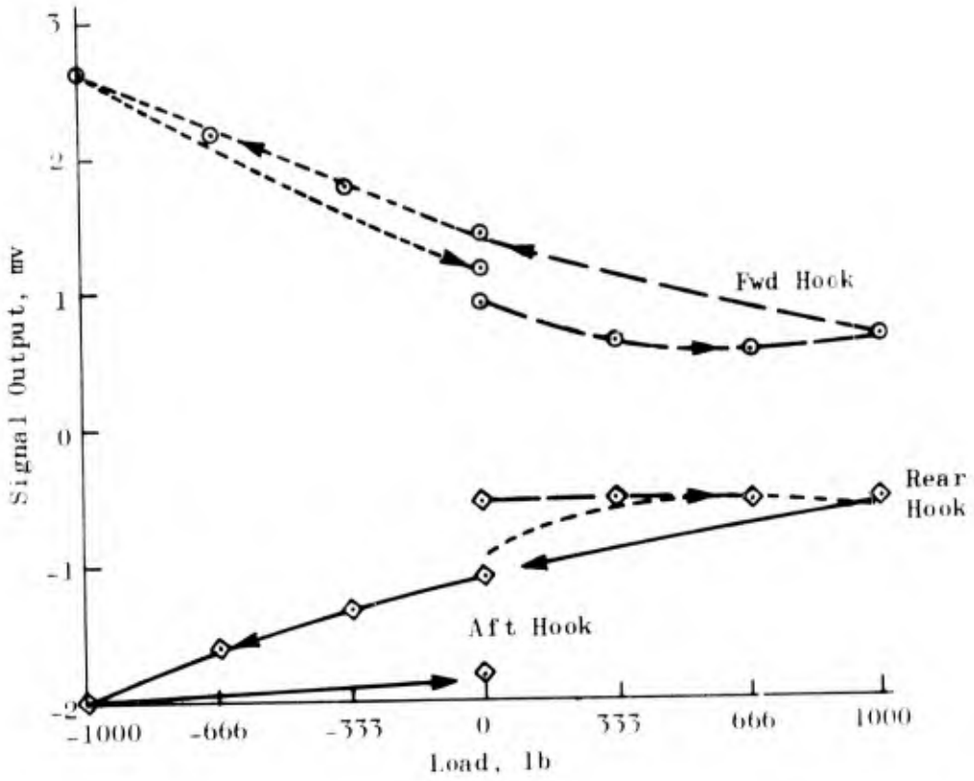

(U) Figure 4-32. Lateral Load Test, X Axis

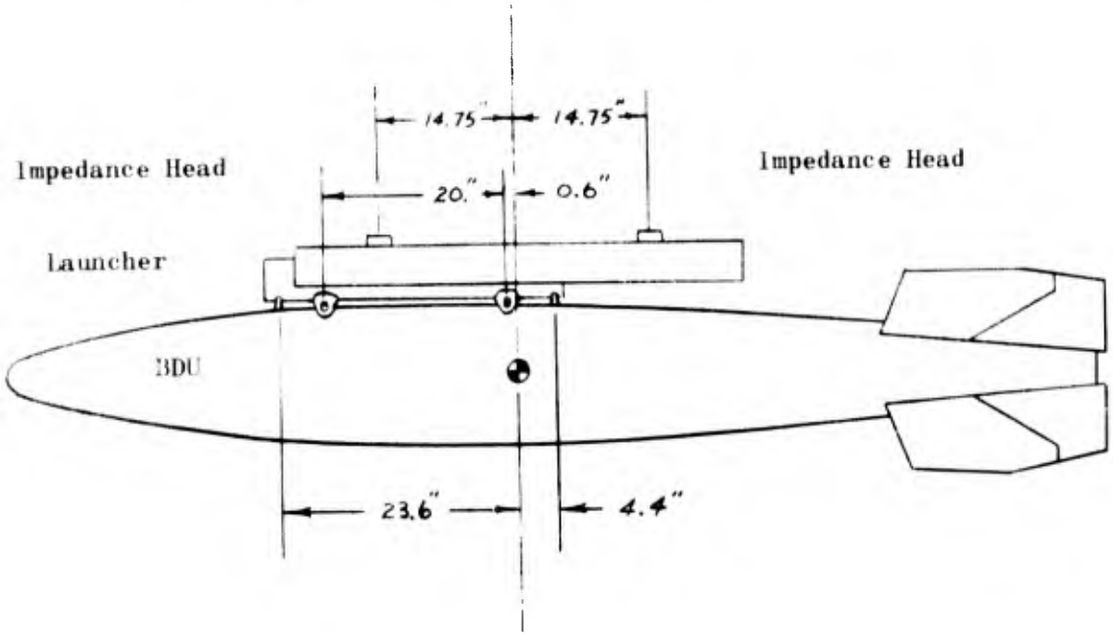

Figure 4-33. Dimensions for Launcher Static Analysis (Z-Axis)

TABLE 4-4

LOADS MEASURING SYSTEM CALIBRATION VALUES

Element	No-Load Output, mv	Calibration Factor, lb/mv
Forward Sway Brace X-Axis	-1.7	35.05
Aft Sway Brace X-Axis	+6.9	35.0
Aft Lug Bending Y-Axis	-0.8	1315.0
Aft Lug Tension Z-Axis	+0.9	258.0
Forward Lug Tension Z-Axis	+0.9	208.0

It should be noted that the sway brace responses were interpreted to result from a horizontal force that is through and perpendicular to the BDU centerline, approximately 8 inches from the launcher. Consequently, moment transfer to the launcher is a horizontal force multiplied by the 8-inch distance.

It is interesting to compare launch-lug calibrations in assembly with those of the lugs alone. When weights were hung on the instrumented lugs only, the factors were found to be 100 lb/mv and 83.3 lb/mv for the aft and forward lugs respectively. The apparent loss in sensitivity (i.e., 100 → 258 lb/mv and 83.3 → 208 lb/mv, see Table 4-4) is introduced by the pretensioning in the launcher. Incidentally, the aft-lug-only factor of 100 lb/mv is 7.5 times more sensitive than that lug when originally instrumented with metal foil strain gages.

One facet of the instrumented launcher assembly that must be regarded with care is the pretensioning of components introduced by the sway brace set screws. If the launcher is disconnected from the BDU the sensing element bridges will be unbalanced. Upon reassembly, those screws must be adjusted to return the bridges to near null balance so that their signal will remain within the band-width capabilities of the data acquisition system. The procedure that was used for calibration

test was as is understood to be standard practice. The steps were as follows:

1. Mount BDU into launcher and snug sway brace screws
2. Turn two aft sway brace screws one-half turn simultaneously
3. Turn two forward sway brace screws one-half turn simultaneously
4. Simultaneously turn two aft sway brace screws one-fourth turn
5. Simultaneously turn two forward sway brace screws one-fourth turn
6. Tighten the locking nuts in place

This completed the static calibration of the flight loads measuring system.

Thermal Calibration

During the final temperature calibration steps of the instrumented launcher and BDU, a calibration shift was incurred on some of the propellant section circuitry due to thermal excursions during the calibration sequence. The new calibration curves for the changed circuits are shown in Fig. 4-34 through 4-38.

X-Axis Instrumented Launcher

0.5-g Sine Sweep Vibration, 20 September 1971. The soft-mount instrumented launcher was used for X-axis 0.5-g sine sweep vibration because the stiffness of the total system with the launcher installed was high enough to permit correlation of impedance head data and instrumented launcher data. Such correlation was essential for the subsequent actual flight test analysis and eventual simulation. Further details are presented in the discussion on launcher flexibility under Section 5.

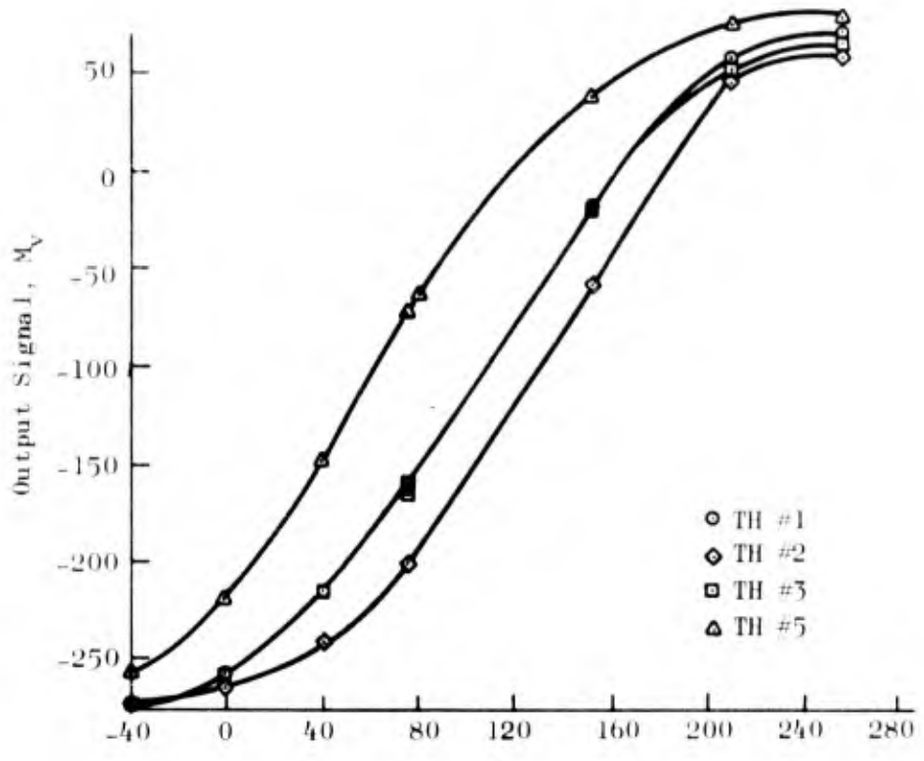

Figure 4-34. Thermistor Circuits No.s 1, 2, 3, and 5, Output Signal vs Temperature

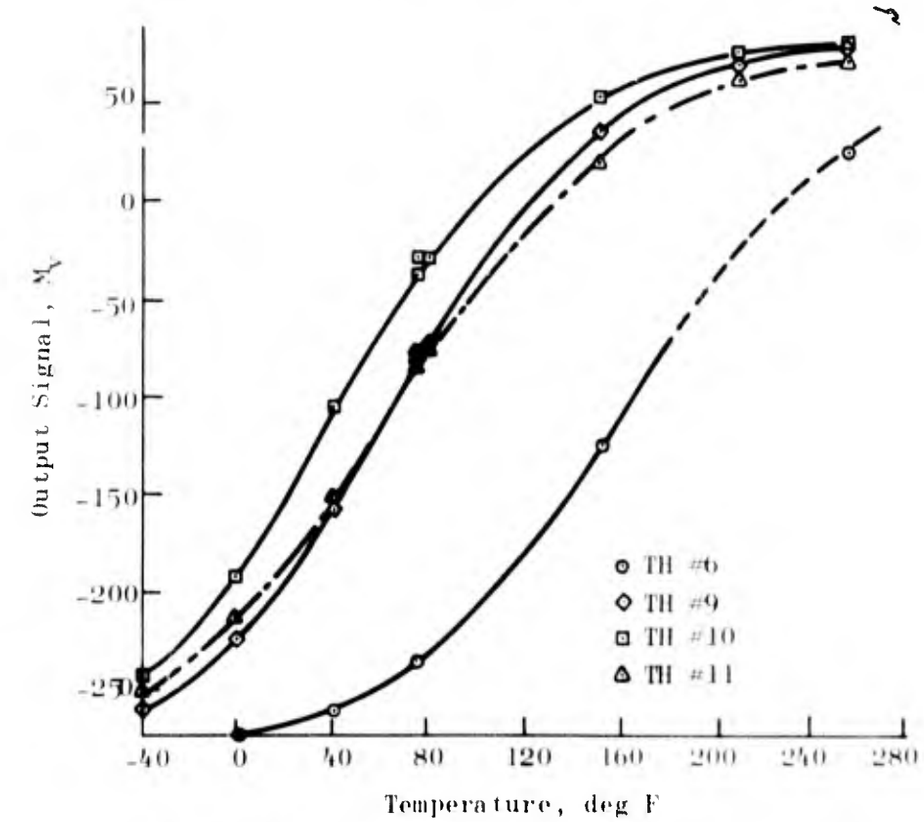

Figure 4-35. Thermistor Circuits No.s 6, 9, 10, and 11, Output Signals vs Temperature

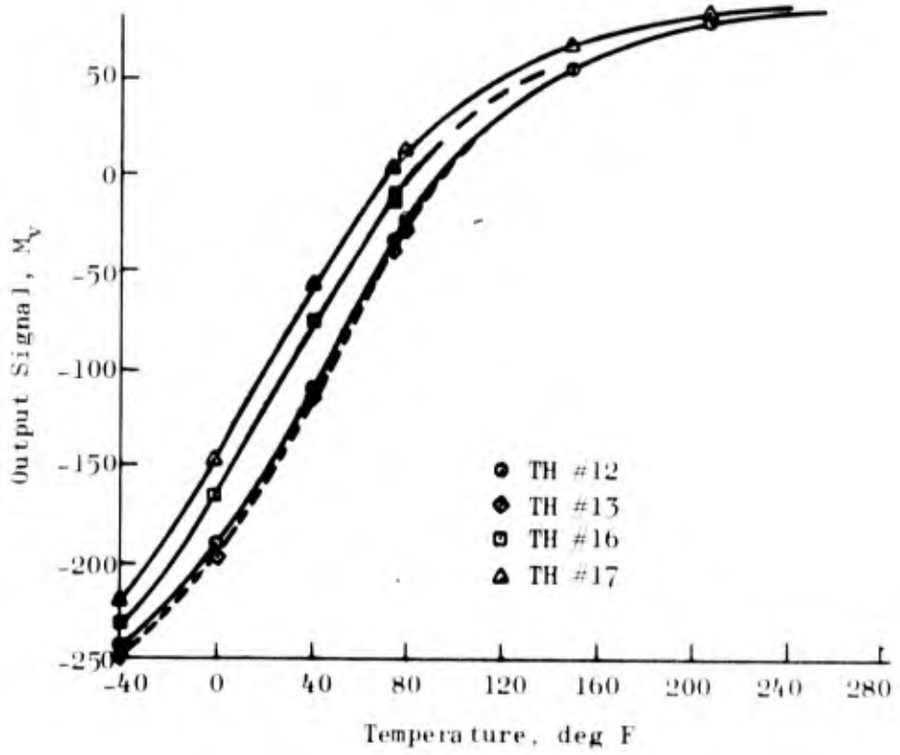

Figure 4-36. Thermistor Circuits No.s 12, 13, 16, and 17, Output Signals vs Temperature

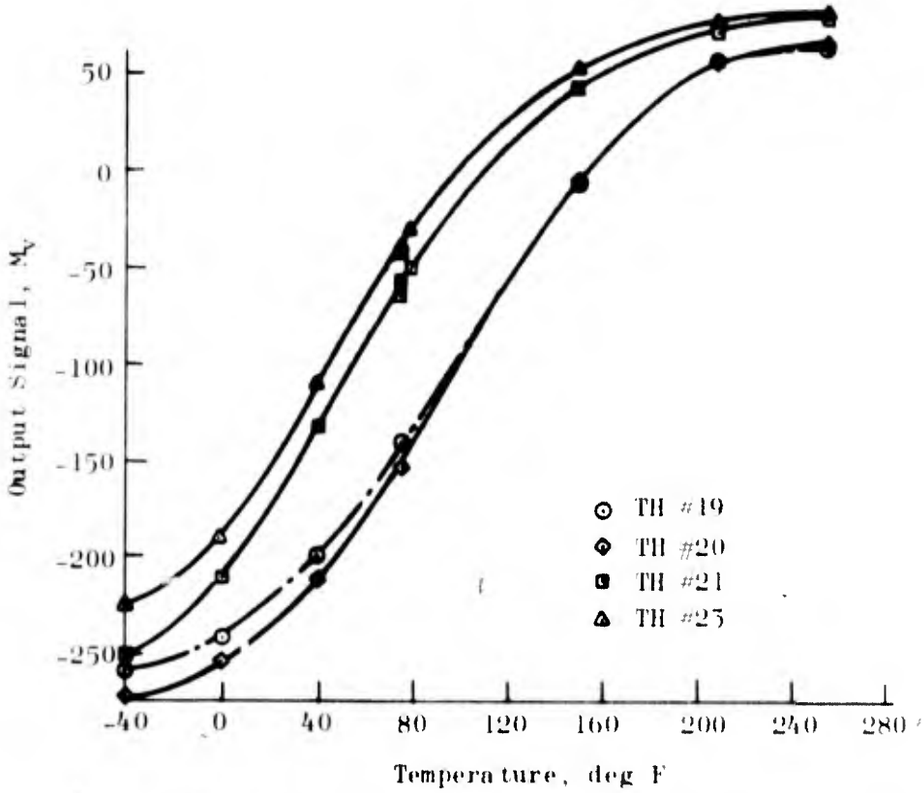

Figure 4-37. Thermistor Circuits No.s 19, 20, 21, and 23, Output Signals vs Temperature

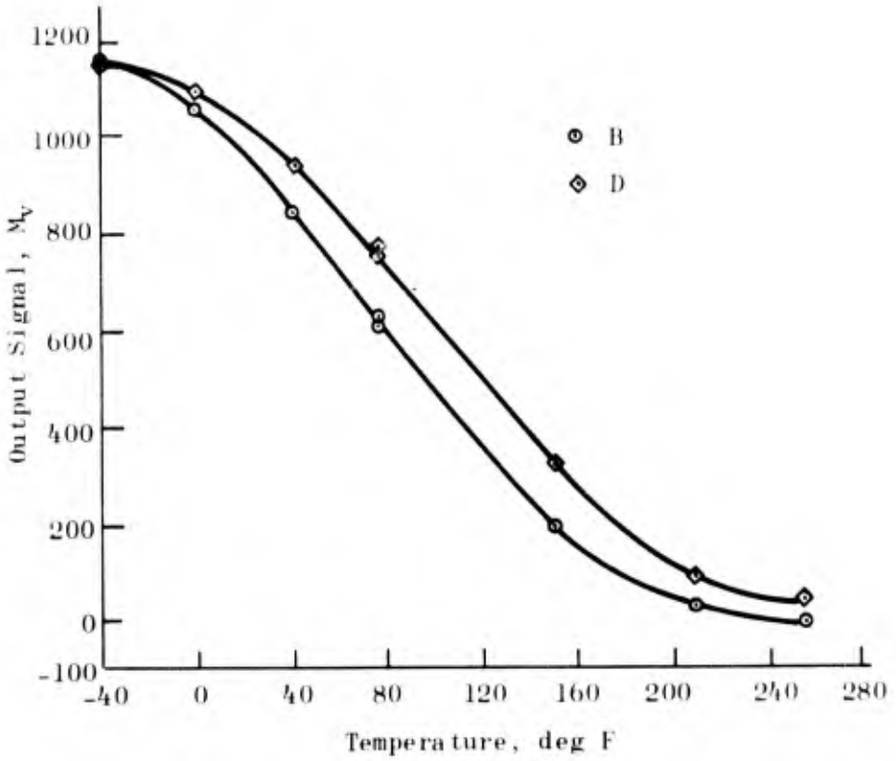

Figure 4-38. Thermistor Circuits B and D, Output Signals vs Temperature

Data from input control channels are shown in Fig. 4-39 and -40. External accelerometer channels (Fig. 4-41) were reduced on all subsequent test cycles because mode shapes defined earlier were not expected to change. Reduced data from this cycle are shown in Appendix G.

Y-axis response indicated by the aft launch lug bending channel was almost constant at 64 millivolts (which corresponds to a very high force). During the review conducted at the end of the test, it was concluded that this signal was a direct-current bridge unbalance caused by shifting the BDU with regard to the launcher and that the response resulting from vibration testing was very low. A more thorough review of the tape recording after the test program was completed shows a direct-current unbalance that saturated the amplifier. Consequently, data from this channel are not valid. It will be necessary to adjust

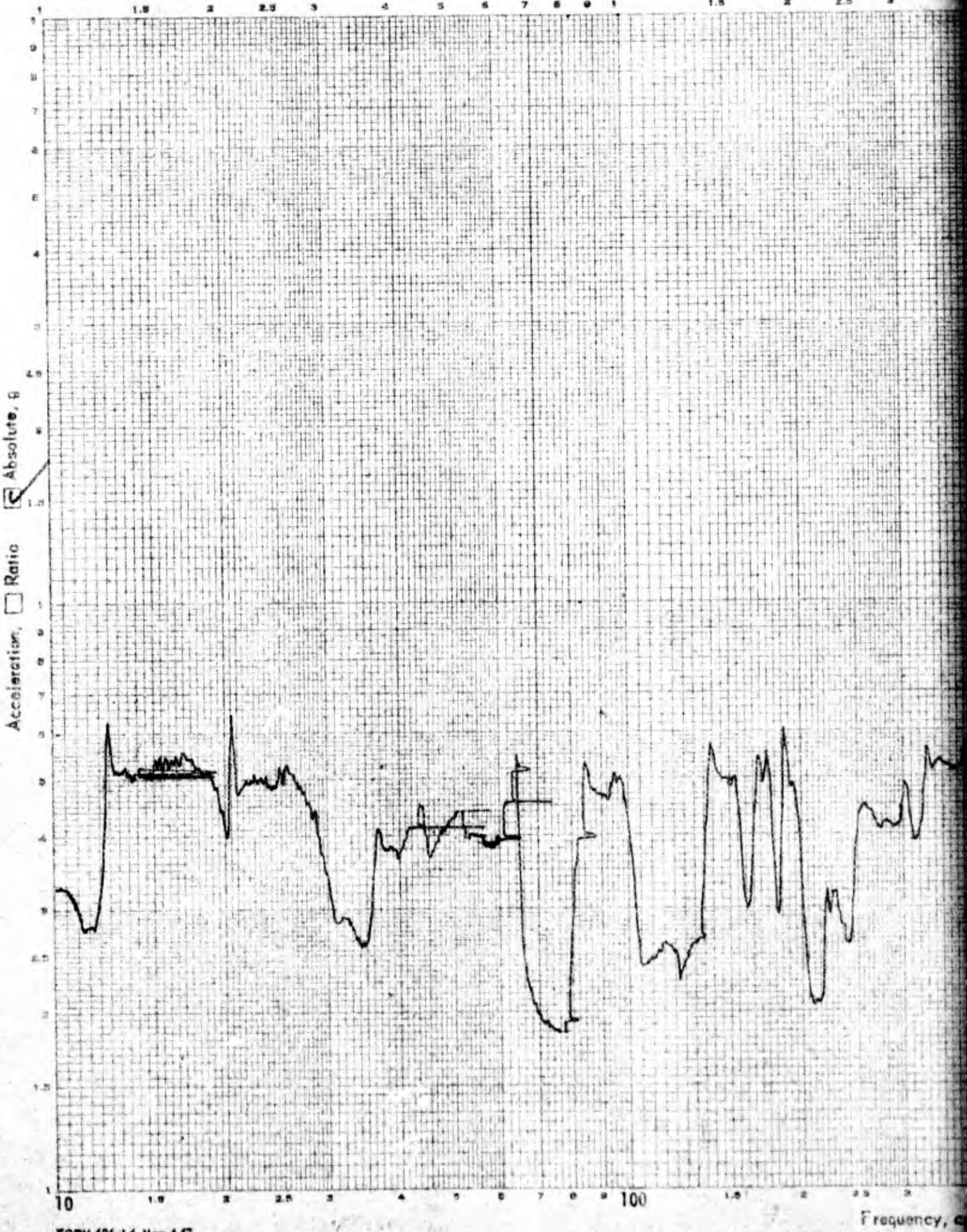

FORM 626-J-6 Nov 4-67

Program BDU

Date 9-20-71 Time 1626

ITO
ETO No. _____ S/N _____
EWR

Test Axis X

Cond Temp AMB

Frequency Range 10-2000 Hz

Sweep Rate .63 OCT/MIN

Input Acceleration Level .5 g

Control Channel 5 E 8

Technician [illegible]

Engineer MULLINS

Amplitude Ratio:

CH _____ ☐ Filtered

CH 15 ☑ Unfiltered

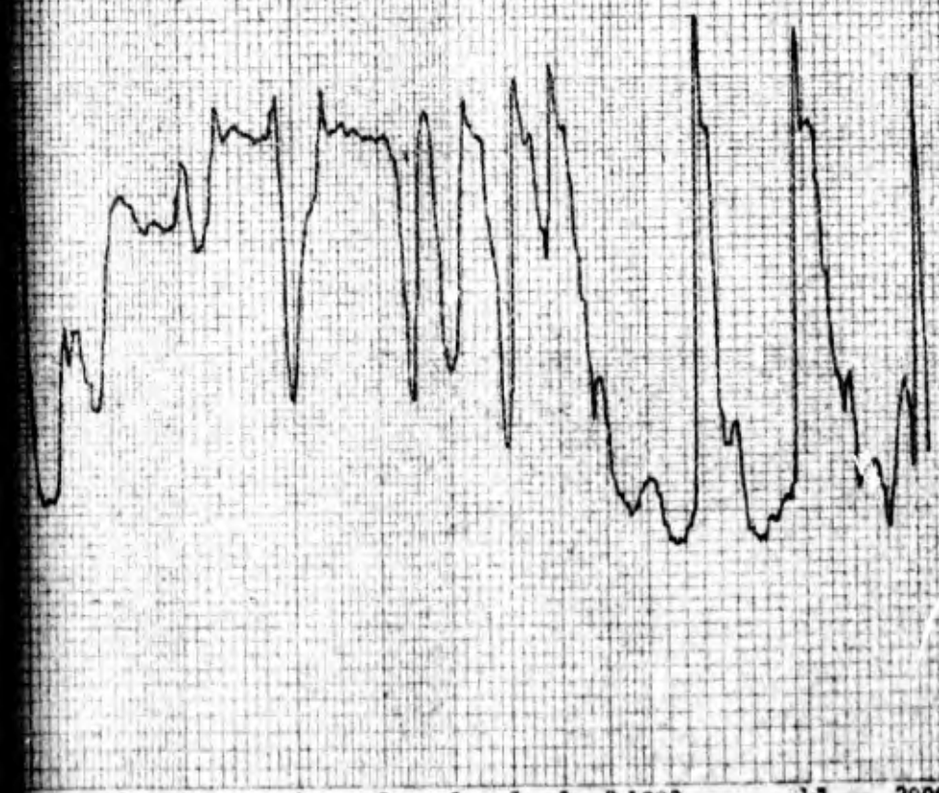

1000 2000

Frequency, cps

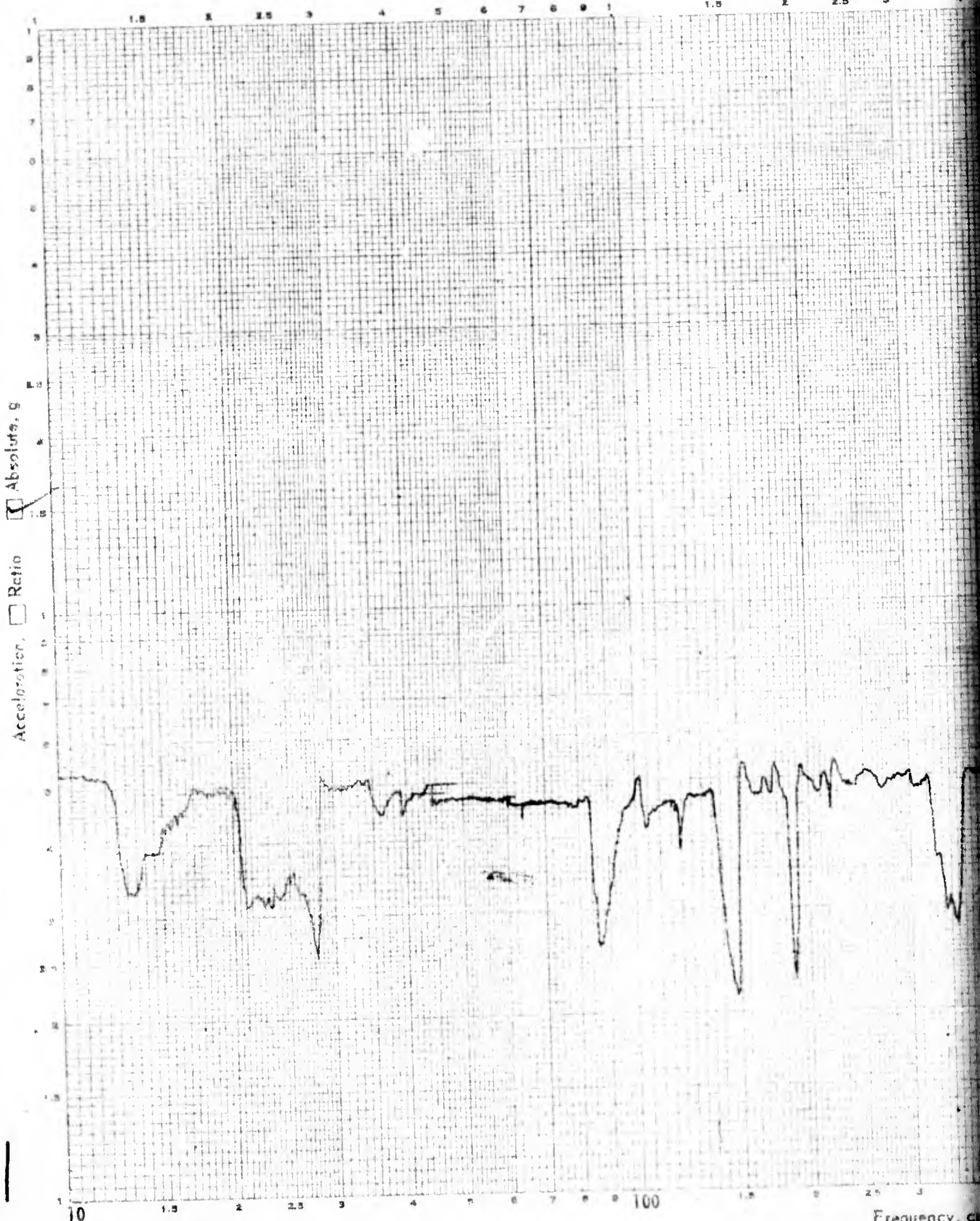

19

FORM 626-J-6 Now 4-67

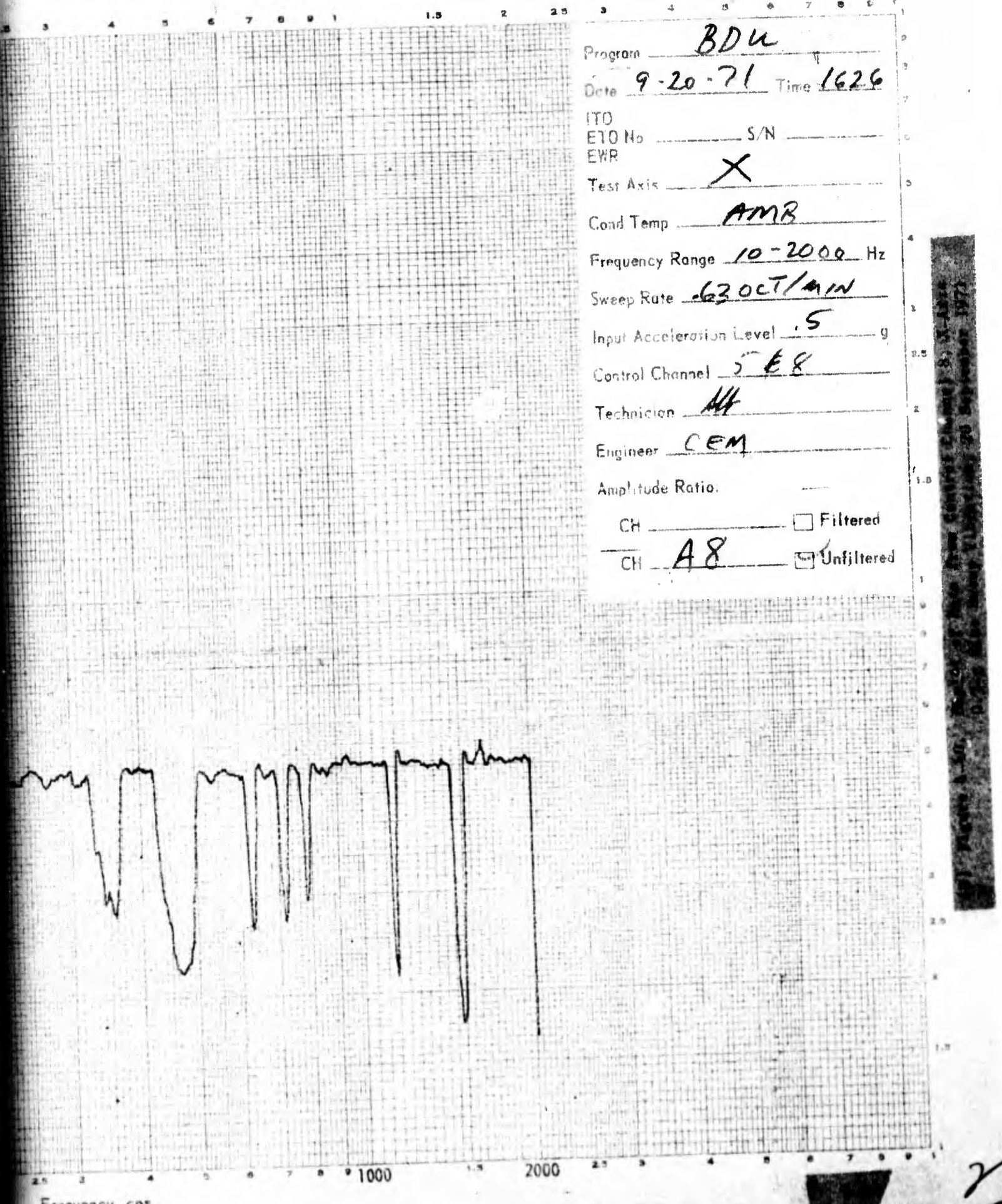
Program BDU
Date 9-20-71 Time 1626
ITO
ETO No S/N
EWR
Test Axis X
Cond Temp AMB
Frequency Range 10-2000 Hz
Sweep Rate .63 OCT/MIN
Input Acceleration Level .5 g
Control Channel 5 E 8
Technician MH
Engineer CEM
Amplitude Ratio
CH Filtered
CH A8 Unfiltered
1000
2000
Frequency, cps

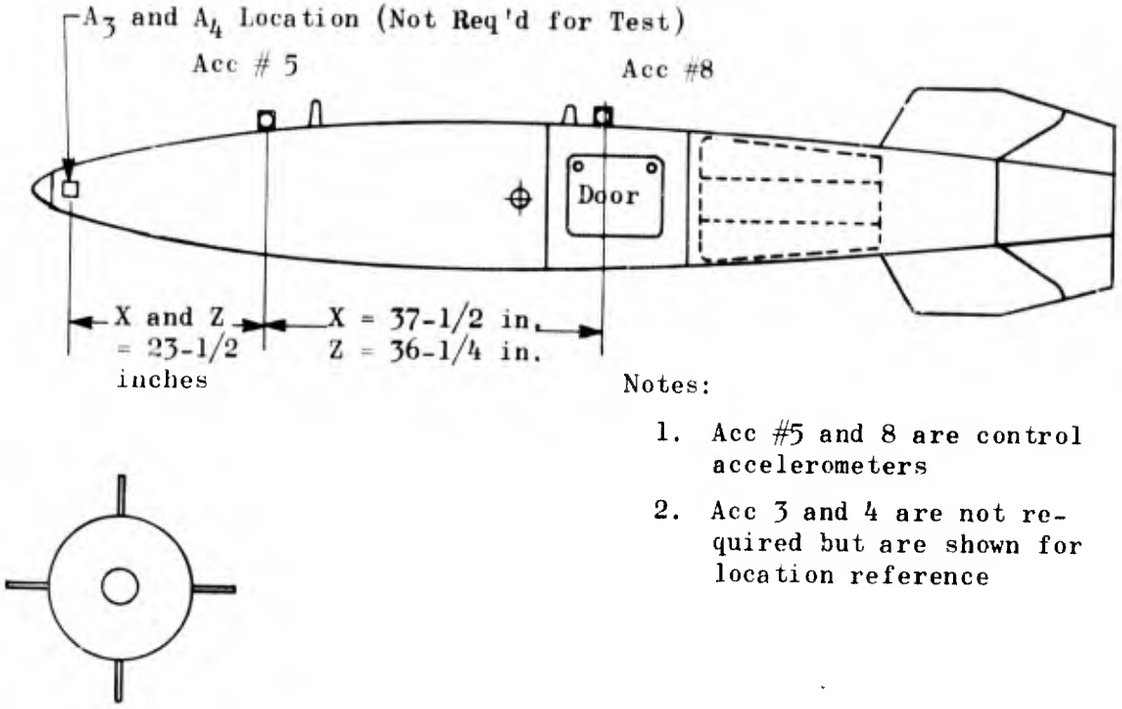

Figure 4-41. Reduced Accelerometer Location Plan

the bridge balance and dynamic range for flight testing and subsequent ground testing.

Data from other channels are valid with the possible exception of that from the forward sway brace between 25 and 32 Hz. The flight recorder tape should be examined in that regime.

Aeroheat Only, 22 September 1971. The BDU was subjected to aeroheat (Fig. 4-42) to provide a baseline for defining gage(s) response due to aeroheating only. Some variation in gage readout was expected to occur due to aeroheating variations from cycle to cycle. (This may be accounted for by analytical adjustments of data obtained from the test.) The aeroheat control section was directly over the propellant section of the BDU. Replots of data obtained during aeroheat are shown in Fig. 4-43. Figure 4-44 shows the location of external thermocouples. Thermistor location was the same as shown earlier. Carbon dioxide was

9-23-71789

Figure 4-42. Aeroheat Setup for BDU

piped into the electronics section to prevent excessive heating on this and all subsequent aeroheat cycles. Reduced data from these cycles are shown on pages 4-19 through 4-26.

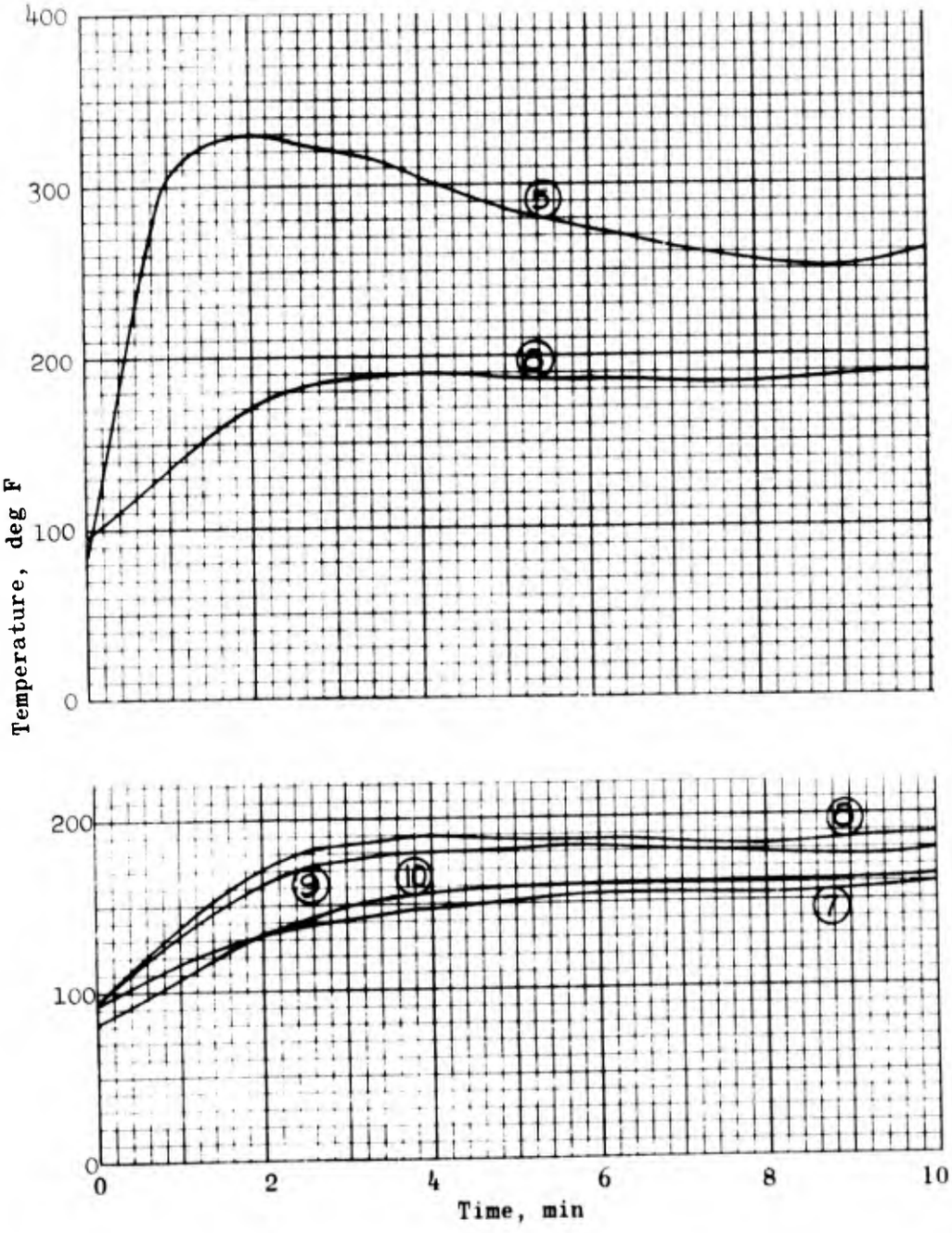

Figure 4-43. Replots of Data Obtained During Aeroheat Only

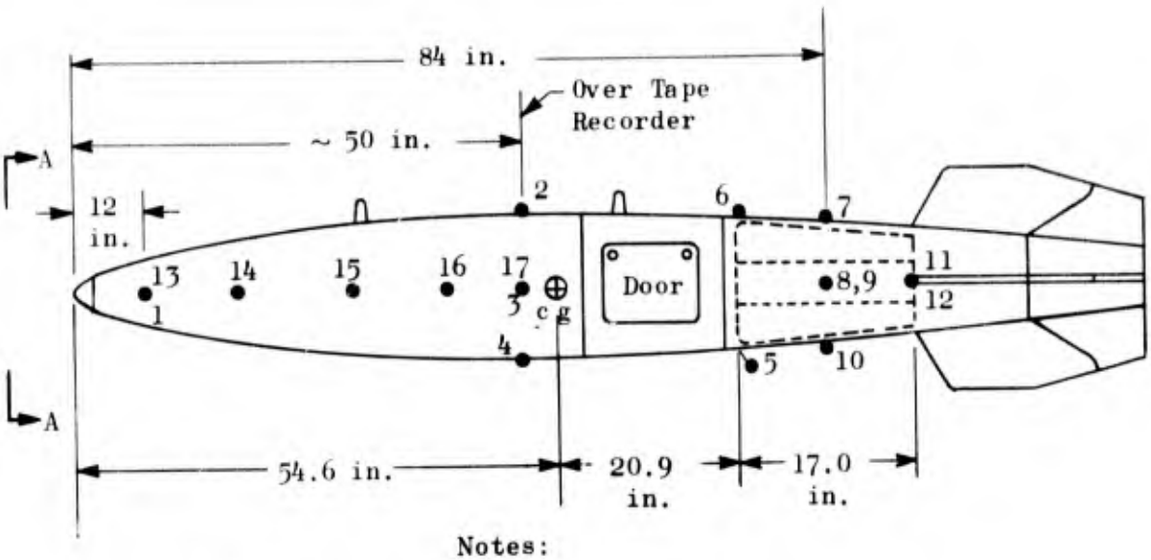

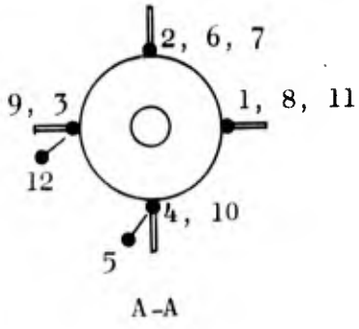

Notes:

1. T.C.'s 7, 8, 9, 10 are control T.C.'s.
2. Five additional T.C.'s (13, 14, 15, 16, and 17) will be located directly opposite NWC installed internal T.C.
3. One additional T.C. will be located on tape recorder. Max temp for this T.C. is 100 F.
4. T.C.'s 5 and 12 will be ~ 1 inch from surface to measure air temperature.

Figure 4-44. Thermocouple Location for Aeroheat Cycle(s)

Combined Random Vibration and Aeroheat, 24 September 1971. The first combined aeroheat and vibration test was conducted 24 September 1971. Aeroheat input data are shown in Fig. 4-45. The input vibration spectrum is shown in Fig. 4-22. Vibration data were obtained the first 4 minutes and about the last 4 minutes of the run since total run time and tape identification data exceeded the on-board tape capacity. Thermocouple location was the same as in the previous aeroheat-only cycle, Ref. Fig. 4-44. Reduced data in the form of spectral analyses for this cycle are shown in Appendix H.

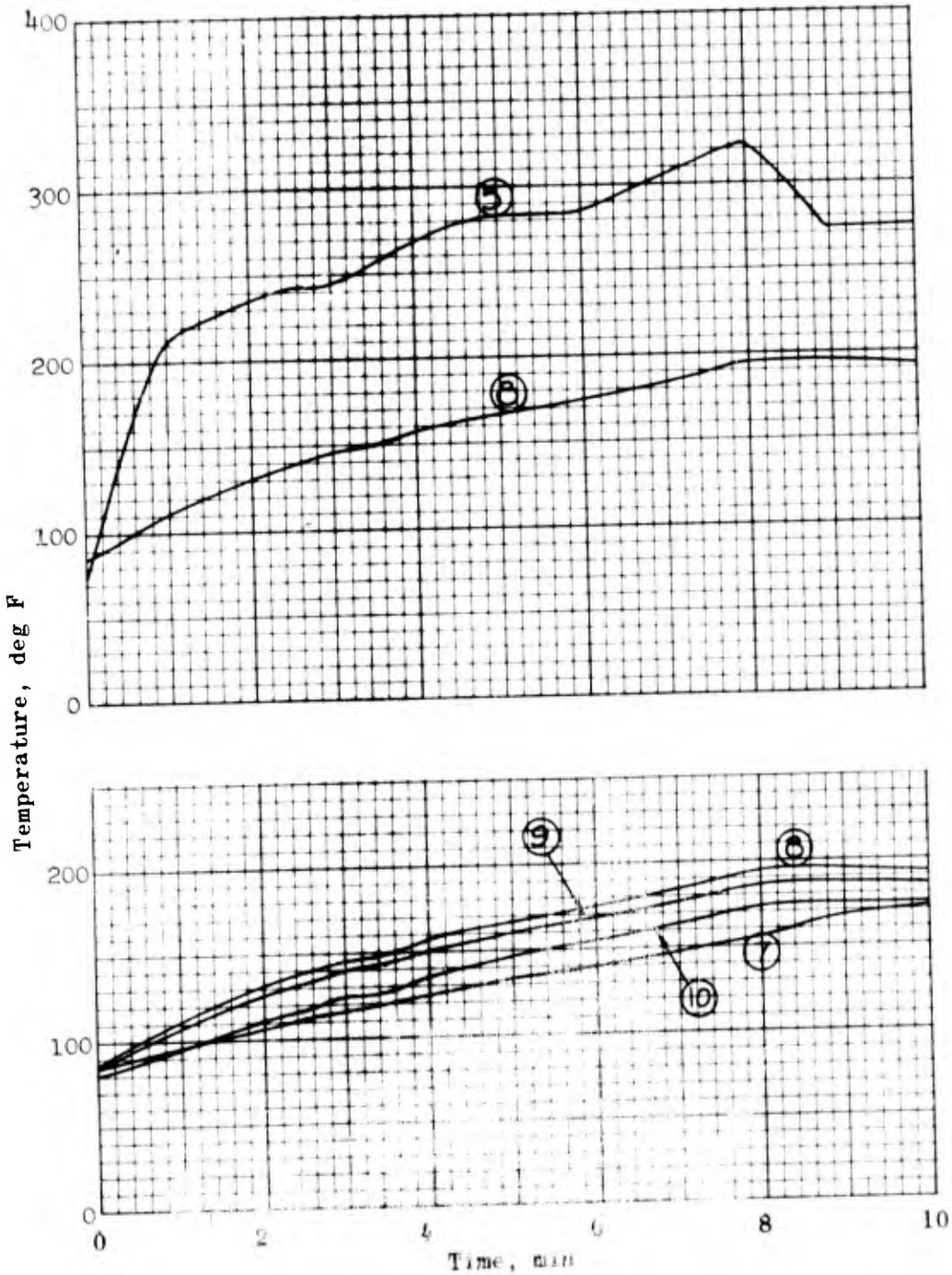

Figure 4-45. Aeroheat Input Data for Combined Random Vibration and Aeroheat

Instrumented Launcher, Z-Axis

0.5-g Sine Sweep Vibration, 28 September 1971. Another 0.5-g sine sweep vibration was conducted to provide a comparison of the impedance head data and the special instrumented sway braces and launch lugs. The reduced external accelerometer location was used for this test since the BDU vibration mode for the Z-axis was already characterized. Reduced data from the cycle are contained in Appendix I.

The aft launch lug (Y axis) bending channel had a large direct-current unbalance that saturated the amplifier, but data from all other launcher channels are valid. Surprisingly, the signal from the forward sway brace and the forward lug were too small to be measured. However, the forward impedance forces were on the order of 100 pounds, which verified the low forward lug response.

Combined Random Vibration and Aeroheat, 28 September 1971. The combined random vibration and aeroheat on 28 September 1971 completed the planned tests for verifying the integrity of the BDU for flight test. Aeroheat and structural data are summarized in Appendix K. Thermocouple locations are shown in Fig. 4-44; resulting case aeroheat data are shown in Fig. 4-46. The input vibration curve is shown in Fig. 4-14. The data accumulation plan on this test was the same as that of the previous combined aeroheat and vibration cycle.

Spectral analysis of several data channels early and late in the aeroheat run shows the response of the unit was only slightly altered by the temperature gradient and rise.

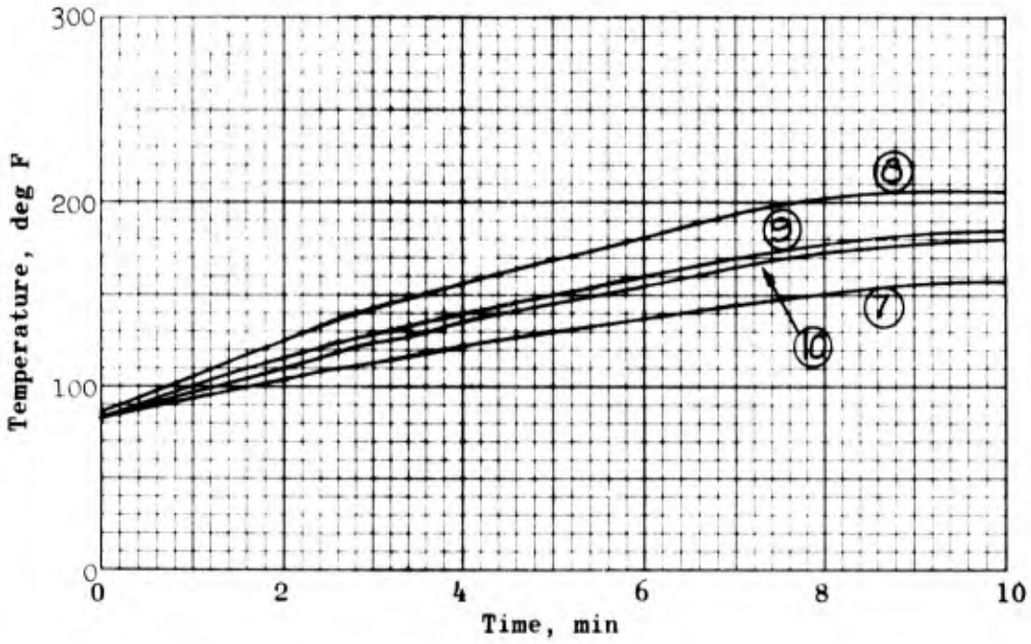

Figure 4-46. Data from Random Vibration and Aeroheat, 28 September 1971

5. PHASE III - DATA ANALYSIS AND INTERPRETATION

MECHANICAL IMPEDANCE

When a force is applied at a point on a mechanical structure, that structure will respond with a deflection. The ratio of the force to deflection is a measure of the stiffness or spring constant of the structure at that point. If the forces are dynamic, one can also measure velocities and acceleration on the structure. The mechanical impedance of a structure is defined as the ratio of the applied force to the resulting velocity at the same frequency. For a sinusoidal force input $F = F_o \sin(\omega t)$ the responding velocity is $V = V_o \sin(\omega t + \varphi)$ where φ is the phase angle between the force and velocity. Then the mechanical impedance

$$Z = \frac{F_o \sin \omega t}{V_o \sin(\omega t + \varphi)} = \frac{F}{V}(\cos \varphi + i \sin \varphi) \qquad (1)$$

can be measured at a point, or the force at one point can be ratioed to the response at other points to give so called transfer impedances.

Mechanical impedance, or its reciprocal, mobility, furnishes information about the dynamic characteristics of a structure. Depending upon the application, related parameters are obtained directly. From basic motion definitions, instantaneous velocity is the time rate of change of displacement; and acceleration is the time rate of change of velocity or;

$$v \equiv \frac{dx}{dt} = \dot{x} \qquad (2)$$

$$a \equiv \frac{dv}{dt} = \frac{d^2x}{dt^2} = \ddot{x} \qquad (3)$$

Ratios of force to these terms are identifiable as follows:

$$\frac{F}{a} = \frac{\text{Force}}{\text{acceleration}} = \text{apparent mass}$$

$$\frac{F}{x} = \frac{\text{Force}}{\text{Displacement}} = \text{dynamic stiffness}$$

Inertness and compliance are the inverse of these respective parameters. The relationship that the phase angle takes for point impedance is as follows:

	F lags a by φ	F lags V by φ_1	F lags X by φ_2
Mass Control	$0 \leq \varphi < +90^0$	$-90 \leq \varphi_1 < 0^0$	$-180 \leq \varphi_2 < -90^0$
Resonance and Anti-Resonance	90^0	0^0	-90^0
Spring Control	$+90 < \varphi \leq +180^0$	$0 < \varphi \leq +90^0$	$-90 < \varphi_2 \leq 0^0$

Note: $\varphi = \varphi_1 - 90^0$; $\varphi_1 = \varphi_2 - 90^0$

With the close relationship existing between apparent mass, impedance, and dynamic stiffness, one can display these parameters on a single graph. A graphical representation typically used in impedance testing is shown in Fig. 5-1. For information, a curve is shown and the resonances identified. Phase angles should also be displayed, as shown at the lower edge of the chart. This phase angle shown is between the force and velocity, and must be adjusted by 90^0 either way to be usable for apparent mass or for dynamic stiffness.

At times it is convenient to plot apparent mass vs survey frequency curves. The mechanical impedance and dynamic stiffness can still be obtained from the plot. Shown in Fig. 5-2 are the associated scales that properly interrelate for interpretation of force over acceleration data. A transparent overlay is included in Appendix K for convenient usage in the test laboratory.

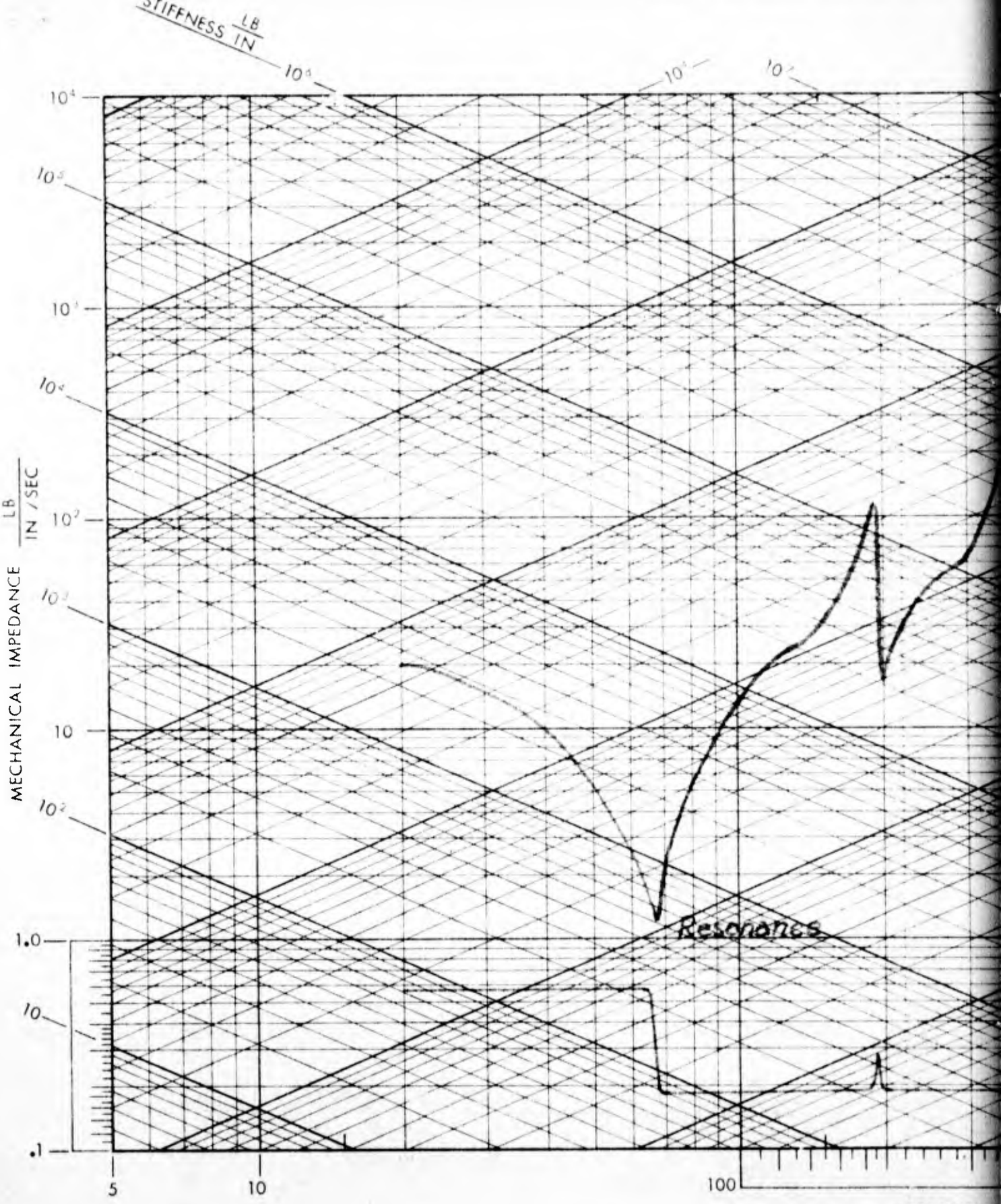

Job No. ..... Item ..... Serial No. .....

Axis/Condition ..... Pickup S/N & Location .....

Analyzer Filter ..... Hz BW Sweep Speed ..... Decades/min. .....

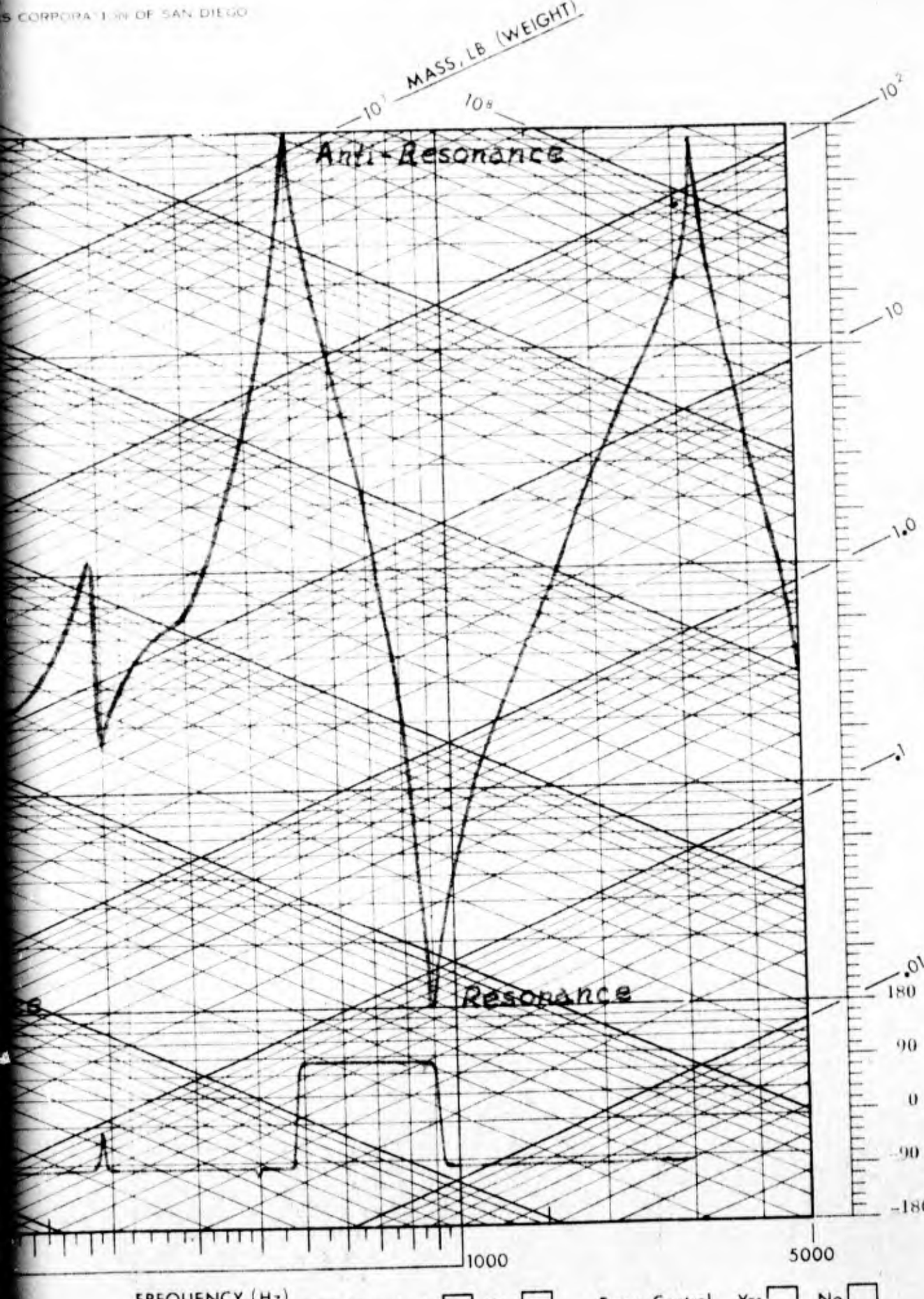

Figure 5-1. A Beam Model Impedance Plot

Mass Cancel In ☐ Out ☐ Force Control Yes ☐ No ☐

Date ..... Time .....

Decades/min. ..... Hz/Sec Operator .....

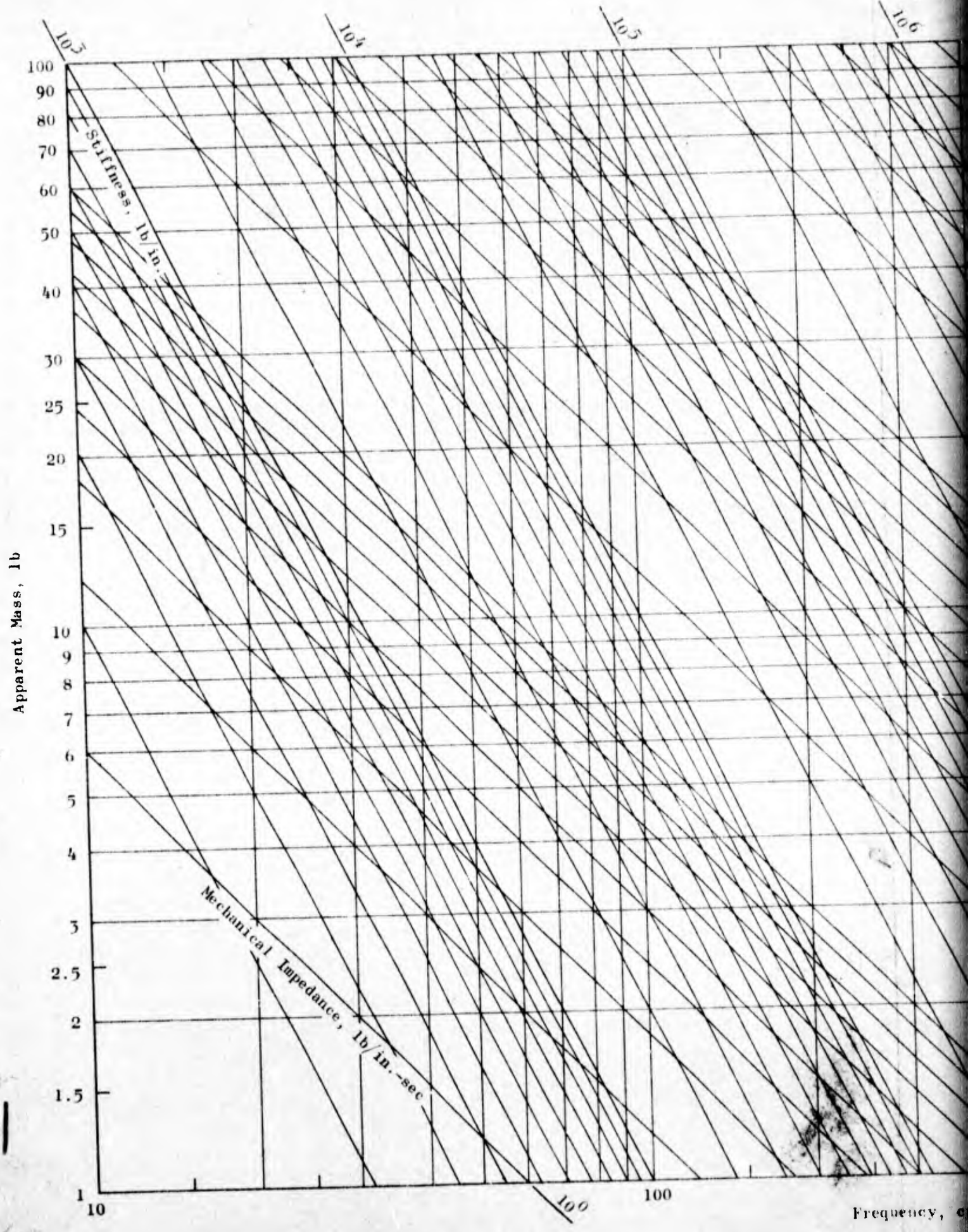
Apparent Mass, lb
Stiffness, lb/in.
Mechanical Impedance, lb/in.-sec
Frequency, c
100
90
80
70
60
50
40
30
25
20
15
10
9
8
7
6
5
4
3
2.5
2
1.5
1
10
100
10^3
10^4
10^5
10^6
10^0

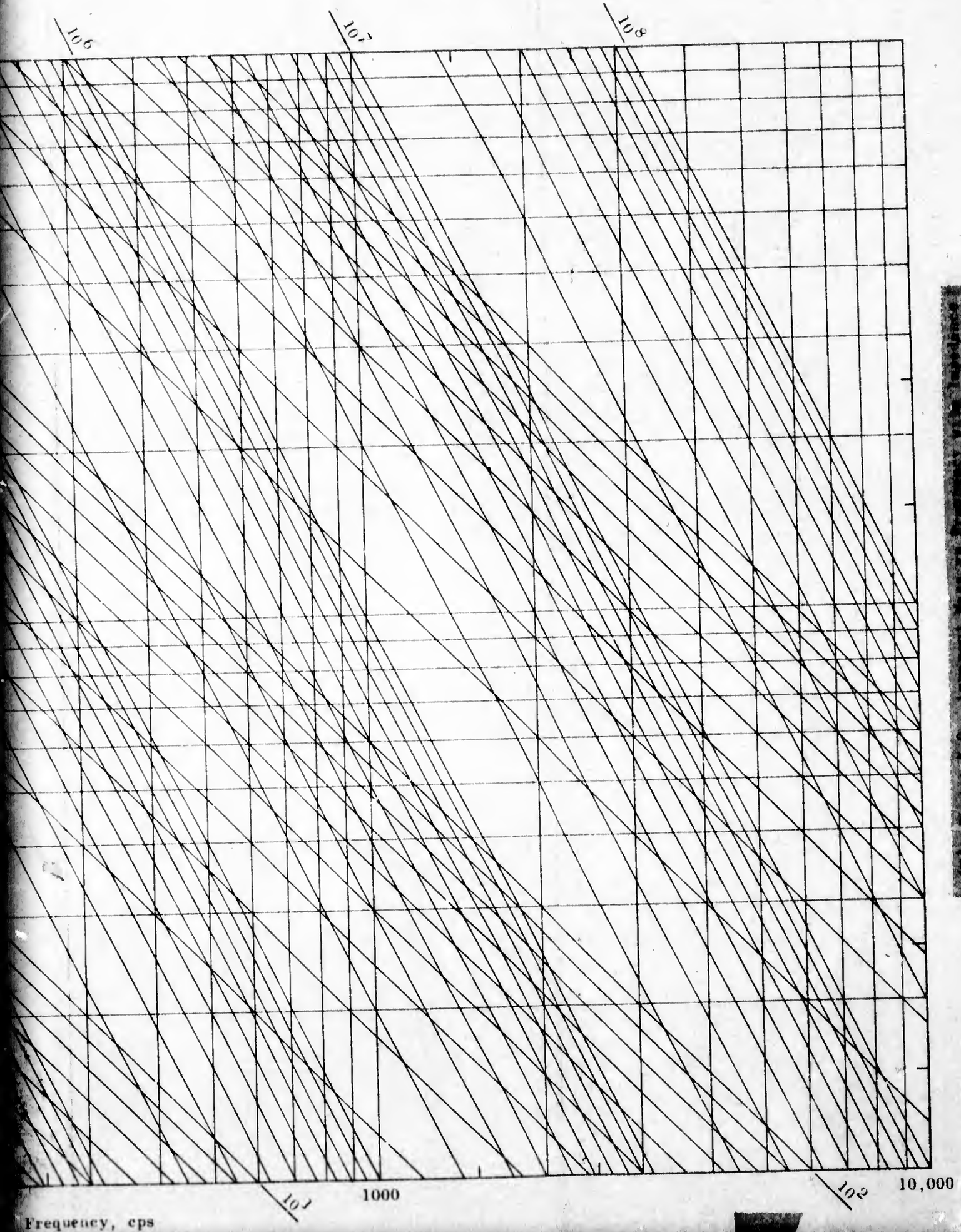
10^6
10^7
10^8
10^1
1000
10^2
10,000
Frequency, cps

In addition to identification of resonant and anti-resonant frequencies of a system, the damping in a system can be determined from the previously described figures. Then if one goes one step further and monitors the velocities at different points on the structure, always maintaining the force input at one point, the resulting (transfer) impedance plots could be overlayed. An exact 3-dimensional picture of the mode shape or mode pattern of the structure is then developed. The phase angles are, of course, an important integral part of these definitions.

BDU impedance measurements are discussed in sections relating to testing axis, and in the section relating to the instrumented launcher.

INSTRUMENTED LAUNCHER DYNAMIC TEST DATA

Data were taken from the instrumented launcher sensor channels simultaneously with other dynamic data during sine survey and random with aeroheat testing. Launcher data were recorded on a magnetic tape along with impedance head measurements for review and for internal comparisons. Signal amplitude-vs-frequency plots of the sine-survey data were made through an analog system. Several amplitude ratio and phase angle comparisons were made between channels that are pertinent. Power spectral density reductions were plotted for the random test data. These data are included in Appendix J and H. Portions of these data are briefly discussed below.

X-AXIS SINE SURVEY

The force necessary to drive the BDU/launcher assembly and a portion of the jig was measured from the impedance head over the frequency range of 10 to 2000 Hz. Since the data are particularly pertinent over the frequency range of 10 to 100 Hz, the force is shown in Fig. 5-3 over that frequency range. The fore and aft sway brace measured response are also shown in this figure. It can be seen that the response between the aft sway brace and the impedance head force compares fairly well for frequencies below the first primary resonance, which appears at approximately 25--35 Hz. At forcing frequencies above this resonance, response indications from both sway braces can be identified with the impedance head force.

Phase angles between the forward and aft sway brace channels were measured. This phase angle remained near zero (i.e., fore and aft end in phase) at frequencies between 10 and 45 Hz. The phase angle then quickly changed so that the aft sway brace led the forward sway brace 180^{o} at 50 Hz and the BDU entered a combination of previously experienced modes, which resulted from several motions being excited simultaneously. This phase passed, and the phase angle remained near 90^{o} between frequencies of 60 and 100 cps.

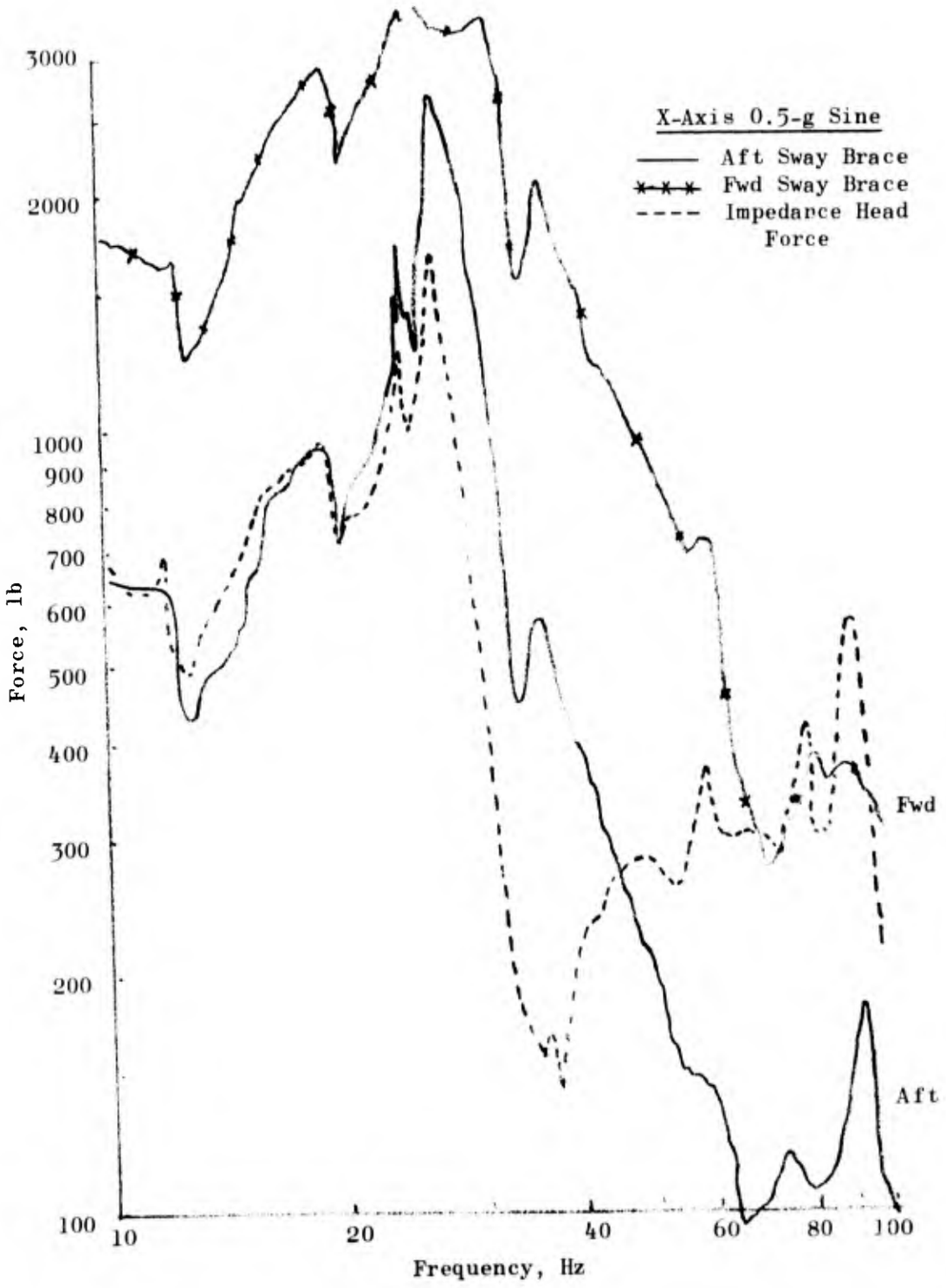

Figure 5-3. Input Force and Sway Brace Response During 0.5-g Sine Survey in X-Axis

Phase angles were also continuously measured between the aft sway brace and the impedance head force. This phase angle remained near zero from 10 to 20 cps then gradually changed to 150^{0} at 32 cps. The angle remained a constant of 150^{0} to about 50 Hz whereupon it quickly switched to -180^{0}. The phase relation then remained near 90^{0} at frequencies between 60 and 100 Hz. It is apparent that the aft sway brace location of the BDU is responding directly with the input forcing function at frequencies below resonance (10--25 Hz) and the foreward sway brace location is responding directly (in phase) to the input at frequencies between 60 and 100 Hz. In the frequency band between 25 and 60 Hz, a coupled transition is occurring that requires little energy to excite. A minimum input energy is required at 36 Hz which is the first resonant frequency for the total system including jig, launcher, and BDU.

An amplification factor of 3 was measured for the forward-to-aft sway brace from 10 to 23 Hz. This factor approaches 1 at 27 Hz then increases to a maximum of 5.9 at 60 Hz. At higher frequencies (70 to 2000 Hz) this factor ranges between 1.4 and 4 and is most usually 3.

The salient features of the dynamic response of the total BDU system, the measured apparent mass in the X axis $\left(\frac{\text{Impedance Head Force}}{\text{Impedance Head Acceleration}}\right)$ are shown in Fig. 5-4. Upon examining this figure, the peaks are identifiable as anti-resonances and occur at frequencies at which the assembly is most difficult (i.e., requires large forces to attain a response) to excite. The valleys are identifiable with resonance frequencies. It is then noted that the first four resonance frequencies are 36, 210, 340, and 600 Hz. There are numerous additional partial valleys in the apparent mass curve that indicate resonances for various components of the system. However, identification of the components and their separate resonance frequencies requires information in addition to that appearing in Fig. 5-4 (see Appendix G).

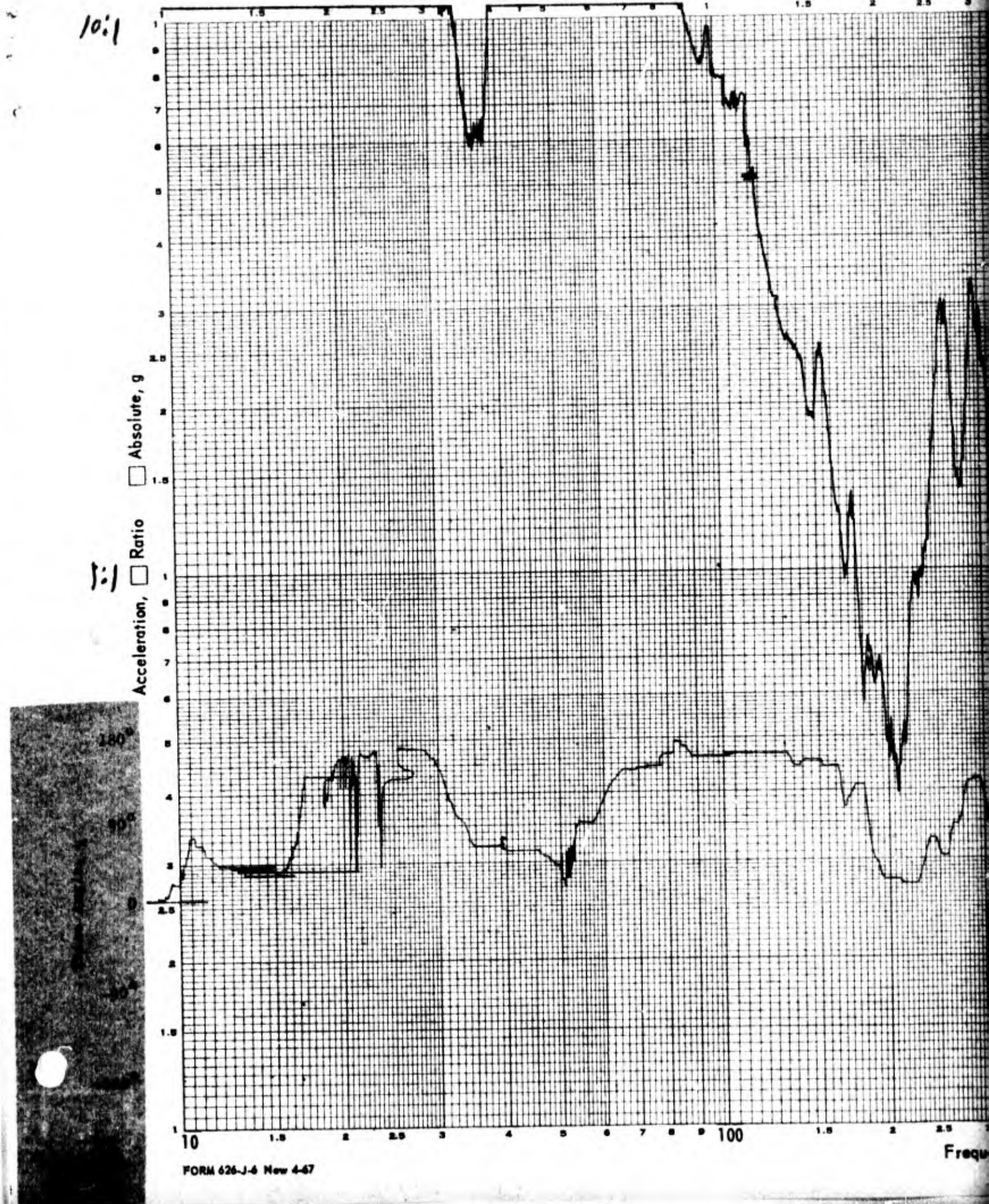
10:1
1:1
Acceleration, ☐ Ratio ☐ Absolute, g
10
100
Freq
180°
90°
0
-90°
FORM 626-J-6 New 4-67

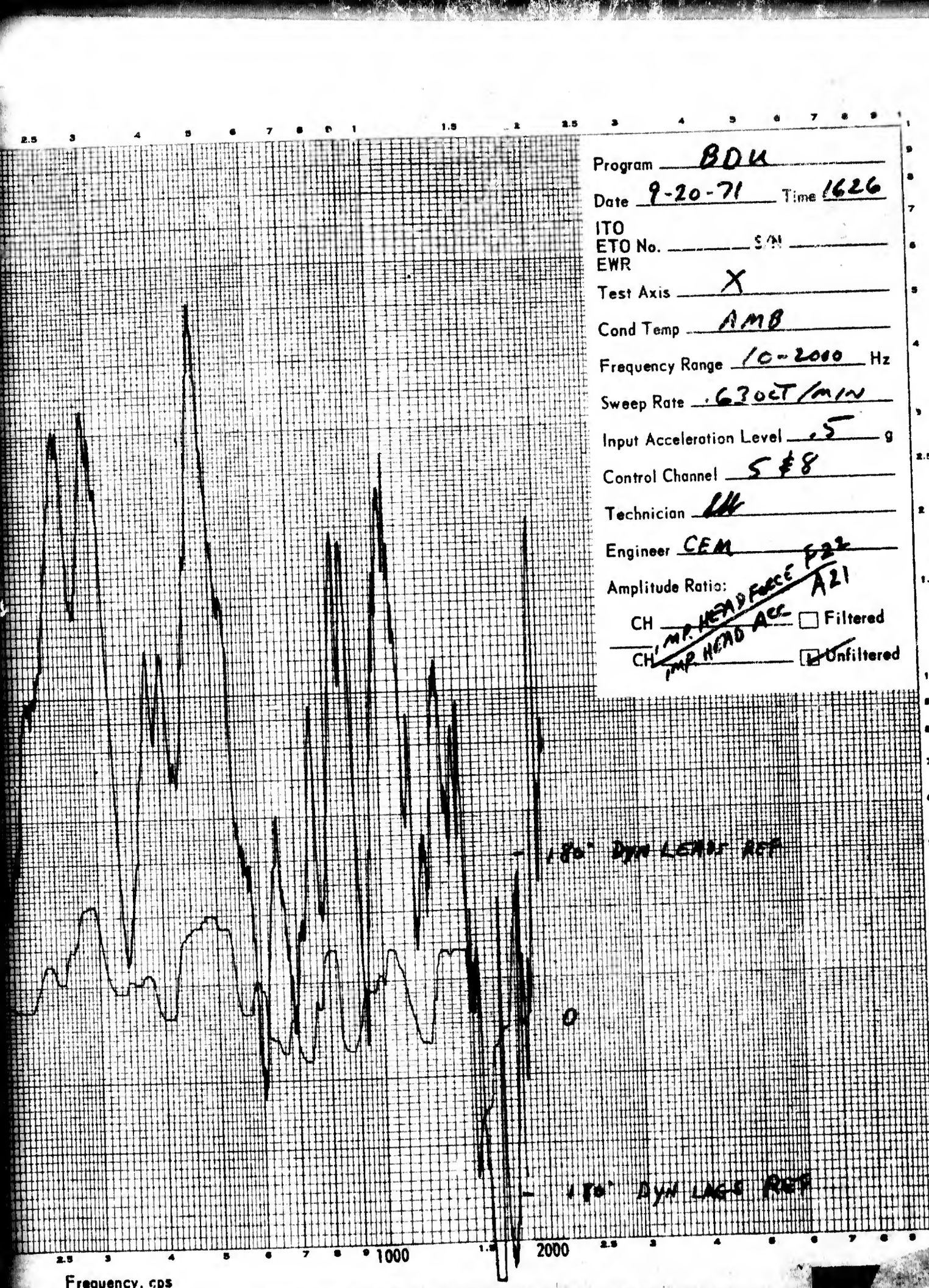
Program BDU
Date 9-20-71 Time 1626
ITO
ETO No. S/N
EWR
Test Axis X
Cond Temp AMB
Frequency Range 10-2000 Hz
Sweep Rate .63 OCT/MIN
Input Acceleration Level .5 g
Control Channel 5 #8
Technician
Engineer CEM
Amplitude Ratio:
CH IMP. HEAD FORCE / IMP. HEAD ACC. F22 / A21
Filtered
Unfiltered
-180° DYN LEADS REF
0
+180° DYN LAGS REF
1000
2000
Frequency, cps

Z-AXIS 0.5-g SINE SURVEY (SOFT MOUNT)

The signal from the fore and aft bending channel on the aft launch hook exceeded the data band width set for this channel during testing, and the amplifier was saturated. The band width for this channel should be changed for subsequent testing.

Aft sway brace data are shown in Fig. 5-5. Equivalent side forces of 290 and 195 pounds are measured at 11.5 and 90 Hz, respectively. Lesser force peaks are measured at 17.5, 35, 180 and 215 Hz. These side forces are not as high as would be expected from the X-axis accelerometers mounted on the BDU measured during the Z-axis testing. Since the instrumented launcher is the direct measuring link in the system, it is concluded that the side forces are low, and that the high accelerometer excursion result from beam flexibility and amplification of (principally) the tail section of the BDU. The forward sway brace measured essentially zero force, which further supports this conclusion. It appears the dynamic motion of the BDU, in both the X and Z axes, are pivoting around the forward launch lug. The tensile force (Z axis) measured by the forward launch lug is also essentially zero.

The aft launch lug measured reaction forces are shown in Fig. 5-6. Forces as high as 8000 pounds (at 24 Hz) were measured. Secondary force peaks of 6000 pounds (at 64 Hz), 6900 pounds (at 95 Hz) and 4400 pounds (at 330 Hz) were also measured. The frequencies at which these peaks occur agree exactly with the force peak frequencies on the aft impedance head. The impedance head forces are also plotted on Fig. 5-6 to show the relationships with the aft launch lug forces, which are substantially higher than the impedance head forces. It is to be expected, in a dynamic system, that forces measured at different locations will be different; however, the differences measured are surprisingly large for the BDU/launcher configuration. Analysis of these data is continuing.

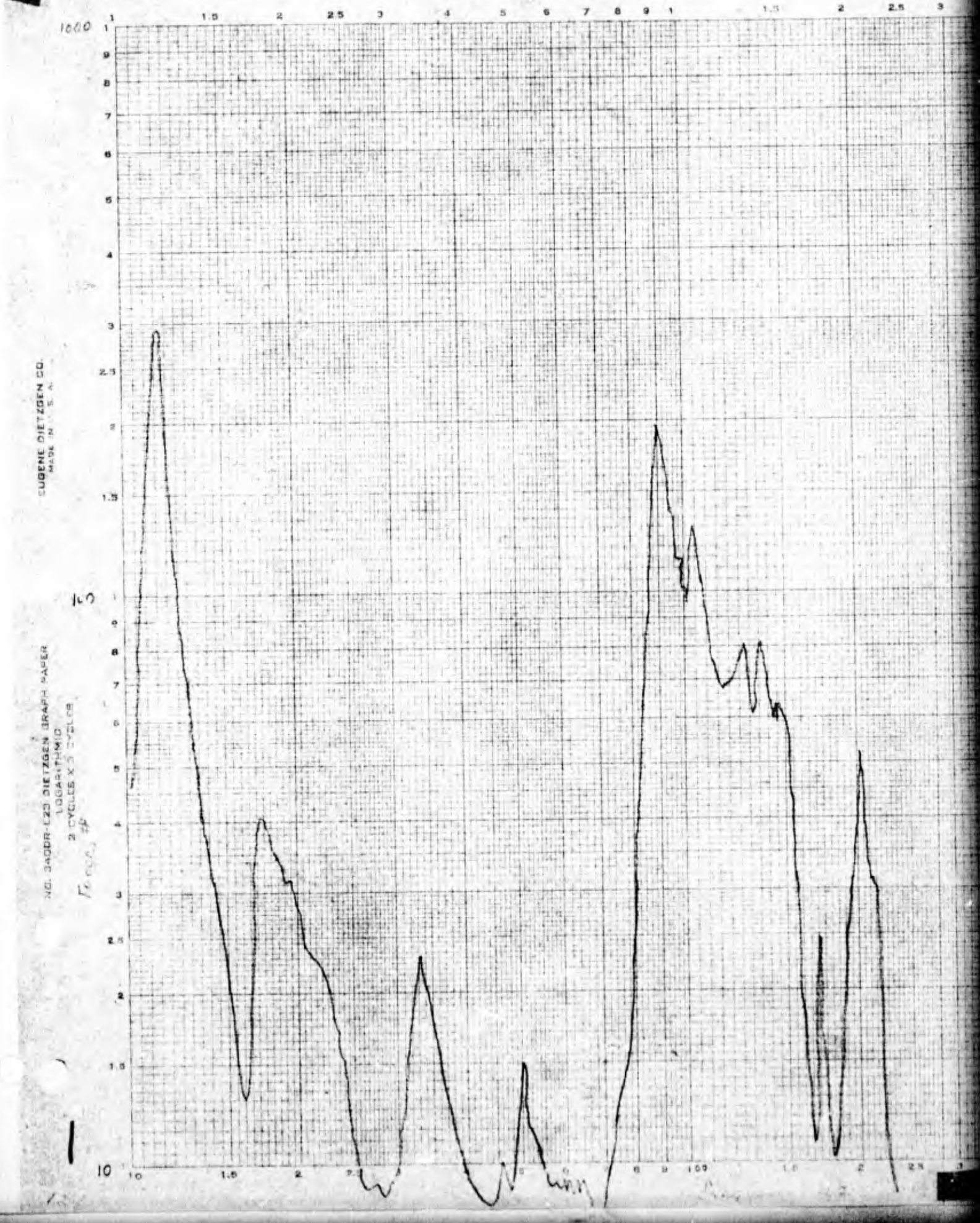
1000
1
1.5
2
2.5
3
4
5
6
7
8
9
10
EUGENE DIETZGEN CO.
MADE IN U.S.A.
NO. 340DR-E20 DIETZGEN GRAPH PAPER
LOGARITHMIC
2 CYCLES X 5 CYCLES

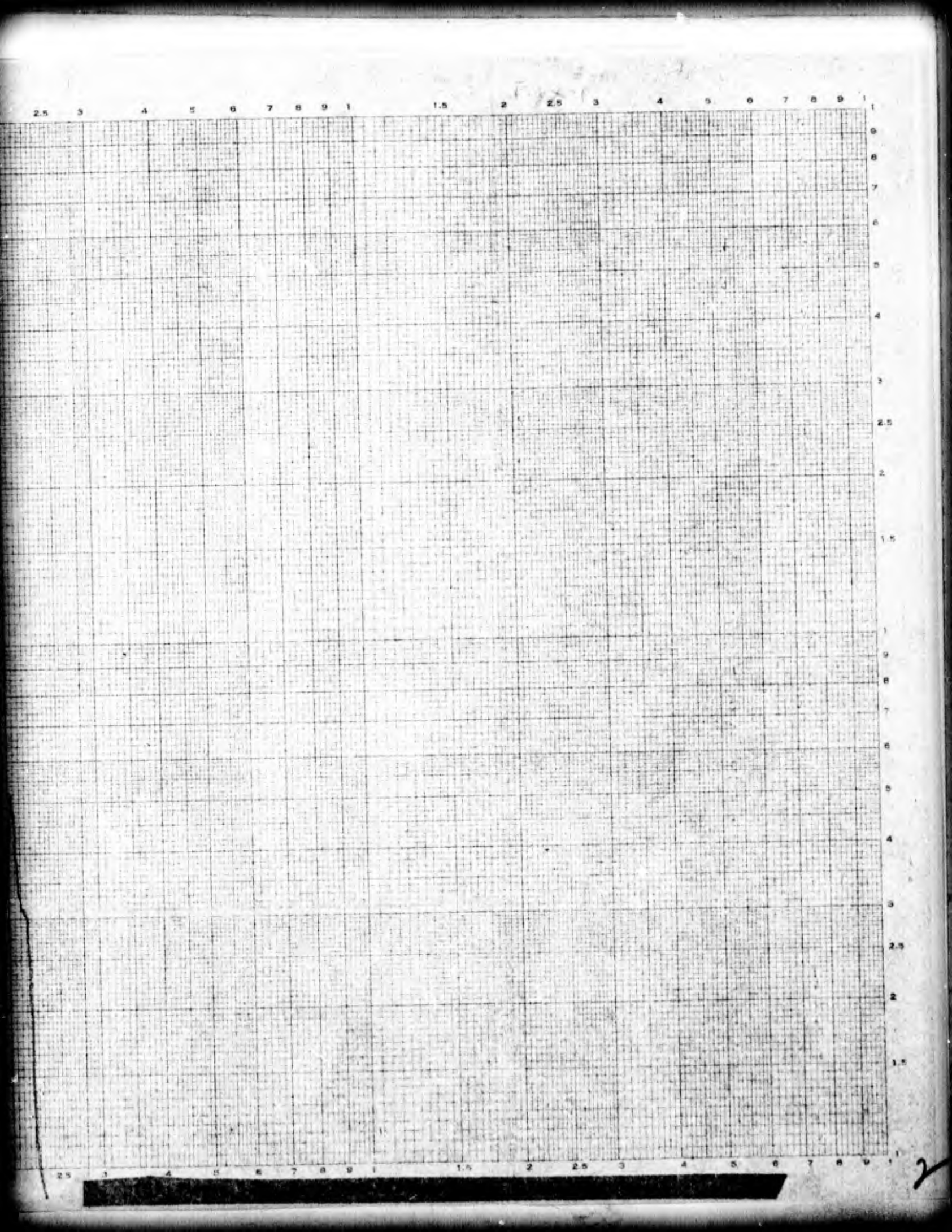

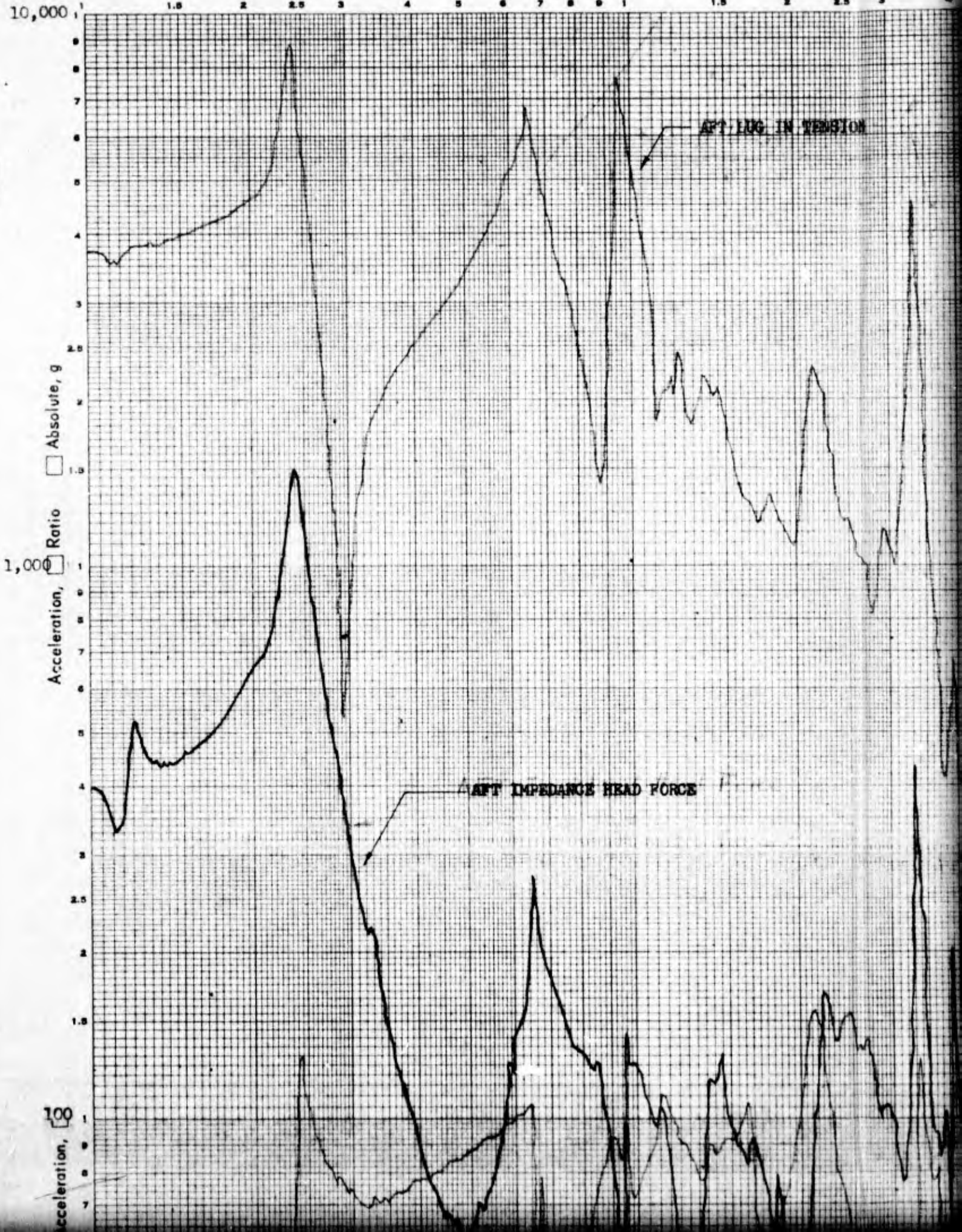
10,000
1,000
100
Acceleration, ☐ Absolute, g
☐ Ratio
AFT LUG IN TENSION
AFT IMPEDANCE HEAD FORCE

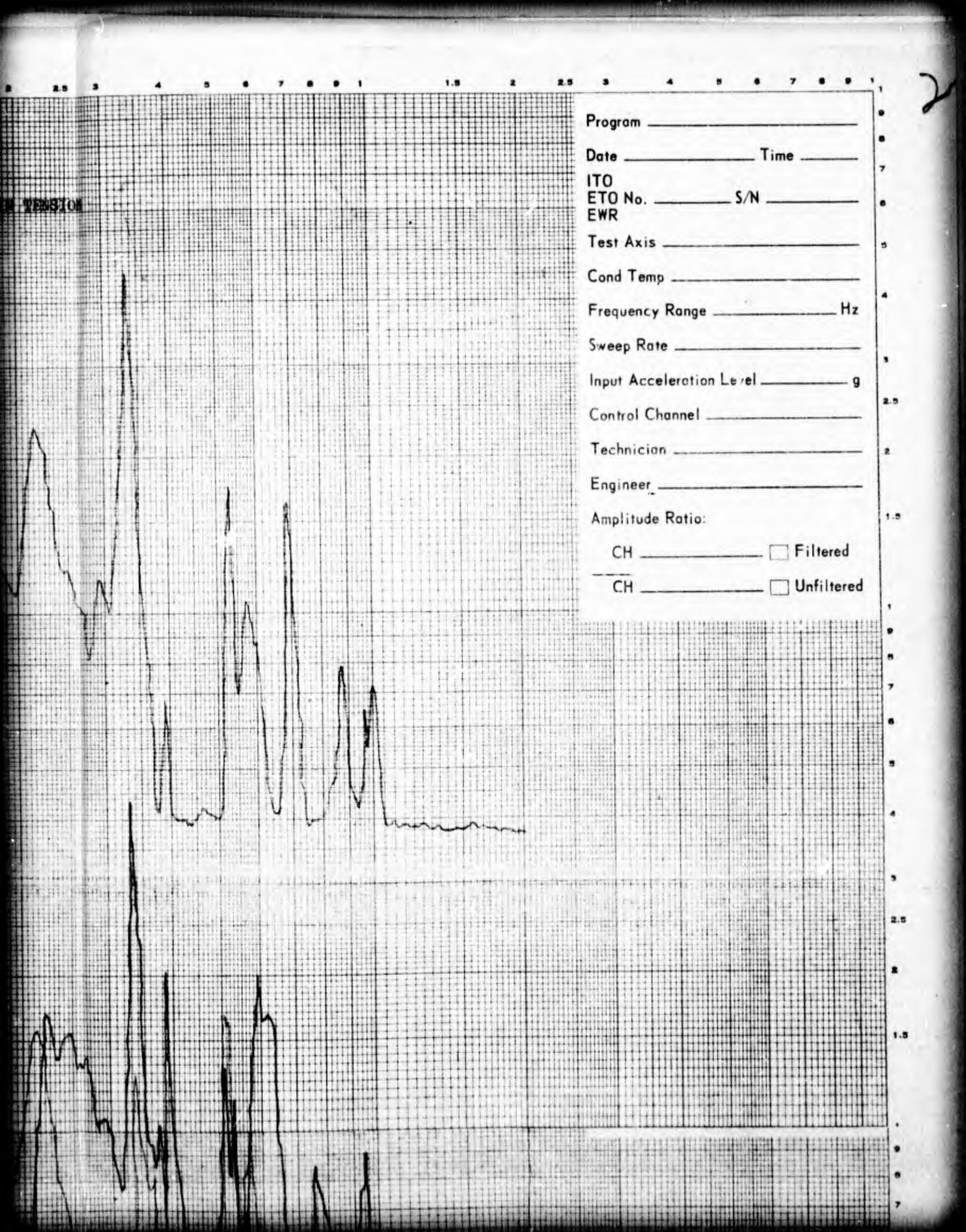
Program
Date
Time
ITO
ETO No.
S/N
EWR
Test Axis
Cond Temp
Frequency Range
Hz
Sweep Rate
Input Acceleration Level
g
Control Channel
Technician
Engineer
Amplitude Ratio:
CH
Filtered
CH
Unfiltered

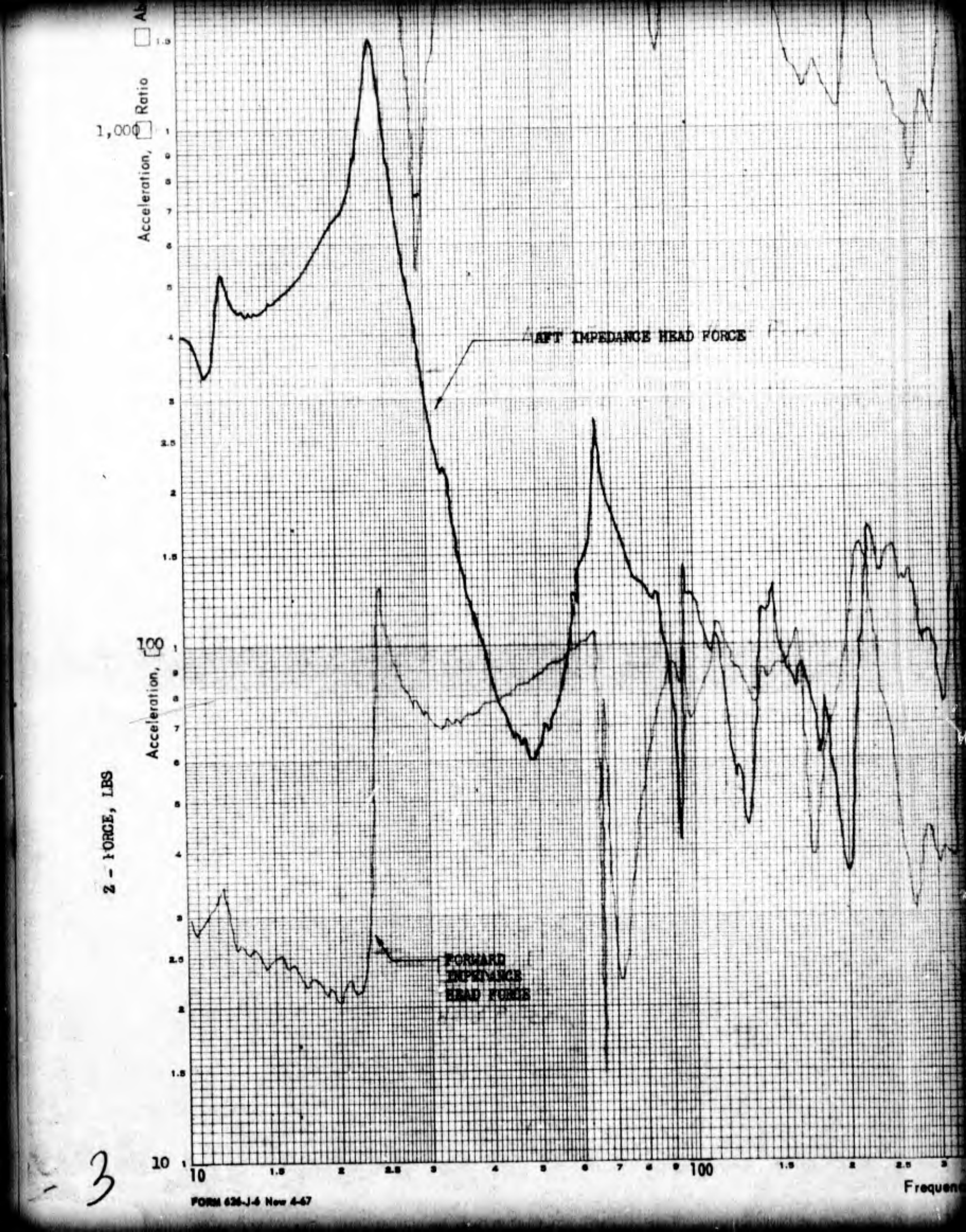

FORM 626-J-6 Nov 4-67

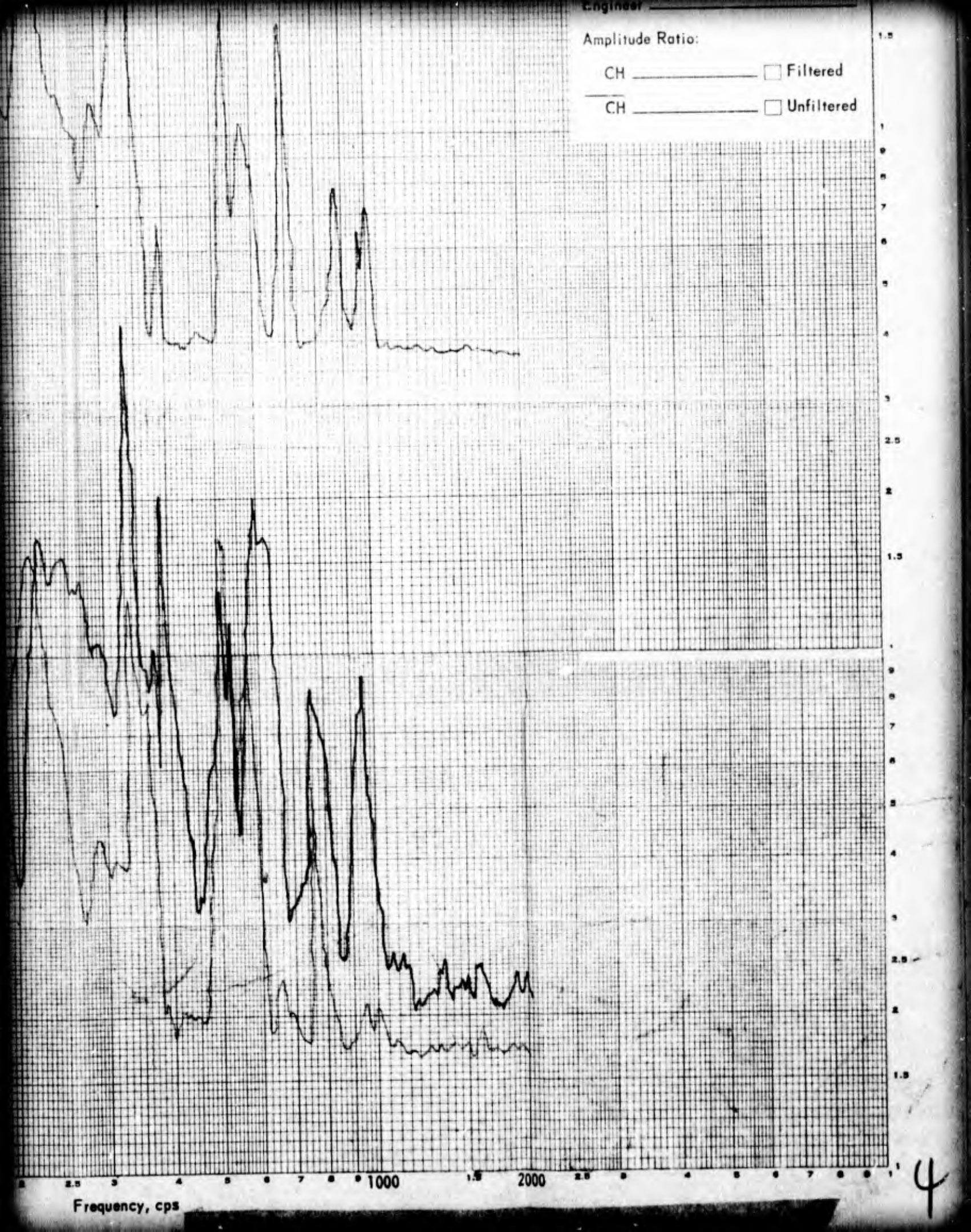
Engineer
Amplitude Ratio:
CH
Filtered
CH
Unfiltered
1.5
1
.9
.8
.7
.6
.5
.4
.3
2.5
2
1.5
1
.9
.8
.7
.6
.5
.4
.3
2.5
2
1.5
1
2
2.5
3
4
5
6
7
8
9
1000
1.5
2000
2.5
3
4
5
6
7
8
9
1
Frequency, cps

SUMMARY

In summary, review of the 0.5-g sine survey data shows the dynamic calibration for the sway braces closely approximates the static values. At frequencies in the neighborhood of resonance, response from the sway braces differs from the impedance head force measurement, which is not surprising in view of the rapidly changing mobility of the system (with frequency) and the different locations in the system from which the measurements were taken. The instrumented launcher provides a direct measure of the load transfer between the BDU and launcher that are valuable for interpretation of the system compliance during dynamic ground and, subsequently, flight testing.

Z-AXIS MODE SHAPES

During a review of the ratios of accelerometers Rocketdyne had attached to the BDU, it was found that complex motion was experienced during the Z-axis vibration testing. The accelerometer ratios and phase angles (related to accelerometer 8, which was used with A-5 in dual control) have been summarized at what appear to be resonant frequencies. The data are shown in Table 5-1. Some of the data that appear more directly related to resonance conditions have been replotted to display mode shapes.

From the standpoint that the test vehicle is excited by and assumed to respond to sinusoidal motion, for input:

$$x = A \sin(\omega t)$$
$$\dot{x} = v = A\omega \cos(\omega t)$$
$$\ddot{x} = a = A\omega^2 \sin(\omega t)$$

The response displacement and acceleration might lag the input by a phase angle φ. (Resonance occurs at $\varphi = 90^{\circ}$.) Then the response would be

$$x_R = A_R \sin(\omega t + \varphi)$$
$$\dot{x}_R = A_R\omega \cos(\omega t + \varphi)$$
$$\ddot{x}_R = A_R\omega^2 \sin(\omega t + \varphi)$$

The ratios would then give

$$\frac{\ddot{x}_R}{\ddot{x}} = \frac{A_R\omega^2}{A\omega^2} = \frac{A_R}{A} = \frac{x_R}{x} \quad \text{at } \varphi$$

TABLE 5-1

Z AXIS AMPLITUDE RATIOS AND PHASE ANGLES

Frequency, Hz	A_1/A_8		A_2/A_8		A_3/A_8		A_4/A_8		A_5/A_8		A_6/A_8		A_{10}/A_{14}	
	Amplitude Ratio	Phase Angle	Amplitude Ratio	Phase Angle	Amplitude Ratio	Phase Angle	Amplitude Ratio	Phase Angle	Amplitude Ratio	Phase Angle	Amplitude Ratio	Phase Angle	Amplitude Ratio	Phase Angle
19	0.73	0	0.84	0	0.36	0	0.14	0	0.63	0	0.96	-90	2.5	0
25	0.42	90	0.36	0	9.0	90	0.17	90	0.34	90	0.59	90	10+	0
27	5.3	90	1.92	0	9.6	90	0.79	0	5.0	90	1.5	180	>10	--
45	1.65	0	1.1	0	3.1	0	0.31	0	2.1	0	1.3	0	0.28	90
60	4.1	-90	0.33	-90	10+	-90	1.6	0	5.5	-90	0.38	-90	10+	-90
72	0.35	-90	0.62	0	0.17	-90	0.16	90	0.14	-180	--	--	--	--
83	--	--	--	--	--	--	--	--	--	--	1.4	0	2.0	180
92	0.56	0	0.52	0	--	--	0.8	-180	0.62	0	--	--	6.4	180
96	0.46	0	0.38	0	2.45	0	--	--	1.4	0	0.62	0	1.7	180
126	1.25	0	2.15	90	8.7	-90	0.33	90	3.2	0	0.72	0	6.9	180
140	0.57	0	--	--	4.3	-90	1.3	90	--	--	--	--	--	--
150	0.82	0	--	--	--	--	2.1	0	--	--	--	--	0.36	90
165	0.5	0	0.69	0	1.35	-180	3.7	-90	0.32	-90	2.5	-90	--	--
170	0.94	0	1.8	0	3.5	-180	--	--	0.95	-90	0.99	-90	4.0	180
210	1.0	90	2.0	90	2.5	-180	0.31	0	0.22	0	4.1	-90	2.0	90

Thus the ratios of the accelerometer signals will serve as ratios of displacement amplitude. These ratios were used to plot the mode shape curves shown in Fig. 5-7.

The mode shape curves, as previously mentioned, are referenced to an input accelerometer, A-8, attached to the BDU approximately 8.5 inches behind the center of gravity. This particular method of display was chosen to facilitate a convenient comparison of the measured BDU dynamic response to the analytical predictions previously made by Lockheed Propulsion Company. The BDU/launcher assembly response is defined by the impedance head data described earlier in this section.

As shown in Fig. 5-7, the normalized displacement amplitude is plotted along the length of the BDU. The forward end is to the left and the aft end is to the right. It appears that there are two basic response modes, typified by the "beam tipping" mode at 27 Hz and the "beam flexure" mode at 60 Hz.

The beam tipping mode is typical of a stiff beam supported by two springs (in this case the fore and aft ends of the launcher) as sketched in Fig. 5-8.

It is observed that the two generalized coordinates, x and θ, may be used to derive the two equations shown below:

$$mZ + (K_1 + K_2)\, Z - (K_1 \ell_1 - K_2 \ell_2)\, \theta = 0 \qquad (4)$$

$$I\ddot{\theta} + (K_1 \ell_1^2 + K_2 \ell_2^2)\, \theta - (K_1 \ell_1 - K_2 \ell_2)\, Z = 0 \qquad (5)$$

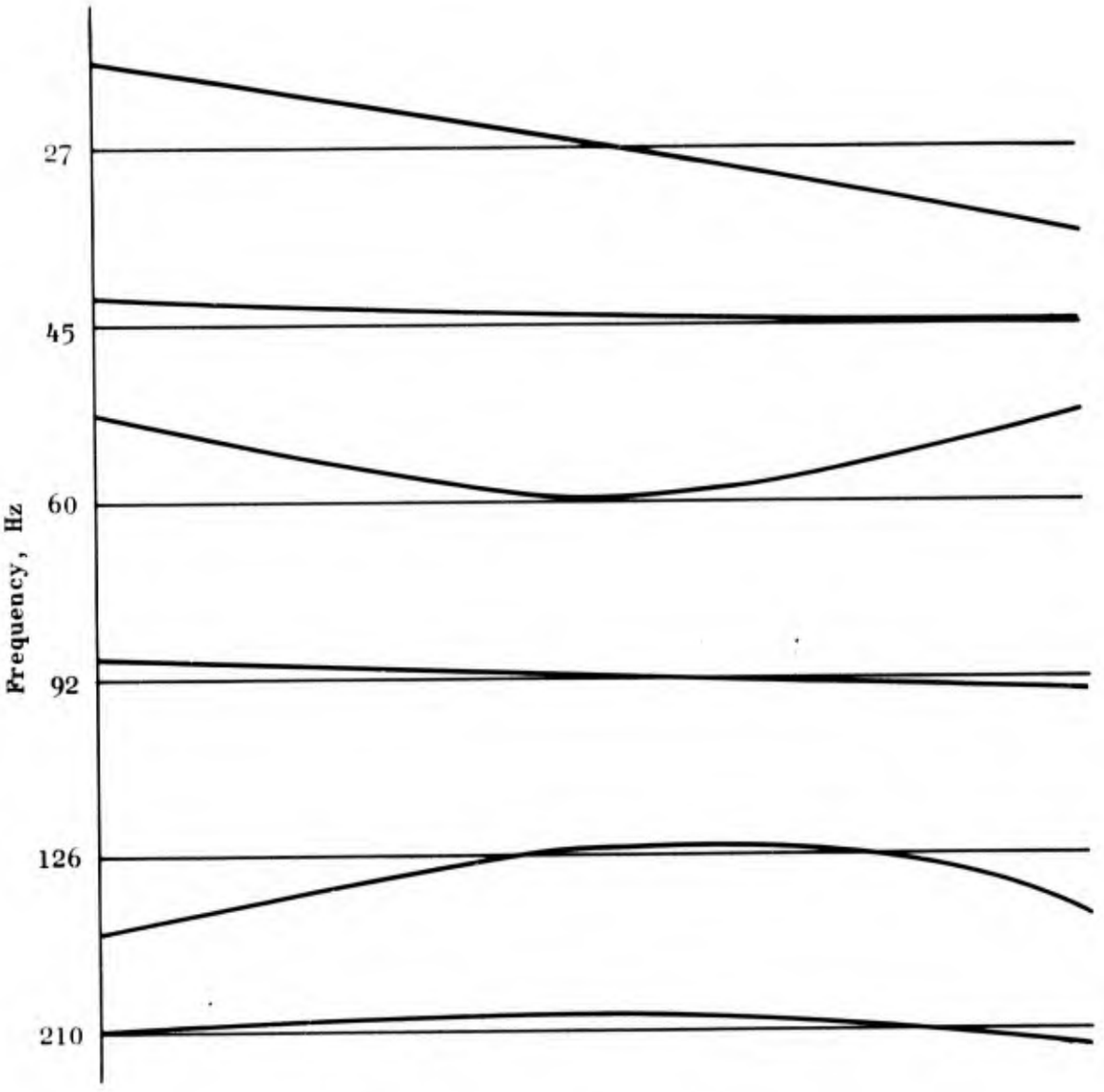

Figure 5-7. Z-Axis Mode Shapes

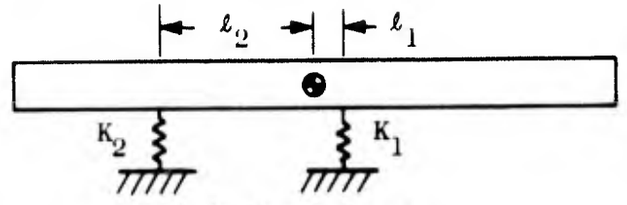

(a) Model Beam

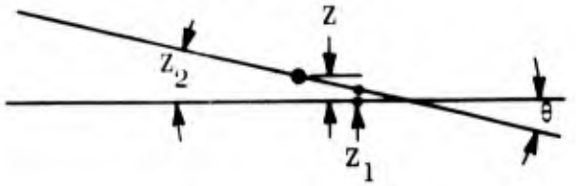

(b) Generalized Coordinates

(U) Figure 5-8. Simplified Stiff Beam Model

The combination $(K_1 \ell_1 - K_2 \ell_2)$ couples these equations. If this term is set to zero, then the equations would no longer be coupled. If

$$K_1 \ell_1 - K_2 \ell_2 = 0 \tag{6}$$

then

$$\frac{K_1}{K_2} = \frac{\ell_2}{\ell_1} \tag{7}$$

But in the case of the BDU tests, the aft section of the launcher is very nearly as stiff as the forward section and $K_1/K_2 \approx 1$. However, the distance from the center of gravity to the aft sway braces is 0.6 inch and 20.6 inches to the forward sway braces. Obviously ℓ_2/ℓ_1 is substantially greater than 1, and the displacement and tipping modes are coupled. Therefore, we can conclude from this simple model that the beam tipping mode for the BDU is a response one might reasonably expect, that this mode can indeed be excited by the Z-axis translation motion

(i.e., coupling), and that the launcher lends primary flexibility to this mode. The modes occurring at 45, 92, and possibly at 210 Hz appear to be harmonics of the fundamental resonance observed at 27 Hz.

The mode shape occurring at 60 Hz appears to be the beam bending mode. The linear nature of the forward end deflections substantiates the stiffness of that section. Flexing would appear to be in the thinner section toward the aft end. A harmonic occurs at approximately 126 Hz.

There are other components contributing to and being excited by the BDU Z-axis response. The fins on the aft end, for example, respond loudly at the 27 Hz frequency. At 165 Hz, X-axis response is excited by the Z-axis input such that the amplitude ratio at the forward end is 3.7, and is greater than 10 at the center of gravity and on the aft fins. The triaxial accelerometers showed Y-axis excitation up to 1 g at frequencies of 27, 66, and 170 Hz. The Y-axis cross response is not too significant. However, the response in the X axis is at times as high as that in the direction being driven. The magnitude of this response, and the apparent low energy level required to excite this cross mode leads us to conclude that the BDU motions along the X-axis should be the limiting criteria relating to adjusting data band widths for the acquisition system, and to evaluation of the structural requirements of the unit.

X-AXIS MODE SHAPES

The technique previously described was used to determine BDU mode shapes in the X axis. Again, these modes are referenced to accelerometer 8 attached to the BDU just behind the aft launch lug. Referencing the accelerometer locations and the sine survey response shown in Appendix G, the output signals were normalized and plotted in Fig. 5-9. These shapes, upon brief review, appear to be variations of the same fundamental mode, amplified at certain frequencies (e.g., 25 Hz) by the flexibility of the launcher. The overall system response will be discussed in more detail in a later section. Nevertheless, it would appear that the beam flexure mode is the primary response that is modified by resonance of BDU components such as the launcher, fins, recorder, and instrumentation racks, etc. The response of these components, particularly relating to the inert propellant grain is discussed in Section 6.

In addition to the acceleration (or displacement) ratios taken to show mode shapes relative to control accelerometer 8, transfer impedance plots were made. Instrument locations are shown in Fig. 5-10. Unfortunately, the phase angle measurements for the F/A-7 and F/A-11 ratios are erroneous due to recording and playback head misalignment on the tape recorder. (Much time and effort were expended adjusting the alignment and most of the other data were recovered. However, the alignment is particularly tedious for the rapid surveys required to accommodate the on-board flight recorder.) The other phase angle channels are correct and the amplitude ratios are close enough for our purposes here.

Review of the data show a primary bell ringing mode at 11.5 Hz and other strong resonance modes at 60, 90, 180, and 600 Hz. The mode shapes agree with those shown in Fig. 5-9, and provide a more comprehensive overview of the BDU dynamic behavior. The measurement of motion relative to a different reference point more clearly elucidates the bell ringing mode. The use of the force (measured at the input excitation

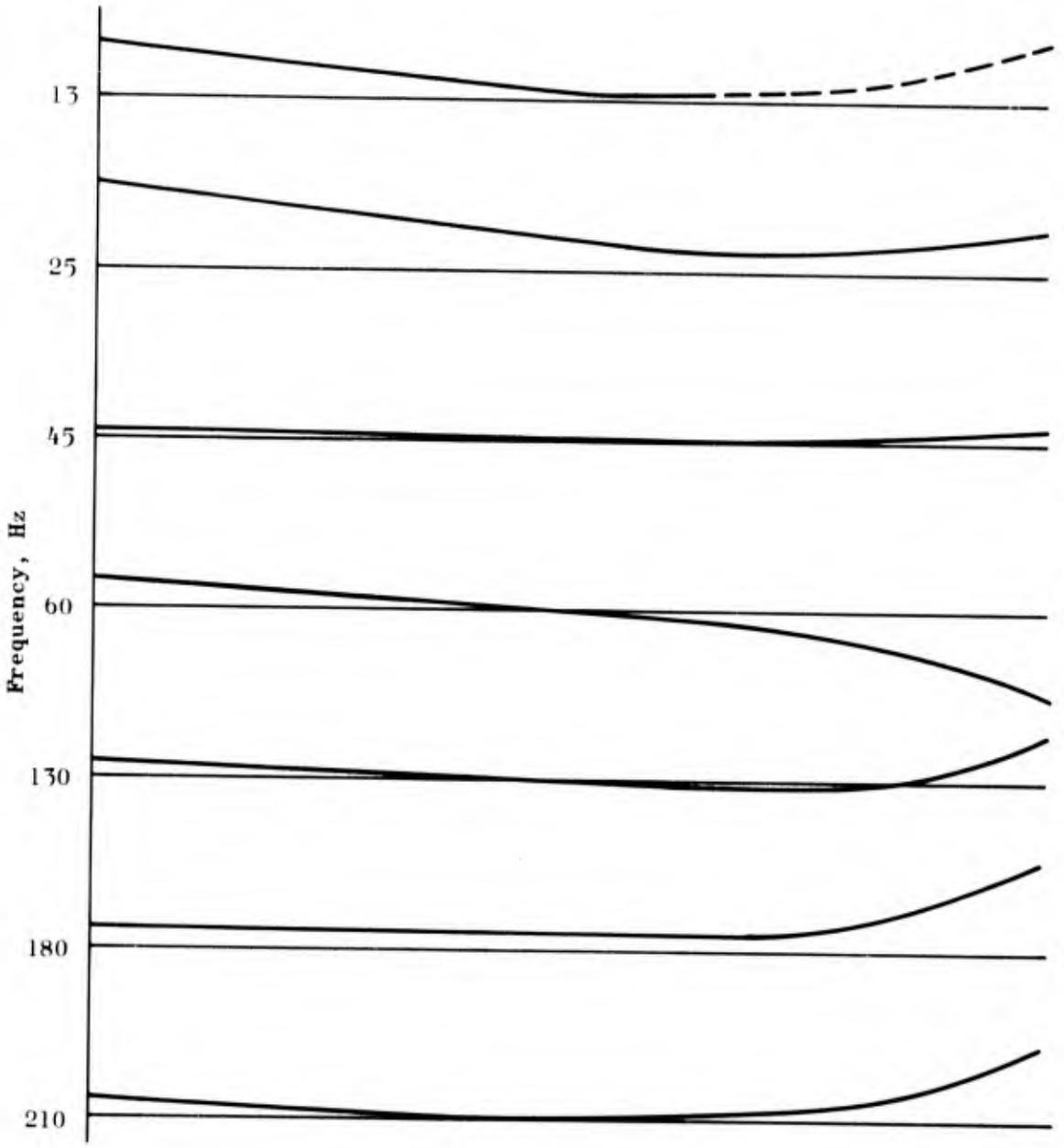

Figure 5-9. X-Axis Mode Shapes

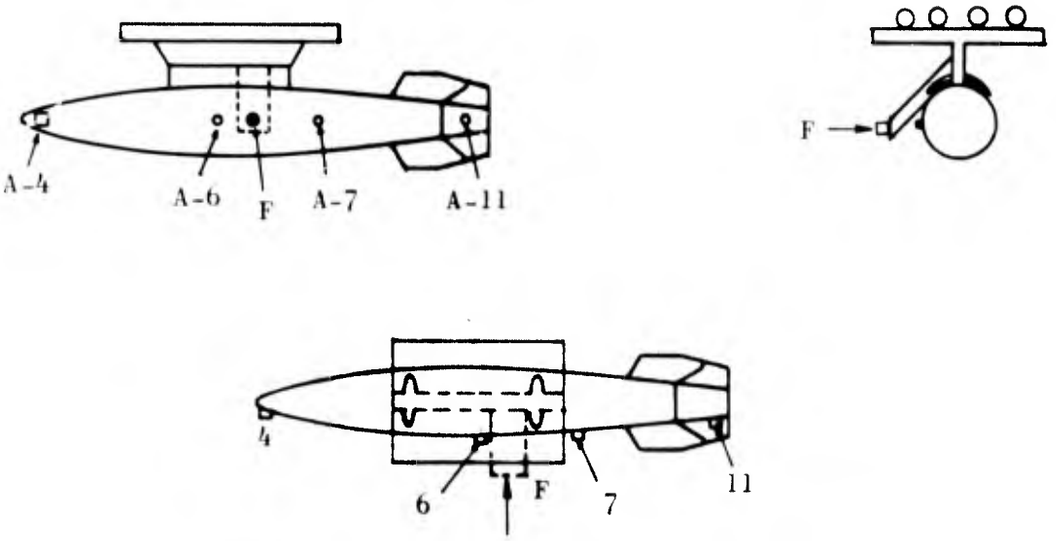

Figure 5-10. Sketch of Transfer Impedance Instrument Locations

point), and the response at several spots on the BDU, provides transfer coefficient data that the analyst may compare with stiffness coefficients in a finite element stiffness method dynamic (computerized) analysis, or more directly, may use to show the more flexible components of the system.

LAUNCHER FLEXIBILITY

The BDU was attached to the vibration jig in two slightly different arrangements for testing during this program. One arrangement ("hard") used a stiff interconnecting member between the jig and the BDU. Attachment to the BDU was accomplished by bolting into the BDU body at the launch lug locations. The other arrangement ("soft") uses the MAU-12A/C launcher, bolted to the jig through clevis fittings as used on the F-111 pylon. The BDU was fitted to the launcher in the usual manner.

Adoption of the different arrangements stemmed from the need to excite the BDU to the spectrum of frequencies between 10 and 2000 Hz. A MAU-12A/B launcher originally scheduled for use in the program

appeared to be so flexible that the BDU would be isolated from high frequency loads input through that launcher. Since aerodynamically induced high frequency loads could be experienced by the BDU in flight, and since it was desired to simulate the environment in ground testing, the hard arrangement was designed and built. Subsequently, a stiffened launcher (the MAU-12A/C) became available and was used throughout the experimental testing.

Initial tests in the X and Z axes were conducted using the hard arrangement. Data from the instrumentation were recorded during sine survey and random tests. (The Z-axis hard sine survey was run at 1-g input. All other tests were made using 0.5-g input.) The impedance head data, plotted in terms of apparent mass, appear to best characterize the system response in the different configurations.

The apparent masses recorded from Z-axis sine surveys in the hard and soft configurations are shown in Fig. 5-11. It is noted that both magnitudes of apparent mass and resonant (and anti-resonant) frequencies are lower for the soft configuration. The launcher is more flexible than the hard arrangement, but the influence on BDU response is relatively small.

The apparent masses for X-axis sine survey tests in the hard and soft configurations are shown in Fig. 5-12. The differences between the curves are less than those displayed in Fig. 5-11.

It was concluded from these data that the differences in BDU response resulting from use of the hard and soft arrangement were small relative to other system complexities. Consequently, subsequent testing was conducted only in the soft (with launcher) configuration, and these data were analyzed and are discussed in more detail earlier in this section.

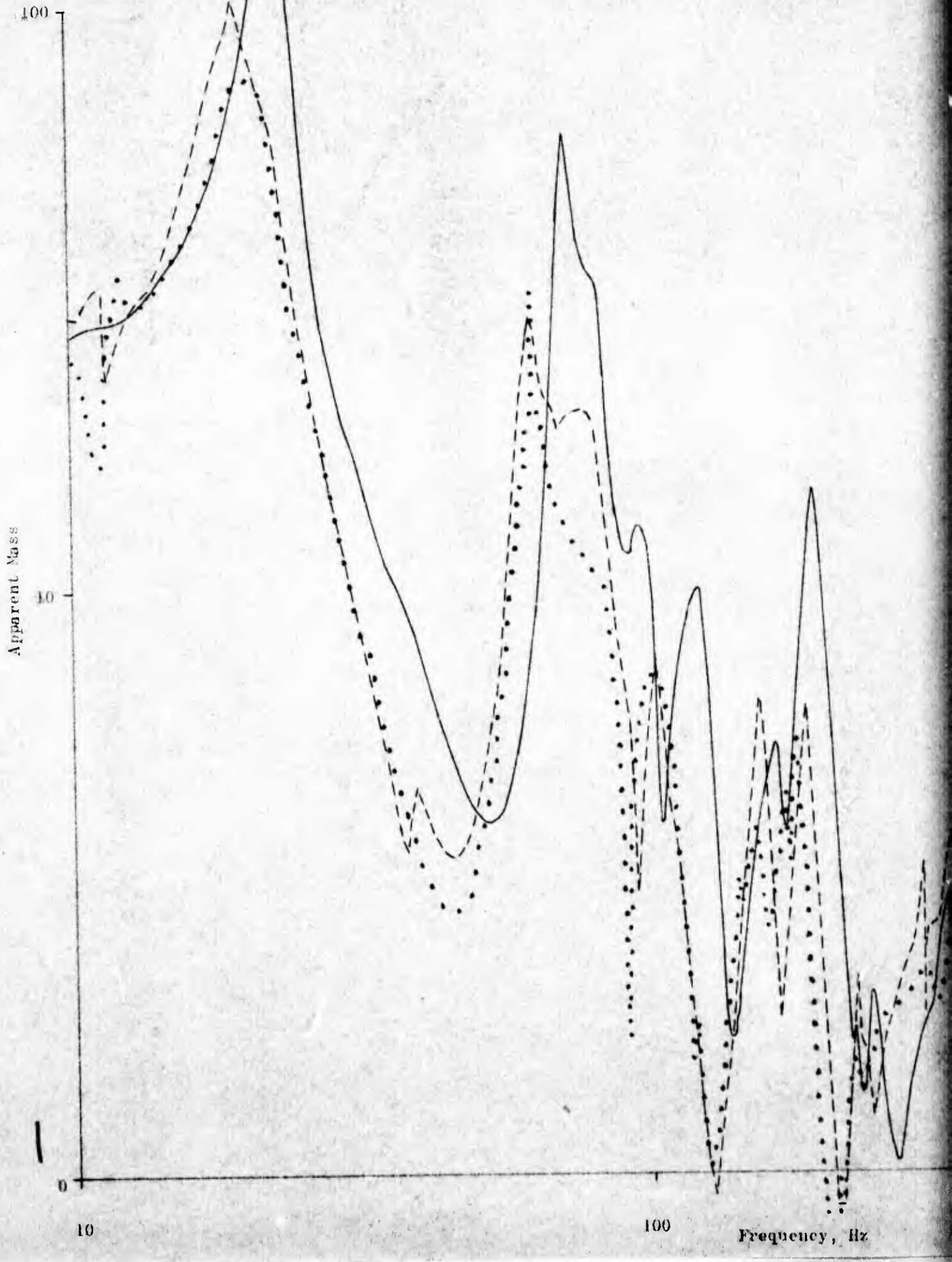
100
10
0
Apparent Mass
10
100
Frequency, Hz

Legend:

1-g Hard, 6/30/71 ——
0.5-g Soft, 7/6/71 – – –
0.5-g Soft, 9/28/71 • • • •

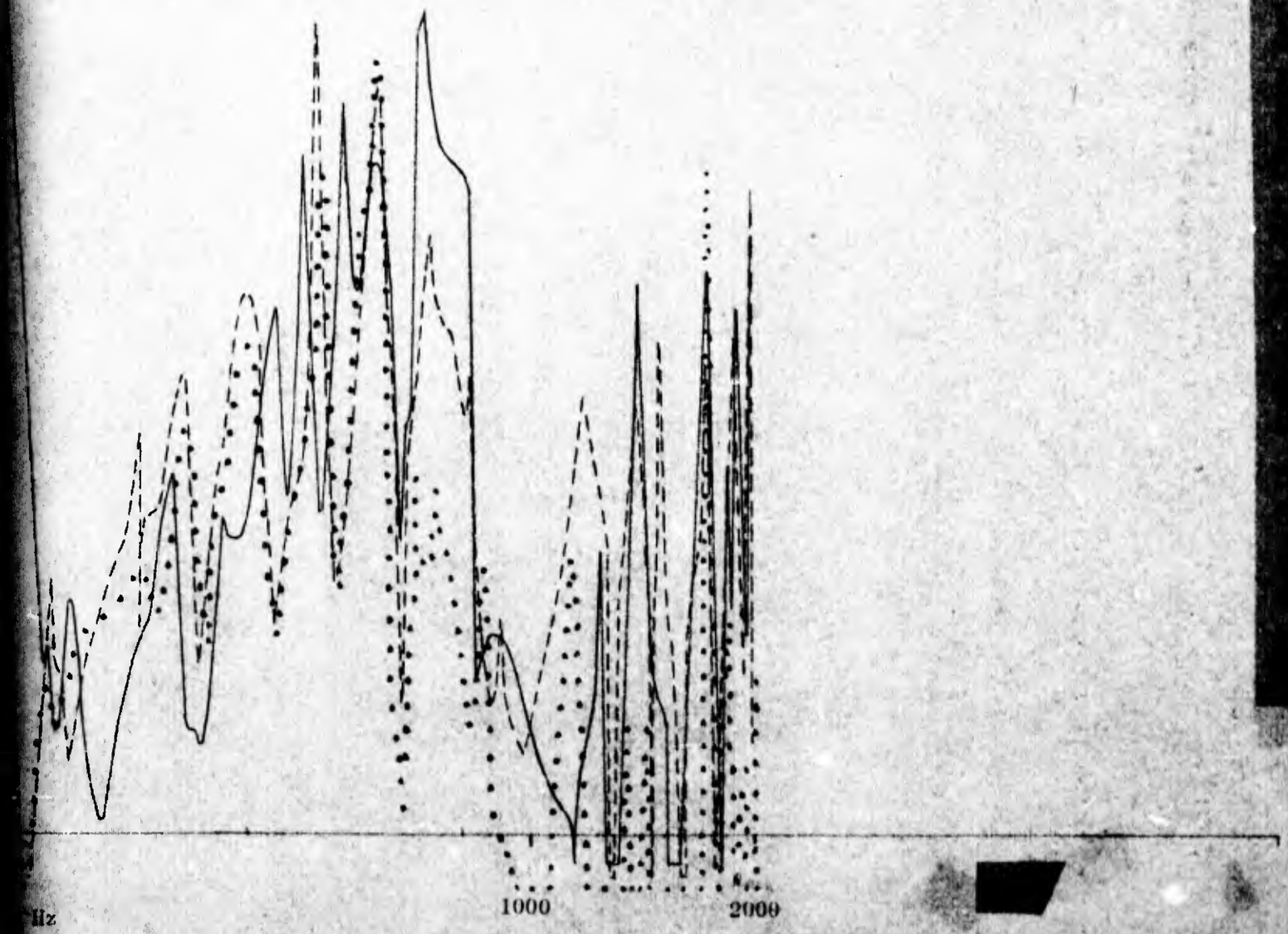

AEROHEAT SIMULATION

The BDU was subjected to aeroheat during three test cycles. One aeroheat-only cycle was conducted to establish a baseline for future thermocouple and thermistor reference. The other two cycles were of combined aeroheat and vibration. The center section of the propellant grain was selected as the control section for the aeroheat cycles. Thermocouples 7, 8, 9, and 10 were on the case at the longitudinal centerline of the propellant grain; while thermocouple 5 was in the air stream just above the case. Data from the three tests are shown in Fig. 4-43, -45, and -46.

Maximum differences in case temperatures were 30 to 50 F at the end of 10 minutes. Air temperature and maximum case temperature are shown in Fig. 4-45.

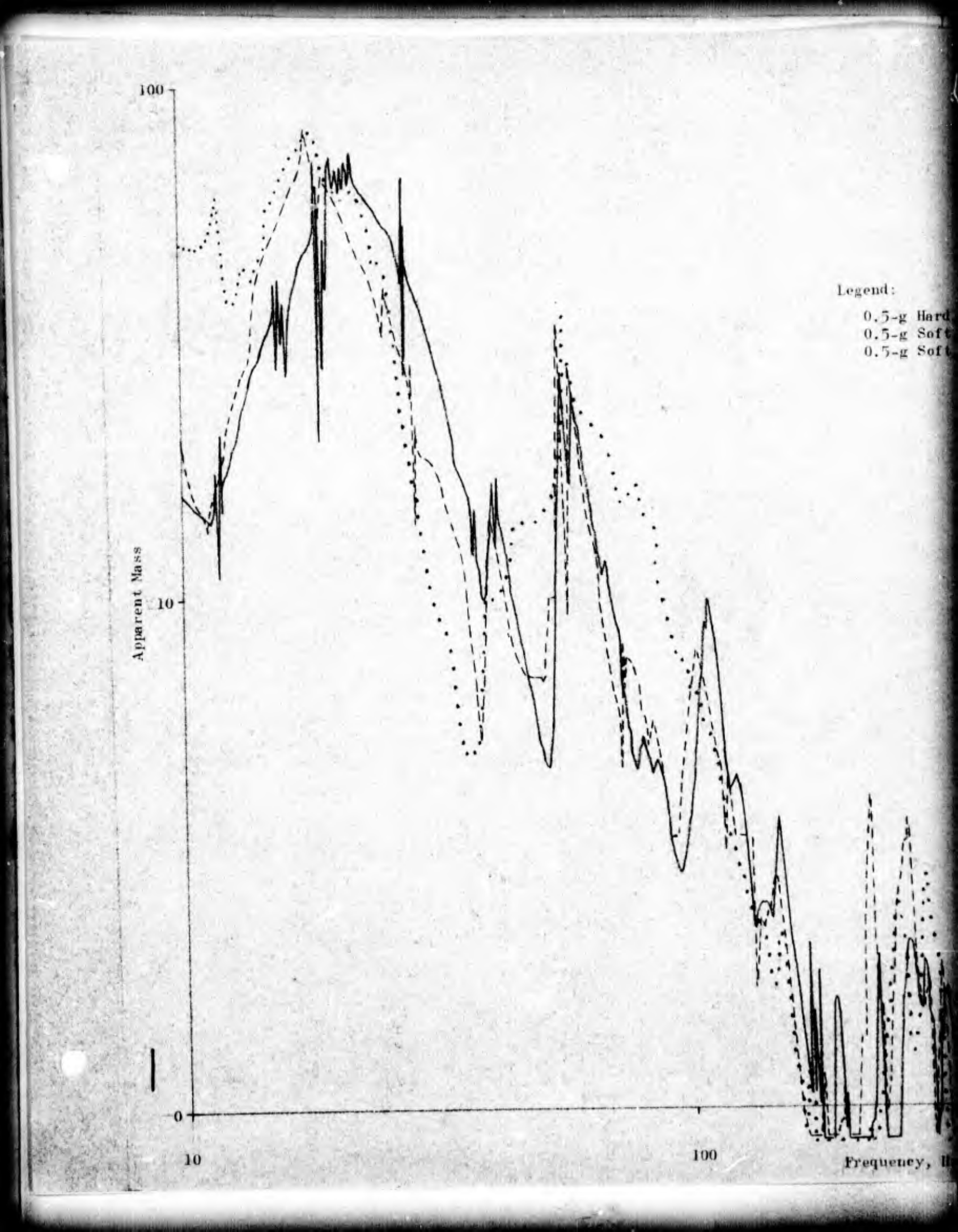
100
10
0
Apparent Mass
10
100
Frequency, H
Legend:
0.5-g Hard
0.5-g Soft
0.5-g Soft

Legend:

0.5-g Hard, 7/14/71 ——
0.5-g Soft, 7/13/71 – – –
0.5-g Soft, 9/20/71 • • • •

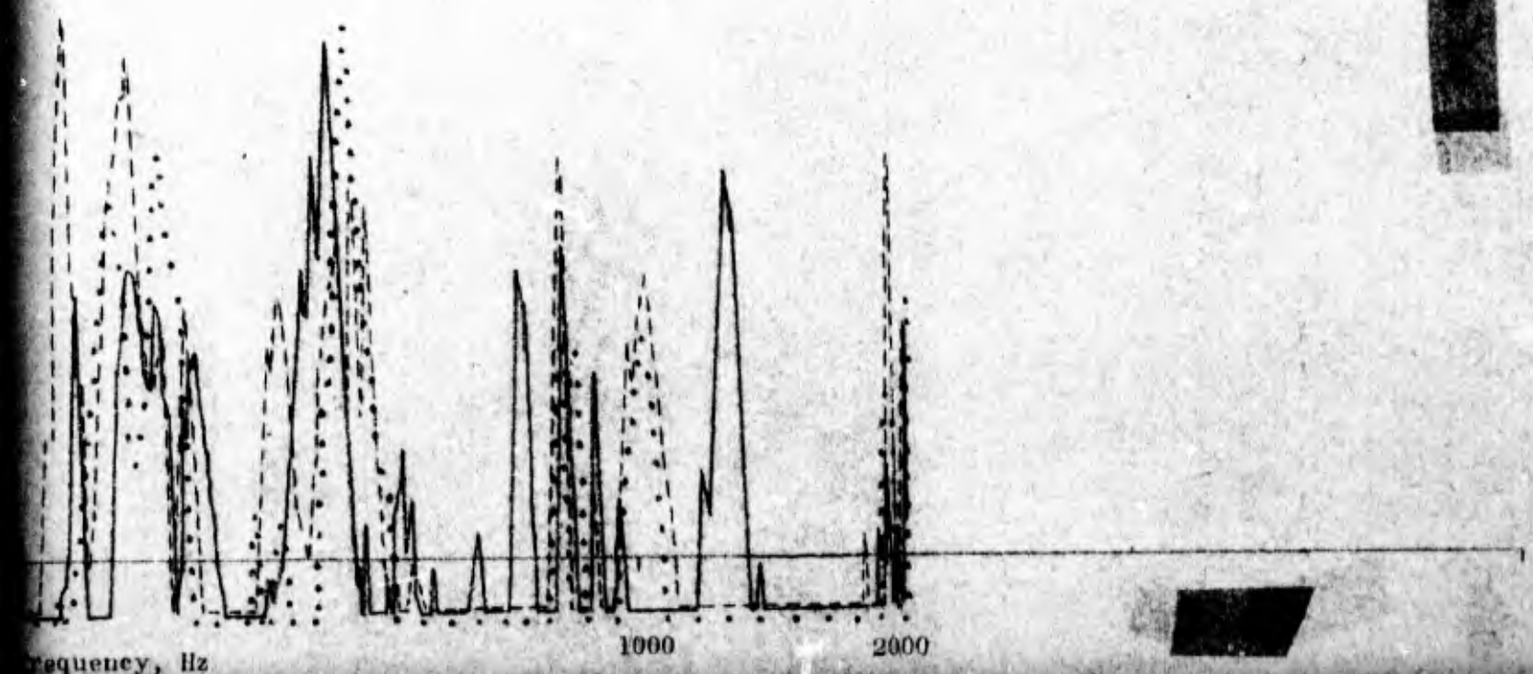

6. PROPELLANT GRAIN RESPONSE DATA

Significant data obtained from the propellant grain instrumentation during vibration and simulated aeroheat testing have been analyzed and are discussed in this section. The identification of the instruments and their location within the inert propellant grain are shown in Table 4-1 and Fig. 4-8.

PROPELLANT INSTRUMENTATION DATA

SINUSOIDAL VIBRATION

A sine wave excitation survey was conducted in both the Z axis (vertical) and the X axis (horizontal and transverse to BDU) at an input acceleration level of 0.5 g.

Table 6-1 shows data from the sine survey in the Z axis and includes the peak-to-peak amplitudes obtained from the normal and shear stress gages and the two bore strain measuring gages. These data represent the maximum amplitudes noted at the various resonance frequencies. The lowest frequency $\sim$ 11.5 Hz is apparently the frequency at which the whole BDU swings like a pendulum (Bell-ringer mode) on its support. This is primarily an X-axis motion, and very low normal stresses (0.15 to 0.25 psi) were obtained in this mode. There was no measurable shear stress in the axial or Y direction.

Higher stress levels were obtained at the higher resonant frequencies of $\sim$ 25 and $\simeq$ 100 Hz. Gage 22 situated at the 180° (bottom) of the forward end of the grain shows the largest stress values at both frequencies, 0.93 and 0.70 psi, respectively. Gage 24 at the rear bottom of the grain shows similar stress levels at 0.64 and 0.61 psi, respectively. Gage 18 located in the middle of the grain was not connected to the Rocketdyne recorder for these tests. Gages 21 and 26, which are arranged to measure the lateral normal stresses, gave extremely small outputs in the noise level during the vertical Z-axis vibration tests.

TABLE 6-1

VIBRATION DATA FROM 0.5 G Z-AXIS SINE SURVEY

Freq, Hz	Gage Number							
	21	22	24	26	101	SH-2	BB 1	BB 2
	Peak-to-Peak Stress/Strain							
	psi	psi	psi	psi	psi	psi	% Ax.	% Hoop
11/12	0.15	0.26	0.22	N	--	--	-	-
23/24	N*	0.93	0.64	N	0.42	0.20	N	N
97/105	N	0.70	0.61	N	0.38	0.31	N	0.014

*Noise level only

Shear gages 101 and SH-2 both showed small shear stresses in the axial or Y direction at the two higher frequencies when the BDU was vibrated in the Z direction. This indicates some coupling between the modes of vibration and demonstrates how difficult it is to obtain a simple pure vibration mode.

The bore strain measuring clip gages showed virtually no vibration strains during the tests. A very small value of 0.014% hoop strain was obtained at the 100 Hz frequency but no other measurable strains were noted.

Table 6-2 shows similar data obtained from the X axis sine survey. In this mode the lateral plane of normal stress gages, i.e., Gages 21, 24, and 26, showed the highest stress values as would be expected. Resonant frequencies noted in these lateral vibration tests were not identical to those obtained in the vertical test mode. Thus, there was no resonance detected at the 11/12 Hz frequency; and the lowest resonant frequency was 28 Hz, which is probably a similar mode to that obtained at 23/24 Hz in the Z axis mode of vibration. There appears to be no equivalent to the 100 Hz mode during vibrations in the X direction but additional peaks were obtained at 140, 220, and 280/300 Hz as noted.

TABLE 6-2

VIBRATION DATA FROM 0.5 G X-AXIS SINE SURVEY

Freq, Hz	Gage Number							
	21	22	24	26	101	SH-2	BB 1	BB 2
	Peak-to-Peak Stress/Strain							
	psi	psi	psi	psi	psi	psi	% Ax.	% Hoop
28	0.66		0.64	0.82	0.50	0.37	N*	0.0085
140	--	--	--	--	0.069	0.051	N	N
220	1.15	--	0.59	0.34	--	--	-	-
280/ 300	0.40	--	0.29	0.27	0.107	0.065	N	N

*Noise level only

At the lowest frequency of 28 Hz the shear gage readings suggest that it is once again a coupled vibration mode, but at the higher frequencies the measured shear stresses are much smaller and almost negligible. There is also essentially no hoop or axial strain in the grain bore during vibration, since only one value of the hoop strain could be measured (i.e. 0.0085% at 28 Hz).

RANDOM VIBRATION WITH SIMULATED AEROHEAT

Random excitation was applied to the BDU in both the X and the Z axes simultaneously with aeroheat. These tests were intended to simulate a flight test as closely as possible. Data from the X-axis vibration test are presented in Table 6-3, and data from the Z-axis vibration test are given in Table 6-4.

The data consist of peak-to-peak amplitudes at the maximum data points observed during the test sequence. Thus the results from the normal stress Gages 21, 24, and 26 in Table 6-3 show maximum values of normal stress of from 2 to 4 psi. Gages 21 and 26, which are located at the

TABLE 6-3

VIBRATION DATA FROM X AXIS RANDOM VIBRATION PLUS AEROHEAT

Time, sec	Gage Number							
	21	22	24	26	101	SH-2	BB 1	BB 2
	Peak-to-Peak Stress/Strain							
	psi	psi	psi	psi	psi	psi	% Ax.	% Hoop
18.8	2.05	1.23		1.78				
57.7	2.16	1.21		1.59				
444.2	3.99	1.80		2.24				

TABLE 6-4

VIBRATION DATA FROM Z AXIS RANDOM VIBRATION PLUS AEROHEAT

Time, sec	Gage Number							
	21	22	24	26	101	SH-2	BB 1	BB 2
	Peak-to-Peak Stress/Strain							
	psi	psi	psi	psi	psi	psi	% Ax.	% Hoop
44.1	0.60	2.23	1.18	1.09				
95.5	0.59	1.10	1.14	1.08				
150.9	0.67	2.18	1.28	1.05				

90^{0} points of the grain, show the maximum data as would be expected. Some coupling between the X and the Z planes is evidenced by the magnitude of the response from Gage 24, which measures the vertical (Z) response at the rear of the grain.

Data in Table 6-4 show maximum stress levels from Gages 22 and 24, but stresses at Gage 26 are not much smaller than those recorded by the two Z-axis plane gages. Again, this demonstrates the complexity of the vibration modes.

AEROHEAT

Results of the aeroheat vibration tests were presented in the preceding paragraph; thermal results from the tests are discussed here. Temperature data were obtained from thermistors located in the grain adjacent to the gages and in a temperature gradient block at the middle of the grain. In Fig. 6-1 through -4, thermistors B and D measure the case temperature while Thermistors 1, 2, 5, and 10 measure the grain temperature inside the insulation layer near the gages. Thermistor 21 is located inside the propellant web at a distance of 1 inch from the insulation layer, and Thermistor 20 is located in line with Thermistor 20 and 1 inch deeper in the grain (2 inches inside the grain from the insulation layer). Thermistor 16 measures the temperature at the bore of the grain.

Data from three aeroheat runs are given. Figure 6-1 shows the temperature data from a simple aeroheat test alone, i.e., no simulataneous vibration; and Fig. 6-2 and -3 show data obtained during the aeroheat plus vibration tests.

All three sets of data show similar results in that the maximum heating is obtained at the bottom of the grain as evidenced by Thermistors D, 1, and 2 all located at the bottom of the grain and Thermistors B, 5, and 10 located at the top of the grain. It will be noted that there is a difference of about 10 F between the bottom and the top of the grain at the end of the aeroheat test alone, a difference of 20 to 25 F in Fig. 6-2, aeroheat plus Z axis vibration, and a difference of about 20 F in the data shown in Fig. 6-3, aeroheat plus X axis vibration.

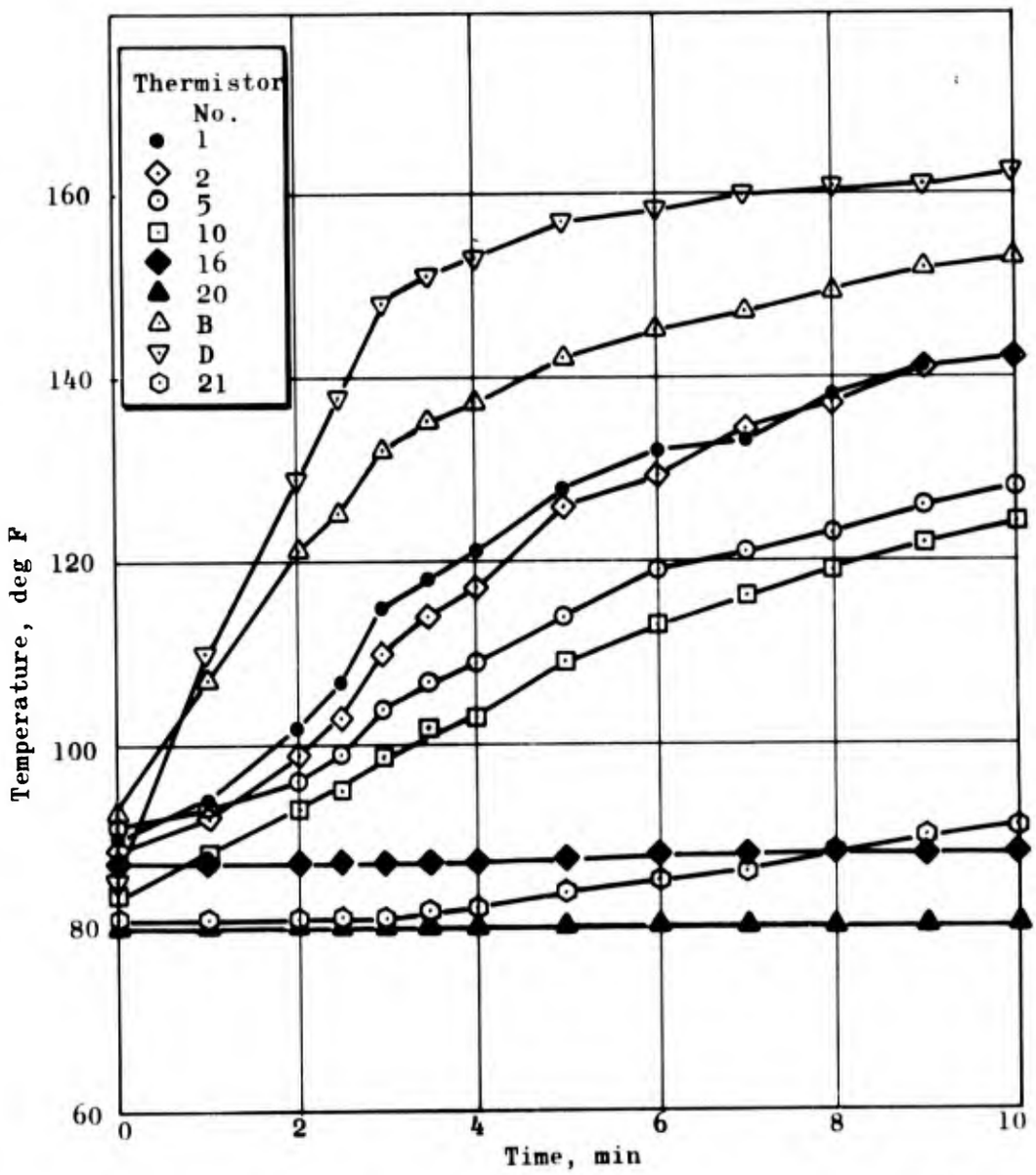

Figure 6-1. BDU Temperature Data from Aeroheat Test 9/22/71

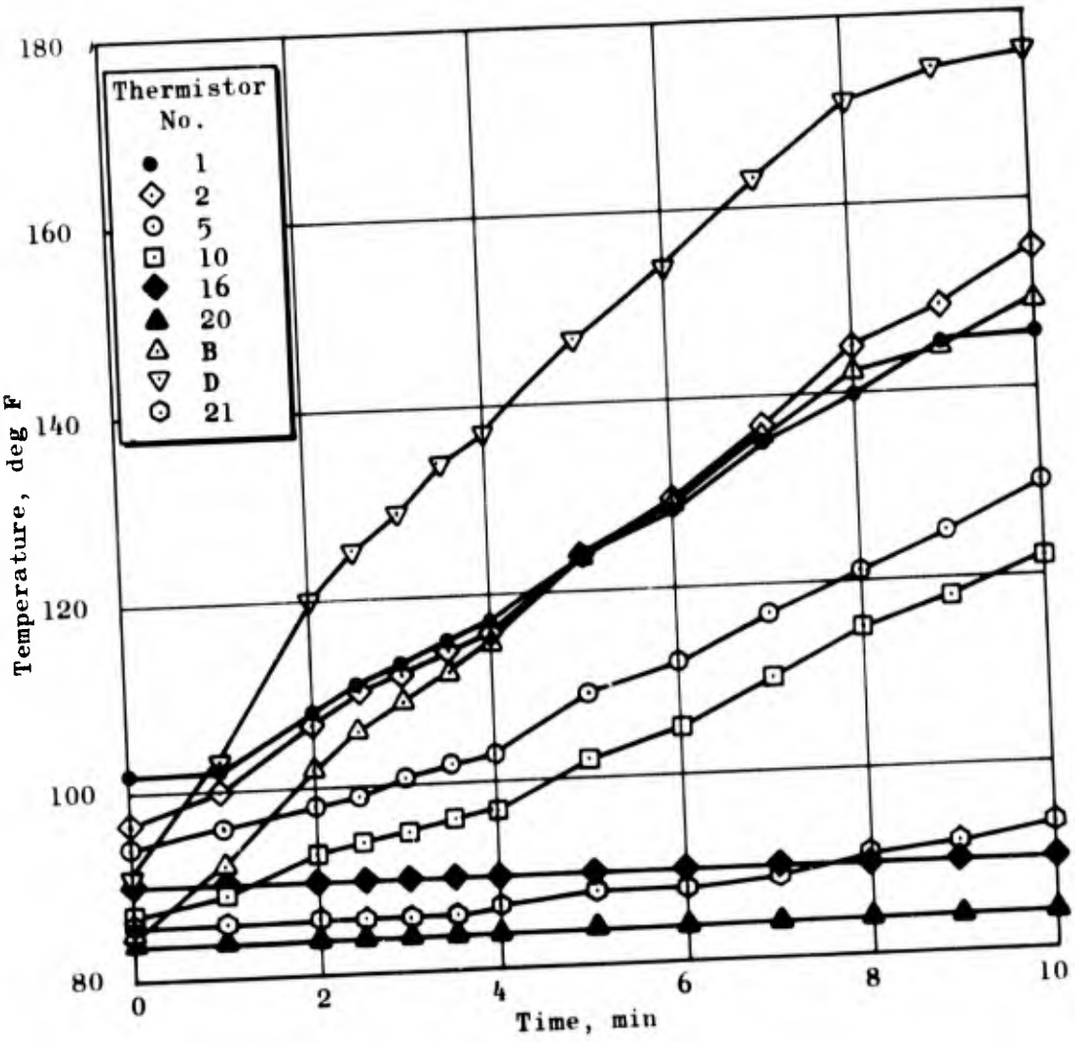

Figure 6-2. BDU Temperature Data from Aeroheat Plus Vibration Test 9/28/71

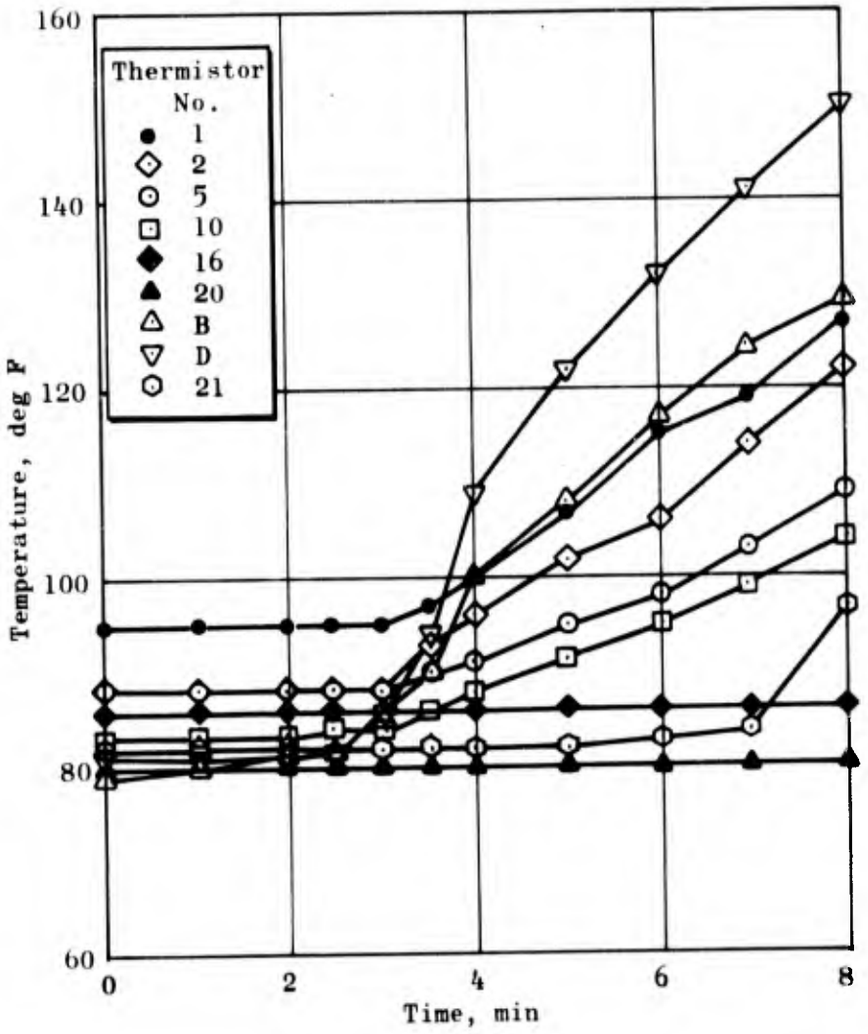

Figure 6-3. BDU Temperature Data from Aeroheat Plus Vibration Test; X Axis Random, 9/24/71

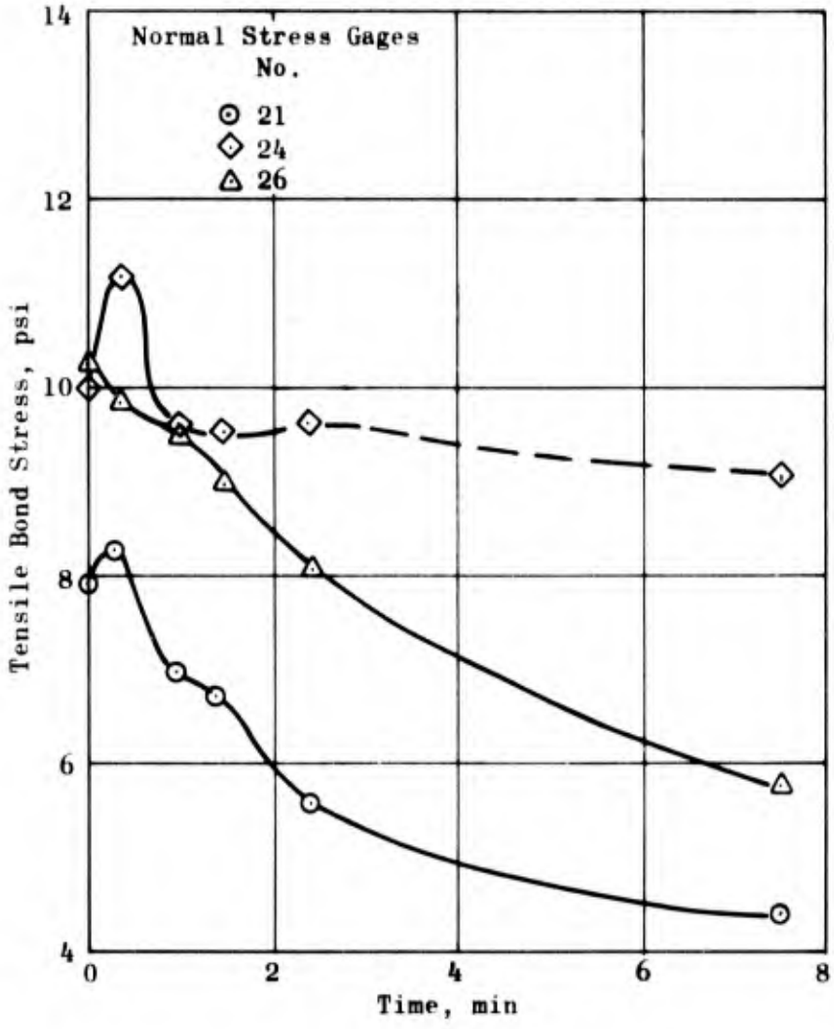

Figure 6-4. Thermal Bond Stresses Measured During Aeroheat Plus X Axis Vibration Test

Data from other thermistors were taken during the tests, but some appear incorrect and suggest that the unit needed another thermistor calibration test.

During the combined Random vibration and simulated aeroheat, the propellant stress transducers were expected to display relatively small amplitude (vibration response) oscillations superimposed on larger (thermal response) variations. In order to record the amplified vibrator response, the signal reference base was manually adjusted during the test.

In this manner, the data presented in Fig. 6-4 were obtained. The curves show the thermally induced changes in the outputs from normal stress Gages 21, 24, and 26 during the aeroheat plus X-axis random vibration test. In the first minute of the aeroheat test Gages 21 and 24 show a small increase in tensile stress after which the stresses become smaller for Gages 24 and 26. Gage 21 shows the initial increase as described above then shows a reduction in tensile stress for a short time interval. The final data point at 444.2 seconds indicates an increase in stress, but it is possible that this is merely an error in signs and that in reality the stress decreases as in the case of the other two gages.

7. CONCLUSIONS

A complete assessment of the program results as to interpretation correlation and accomplishments must await reduction and receipt of the Air Force on-board flight data. Accordingly the following remarks are limited by this consideration and will be revised as the data becomes available.

The basic objectives to perform a system checkout of the BDU under simulated environmental and dynamic conditions prior to captive flight tests (Project DAME) in conjunction with the F-111 aircraft were achieved or exceeded. These tests revealed the necessary corrections and/or modifications (gage settings, gains, launch lug instrumentation, on-board tape recorder repair, etc.) in a timely manner. The corresponding technical schedule, and cost effectiveness is significant compared to that of similar corrective activities resulting from actual flight tests. Data resulting from the forthcoming Project DAME flight tests will be unique and invaluable in establishing requirements and specifications for current and future tactical solid propellant propulsion units.

The volumes of data collected successfully from static, dynamic, and thermal testing of the BDU lead to the conclusion that data management and analysis can be made more cost effective through the use of advanced data acquisition equipment. Redundant data collected at the ground test station are available as a standard for comparison with data recorded by the on-board system. All data were not analyzed in detail, yet pertinent features of dynamic mechanical response were defined. Three fundamental mechanical vibration modes were defined: (1) bell-ringing (X axis) at 11.5 Hz, (2) pitching (Z axis) at 27 Hz, and (3) bending (both axes) at 60 Hz. Reinforcement and harmonic resonances occur at numerous other (higher) frequencies.

Recorded point and transfer impedance measurements clearly show resonances, mode shapes, and the mechanical flexibility of components. Mechanical impedance peak values of 30 lb-sec/in. are typical in both X and Z axes. Impedance head force data obtained during vibration tests provided a dynamic check with data from the instrumented launcher. Dynamic sensitivity of the launcher compares well with static calibration.

Data from the aft launch lug bending channel exceeded the range of the ground data acquisition system, and valid data were not obtained. The range must be increased for subsequent testing.

Random and aeroheat simulation tests conducted are reasonably comparable to environments specified by General Dynamics.

Unclassified
Security Classification

DOCUMENT CONTROL DATA - R & D

(Security classification of title, body of abstract and indexing annotation must be entered when the overall report is classified)

1. ORIGINATING ACTIVITY *(Corporate author)*
North American Rockwell Corporation
Rocketdyne, Solid Rocket Division
McGregor, Texas 76657

2a. REPORT SECURITY CLASSIFICATION
Unclassified

2b. GROUP

3. REPORT TITLE
Simulation Testing of a Modified Bomb Dummy Unit (BDU)
(AFRPL Project DAME)

4. DESCRIPTIVE NOTES *(Type of report and inclusive dates)*
Final Report

5. AUTHOR(S) *(First name, middle initial, last name)*

6. REPORT DATE
24 February 1973

7a. TOTAL NO. OF PAGES
122

7b. NO. OF REFS
0

8a. CONTRACT OR GRANT NO.
F04611-69-C-0075

b. PROJECT NO.

c.

d.

9a. ORIGINATOR'S REPORT NUMBER(S)
R-4739

9b. OTHER REPORT NO(S) *(Any other numbers that may be assigned this report)*
AFRPL-TR-72-107

10. DISTRIBUTION STATEMENT
Distribution limited to U. S. Government agencies only: Test & Evaluation; October 1972. Other requests for this document must be referred to AFRPL (STINFO), Edwards, CA 93523.

11. SUPPLEMENTARY NOTES

12. SPONSORING MILITARY ACTIVITY

13. ABSTRACT
This report documents results of a system checkout of the completed flight test vehicle (BDU) for Project DAME while it was exposed in a static environment test simulator to a predicted flight vibration and thermal environment. The BDU was subjected to numerous vibration and aeroheat test cycles using both soft- and hard-mounting systems. Both ground station and on-board data were acquired and are presented in the report.

DD FORM 1 NOV 65 1473

Unclassified
Security Classification

14 KEY WORDS	LINK A		LINK B		LINK C	
	ROLE	WT	ROLE	WT	ROLE	WT
Mechanical Impedance						
Data Acquisition						
Solid Rocket Propellants						
Vibration						